



January 2016

Synthesis And Exploration Of Catalytic Activity Of Amidooxazolate Zinc Complexes And A Manganese Salen Complex

Vamshi Krishna Chidara

Follow this and additional works at: <https://commons.und.edu/theses>

Recommended Citation

Chidara, Vamshi Krishna, "Synthesis And Exploration Of Catalytic Activity Of Amidooxazolate Zinc Complexes And A Manganese Salen Complex" (2016). *Theses and Dissertations*. 2003.
<https://commons.und.edu/theses/2003>

This Dissertation is brought to you for free and open access by the Theses, Dissertations, and Senior Projects at UND Scholarly Commons. It has been accepted for inclusion in Theses and Dissertations by an authorized administrator of UND Scholarly Commons. For more information, please contact zeinebyousif@library.und.edu.

SYNTHESIS AND EXPLORATION OF CATALYTIC ACTIVITY OF
AMIDOOXAZOLINATE ZINC COMPLEXES AND A MANGANESE SALEN
COMPLEX

by

Vamshi Krishna Chidara
Masters of Science, Osmania University, Hyderabad, India, 2011

A Dissertation

Submitted to the Graduate School

of the

University of North Dakota

in partial fulfillment of the requirements

for the degree of

Doctor of Philosophy

Grand Forks, North Dakota

December

2016

This dissertation, submitted by Vamshi Krishna Chidara in partial fulfillment of the requirements for the degree of Doctor of Philosophy from the University of North Dakota, has been read by the Faculty Advisory Committee under whom the work has been done, and is hereby approved.

Dr. Guodong Du (Chair person)

Dr. Harmon Abrahamson

Dr. Lothar Stahl

Dr. Qianli (Rick) Chu

Dr. Brian Tande

This dissertation meets the standards for appearance, conforms to the style and format requirements of the Graduate School at the University of North Dakota, and is hereby approved.

Grant McGimpsey
Dean of the School of Graduate Studies

Date

PERMISSION

Title SYNTHESIS AND EXPLORATION OF CATALYTIC
ACTIVITY OF AMIDOOXAZOLINATE ZINC COMPLEXES
AND A MANGANESE SALEN COMPLEX

Department Chemistry

Degree Doctor of Philosophy

In presenting this dissertation in partial fulfillment of the requirements for a graduate degree from the University of North Dakota, I agree that the library of this University shall make it freely available for inspection. I further agree that permission for extensive copying for scholarly purposes may be granted by the professor who supervised my dissertation work or, in his absence, by the chairperson of the department or the dean of the Graduate School. It is understood that any copying or publication or other use of this dissertation or part thereof for financial gain shall not be allowed without my written permission. It is also understood that due recognition shall be given to me and to the University of North Dakota in any scholarly use which may be made of any material in my dissertation.

Vamshi Krishna Chidara

Signature

December 09, 2016

Date

TABLE OF CONTENTS

LIST OF FIGURES	viii
LIST OF TABLES	x
LIST OF CHARTS	xii
LIST OF SCHEMES.....	xiii
LIST OF ABBREVIATIONS.....	xiv
ABSTRACT.....	xix
CHAPTER	1
1. GENERAL INTRODUCTION	1
1.1. Poly(carbonates)	1
1.2. Poly(esters)	5
1.3. Silyl ethers	9
1.4. Value-added intermediates	12
1.5. References.....	14
CHAPTER	19
2. SYNTHESIS OF CHIRAL C ₂ -SYMMETRIC BIMETALLIC ZINC COMPLEXES OF AMIDO-OXAZOLINATES AND THEIR APPLICATION IN COPOLYMERIZATION OF CO ₂ AND CYCLOHEXENE OXIDE	19
2.1. Introduction.....	19
2.2. Results and discussion	22
2.2.1. Ligand design and synthesis	22
2.2.2. Synthesis of zinc complexes	26
2.2.3. Copolymerization of CO ₂ and CHO	27
2.3. Conclusions.....	34

2.4. Experimental section	34
2.5. References.....	44
CHAPTER	49
3. RING OPENING COPOLYMERIZATION OF STYRENE OXIDE AND CYCLIC ANHYDRIDES CATALYZED BY CHIRAL ZINC AMIDO- OXAZOLINATE COMPLEXES.....	49
3.1. Introduction.....	49
3.2. Results and discussion	51
3.2.1. Screening of the polymerization reaction conditions	51
3.2.2. Effect of catalyst structure on catalytic behavior....	53
3.2.3. Effect of anhydrides.....	55
3.3. Conclusions.....	56
3.4. Experimental section	57
3.5. References.....	59
CHAPTER	61
4. RING OPENING COPOLYMERIZATION OF CYCLOHEXENE OXIDE AND CYCLIC ANHYDRIDES CATALYZED BY CHIRAL ZINC AMIDO- OXAZOLINATE COMPLEXES.....	61
4.1. Introduction.....	61
4.2. Results and discussion	62
4.2.1. Screening of reaction conditions.....	62
4.2.2. Effect of catalyst structure on catalytic activity.....	65
4.3. Conclusions.....	66
4.4. Experimental section	67
4.5. References.....	69

CHAPTER	71
5. AN EFFICIENT CATALYST BASED ON MANGANESE SALLEN FOR HYDROSILYLATION OF CARBONYL COMPOUNDS	71
5.1. Introduction.....	71
5.2. Results and discussion	72
5.3. Conclusions.....	78
5.4. Experimental section	78
5.5. References.....	88
CHAPTER	92
6. VERSATILE MANGANESE CATALYSIS FOR THE SYNTHESIS OF POLYSILYLEETHERS FROM DIOLS AND DICARBONYLS WITH HYDROSILANES	92
6.1. Introduction.....	92
6.2. Results and discussion	94
6.2.1. Optimization reactions	94
6.2.2. Step-growth polymerization.....	98
6.2.3. Diols.....	99
6.2.4. Dicarbonyls.....	101
6.2.5. Substrates with mixed functional groups.....	103
6.3. Conclusions.....	105
6.4. Experimental section	105
6.5. References.....	109
CHAPTER	112
7. CATALYTIC EPOXIDATION OF BIOBASED ESTERS OF SUCROSE SOYATE	112
7.1. Introduction.....	112

7.2. Results and discussion	116
7.2.1. Epoxidation of SS catalyzed by MTO	116
7.2.2. Epoxidation of SS catalyzed by Mn ^{II} [(<i>R,R</i>)- mcp](OTf) ₂ complex	117
7.2.3. Epoxidation of SS catalyzed by FeCl ₃ .6H ₂ O complex	120
7.2.4. Epoxidation of SS catalyzed by Mo{ 132} nanoball	121
7.3. Conclusions.....	122
7.4. Experimental section	123
7.5. References.....	126
APPENDICES	128
APPENDIX-A.....	129
X-RAY DATA TABLES OF COMPLEX 1d (Chapter 2).....	129
APPENDIX B	137
X-RAY DATA TABLES OF COMPLEX 3b (Chapter 2).....	137

LIST OF FIGURES

Figure	Page
1. Selected applications of CO ₂	2
2. Zinc-phenoxide catalysts for poly(carbonate) synthesis.....	4
3. Bimetallic phenolate complexes for poly(carbonate) synthesis.....	5
4. Porphyrin complexes for the ROCOP of epoxides with anhydrides.	6
5. Series of chloro salen complexes for ROCOP of epoxides with anhydrides.....	7
6. β-Diiminate zinc complexes for ROCOP of epoxides with anhydrides.	8
7. General mechanism for the ROCOP of epoxide with anhydride.....	8
8. Chalk-Harrod mechanism for hydrosilylation of alkenes.	11
9. Ojima mechanism for hydrosilylation of carbonyl compounds.....	12
10. A set of dinuclear zinc complexes for CHO/CO ₂ copolymerization.	21
11. A ball and stick representation of complex 1d	25
12. Carbonyl region of the ¹³ C NMR spectrum of the poly(cyclohexene carbonate) generated by catalyst 2d	30
13. ORTEP drawing of complex 3b with thermal ellipsoids drawn at the 50 % probability level.....	32
14. Regiostructures of polystyrene succinate: Tail-Tail (TT), Head-Tail (HT), and Head-Head (HH) junctions.	54
15. Carbonate region of the PSS of ¹³ C NMR spectrum generated from SO and SA by catalyst 3	55
16. copolymerization of SO and anhydrides catalyzed by 1-4	56

17. Hammett plot for benzaldehyde derivatives.	77
18. The conversion-time profile of PhCHO and PhCOMe under standard conditions. ...	86
19. NMR for observed upfield peak..	87
20. ¹ H and ¹³ C NMR of the poly(silylether) from 1,4-benzenedimethanol and diphenylsilane.	97
21. FT-IR spectra of 1,4-benzenedimethanol, diphenylsilane and poly(silylether).....	97
22. Conversion vs molecular weight of 1,4-benzenedimethanol and diphenylsilane poly(silylether).....	98
23. Time profile for 1,4-benzenedimethanol and diphenylsilane poly(silylether).....	99
24. Completely epoxidized sucrose soyate	113
25. ¹ H NMR spectrum of epoxidized sucrose soyate, hydrolyzed sucrose soyate, sucrose soyate in CDCl ₃	118

LIST OF TABLES

Table	Page
1. Screening the reaction conditions for copolymerization of CO ₂ and CHO.....	27
2. Asymmetric copolymerization of CO ₂ and CHO with catalysts 2a-2d and 3b	29
3. Screening the reaction conditions of ring opening co-polymerization process of styrene oxide and maleic anhydride	52
4. Results of copolymerization of styrene oxide with different anhydrides	54
5. Optimization of reaction conditions.....	64
6. Results of ROCOP of CHO with anhydrides.....	66
7. Hydrosilylation of benzaldehyde and acetophenone	74
8. Hydrosilylation of carbonyl compounds catalyzed by 1	76
9. Initial screening experiments of catalytic hydrosilylation of benzaldehyde and acetophenone.....	84
10. Data for competition reactions of benzaldehydes.	85
11. Dehydrogenative coupling of 1,4-benzenedimethanol with diphenylsilane.....	96
12. Dehydrogenative coupling of symmetrical diols with diphenylsilane.....	100
13. Poly(silylethers) of dicarbonyls, hydroxy carbonyls and unsymmetrical diols.....	103
14. Epoxidation of SS catalyzed by MTO	117
15. Epoxidation of SS catalyzed by Mn ^{II} [(R,R)-mcp](OTf) ₂ complex	119
16. Epoxidation of SS catalyzed by FeCl ₃ .6H ₂ O.....	120
17. Epoxidation of SS catalyzed by Mo{132} nanoball.....	122
18. Crystal data, data collection, structure solution and structure refinement for 1d	129

19. Selected bond lengths for 1b (Chapter 2).	130
20. Selected bond angles for 1b (Chapter 2).....	131
21. Selected torsional angles for 1b (Chapter 2).....	134
22. Crystal data, data collection, structure solution and structure refinement for 3b	137
23. Selected bond lengths for 3b (Chapter 2).	138
24. Selected bond angles for 3b (Chapter 2).....	140

LIST OF CHARTS

Chart	Page
1. Examples of non-degradable polymers.....	1
2. Various classes of bio-degradable polymers.....	1
3. Schematic representation of protons of ligands 1a–d for listing NMR data	35
4. Structures of amido-oxazolate zinc complexes.	51
5. Various catalysts used in this study. 1. Methyltrioxorhenium(VII), 2. Mn ^{II} (R,R-mcp)(CF ₃ SO ₃) ₂ , 3. Iron(III)chloride hexahydrate, 4. {(NH ₄) ₄₂ [Mo ^{VI} ₇₂ Mo ^V ₆₀ O ₃₇₂ (CH ₃ COO) ₃₀ (H ₂ O) ₇₂]}.	115

LIST OF SCHEMES

Scheme	Page
1. General scheme for the ring-opening copolymerization of epoxide and CO ₂	3
2. Synthesis of poly(bisphenol-A) polycarbonate.....	3
3. General procedures for the synthesis of poly(esters).....	6
4. Synthesis of dinucleating ligands 1a–c	24
5. Synthesis of ligand 1d	25
6. Synthesis of zinc complexes 2a–2d	26
7. Synthesis of zinc complex 3b	32
8. Copolymerization of styrene oxide with cyclic anhydrides.....	52
9. Amido-oxazolate zinc complexes for ROCOP of CHO with anhydrides.	63
10. General scheme representing the hydrosilylation of carbonyl compounds catalyzed by a manganese salen complex.....	73
11. Initial products in Mn-catalyzed hydrosilylation.....	80
12. Poly(silylether)s from hydrosilanes.	94

LIST OF ABBREVIATIONS

ACN	Acetonitrile
BDI	β -diketiminat
BINAP	Bis(diphenylphosphino)-1,1'-binaphthyl
BPA	Bisphenol-A
BPA-PC	Poly(bisphenol-A carbonate)
^t Bu	<i>tert</i> -Butyl
CHO	Cyclohexene oxide
CO ₂	Carbon dioxide
Cy	Cyclohexyl
dba	Dibenzylideneacetone
DCM	Dichloromethane
DMAP	4-dimethylaminopyridine
DMP	Dimethylphenyl
ee	Enantiomeric excess
EO	Ethylene oxide
ESS	Epoxidized sucrose soyate
Et	Ethyl
Et ₃ SiH	Triethylsilane
EtOAc	Ethyl acetate
(EtO) ₃ SiH	Triethoxysilane

EtOH	Ethanol
ESEFA	Epoxidized sucrose esters of fatty acids
FTIR	Fourier transform infrared spectroscopy
GC	Gas chromatography
GPC	Gel permeation chromatography
H ₂ O ₂	Hydrogen peroxide
HMDS	Hexamethyldisilazane
HPLC	High performance liquid chromatography
HRMS	High resolution mass spectrometry
MA	Maleic anhydride
Me	Methyl
MeOH	Methanol
M_n	Number average molecular weight
M_w	Weight average molecular weight
MTO	Methyltrioxorhenium
Naph	Naphthyl
NMR	Nuclear magnetic resonance
ORTEP	Oak Ridge Thermal-Ellipsoid Plot
PA	Phthalic anhydride
PAA	Peracetic acid
PC	Poly(carbonate)

PCC	Poly(cyclohexene carbonate)
PCHC	Poly(cyclohexene carbonate)
Pd(OAc) ₂	Palladium acetate
PDI	Polydispersity index
PE	Polyethylene
P&G	Proctor and Gamble
Ph	Phenyl
PhMeSiH ₂	Phenylmethylsilane
PhSiH ₃	Phenylsilane
Ph ₃ SiH	Triphenylsilane
PO	propylene oxide
PP	Polypropylene
Pr	Propyl
PS	Polystyrene
ⁱ Pr	Isopropyl
PVC	Polyvinylchloride
ROCOP	Ring-opening copolymerization
ROP	Ring-opening polymerization
SA	Succinic anhydride
Salcy	Salicylidene
Salen	<i>N,N</i> -bis(salicylidene)-1,2-diaminoalkane

SEFA	Sucrose esters of fatty acids
SO	Styrene oxide
SS	Sucrose soyate
TBS	<i>tert</i> -Butyldimethylsilyl
TEA	Triethylamine
TLC	Thin-layer chromatography
T_g	Glass transition temperature
THF	Tetrahydrofuran
T_m	Melting point
TMEDA	<i>N,N,N',N'</i> -Tetramethylethylenediamine
TMS	Tetramethylsilane
TOF	Turnover frequency
TON	Turnover number
TPP	5,10,15,20-tetraphenylporphinato
Zn(OAc) ₂	Zinc acetate
ZnEt ₂	Diethylzinc

ACKNOWLEDGEMENTS

I thank my graduate advisor, Dr. Guodong Du for his continuous guidance, support, and patience over the past 5 years. I would like to thank my graduate committee members, Dr. Harmon Abrahamson, Dr. Lothar Stahl, Dr. Qianli (Rick) Chu, Dr. Brian Tande, for shaping my path through their suggestions.

I thank my previous lab member, Dr. Srinivas Abbina for being a great mentor, and more than a brother during and after his time at UND. I thank the current graduate students, Shi Bian, Srikanth Vijjamari, Muneer Shaik, Samuel Njie and previous undergraduate student, Samuel Stadem, for being cooperative and for all the good times at UND.

I thank Dr. Alena Kubatova and her group members for allowing us to use their instruments. I thank Dr. Irina P. Smoliakova, Dr. David T. Pierce, Dr. Julie Abrahamson, Dr. Kathryn A. Thomasson, Mr. Michael Whitney for their mentorship as instructors and for teaching me professional skills during my time as a TA.

I thank UND Chemistry Department, Graduate School, and ND EPSCoR for all the financial support they provided.

I thank all co-graduate students and my friends with whom I have shared my time over the past 5 years in Grand Forks.

Finally, special thanks to my family, who gave me freedom to make my own choices, supported my decisions, and watched me grow over the years.

ABSTRACT

A family of new chiral C_2 symmetric amido-oxazolate ligands with three different linkers has been synthesized and the respective bimetallic zinc complexes were generated with two equiv. of $Zn[N(SiMe_3)_2]_2$, a while bischelating zinc complex was synthesized with one equiv. $Zn[N(SiMe_3)_2]_2$. The bimetallic catalyst with *m*-phenylenediamine linker afforded poly(cyclohexene carbonate) (PCHC) formation with 78% carbonate linkages, while the catalyst with 1,8-diaminoanthracene linker generated isotactic PCHC with 86% *m*-centered tetrads.

A monometallic version of the amido-oxazolate zinc complexes were also used to catalyze ring-opening copolymerization (ROCOP) of styrene oxide (SO) or cyclohexene oxide (CHO) with different anhydrides. Type of substituents on the ligand frame work was observed to influence the catalytic activity of the reaction. These complexes were observed to be viable initiators for ROCOP of epoxides and anhydrides.

A manganese(V) salen complex was used as an effective pre-catalyst in hydrosilylation of aldehydes and ketones, dehydrogenative coupling of hydroxyl groups with hydrosilanes, condensation of diols and dicarbonyls with hydrosilanes to synthesize poly(silylethers). The catalyst was active in all cases and a range of functional groups, such as chloro, nitro, methoxy, carbonyl, and carbon-carbon multiple bonds were tolerated in these reactions. Mechanistic studies suggest that the reaction likely proceeds through a reduced manganese(III) hydride species that undergoes electrophilic attack by the substrates.

In addition, inexpensive, easy-to-make, readily available metal complexes were used for the epoxidation of sucrose soyate (SS) using environment benign, non-toxic

oxidants like H₂O₂, and molecular oxygen. Methyltrioxorhenium (MTO) was proved to be an effective biphasic catalyst to afford 100% epoxide content with complete conversion using H₂O₂ and 2-methyl THF. Further details regarding the activity of iron, manganese, and molybdenum complexes were also discussed.

CHAPTER 1

GENERAL INTRODUCTION

Fossil fuels are non-renewable sources, constituting coal, petroleum, and natural gas, used in a variety of applications including transportation industries, manufacturing industries, and more importantly for the generation of electricity.¹ Approximately 81% of the total energy consumed worldwide is derived from fossil fuels.² Consumption of fossil fuels has increased with a rapid increase in global human population.³ Currently, plastics are produced on a scale of 150 million tons per year and majority of them are derived from petrochemical feed stocks, with annual consumption of 7–8% worldwide reserves.^{4,5,6} At this pace, the majority of the oil reserves are estimated to be depleted by 2050.^{6,7} Polyethylene (PE), polyvinylchloride (PVC), polypropylene (PP), polystyrene (PS) (Chart 1) are few examples of the most important polymers. In spite of non-degradable nature of majorly used plastics, excellent thermal and physical properties of these polymers overruled them to be commercially successful and vastly used for various day-to-day life applications.

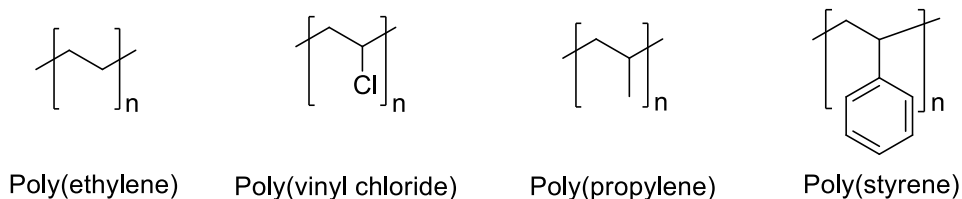


Chart 1. Examples of non-degradable polymers.

Concerns regarding the future availability of crude oil, combined with growing population, ecological imbalance, environmental pollution have led to the investigation of alternate synthetic methodologies to produce polymers from sustainable materials other than petrochemicals. Even though, production of bio-derived polymers is of interest, research is also focused to improve the properties of already existing degradable polymers compared to conventional non-degradable polymers.⁸ To develop biodegradable polymers with degradable functional groups, various classes of polymers like poly(amides), poly(urethanes), poly(anhydrides), poly(carbonates) and poly(esters) have been reported (Chart 2).

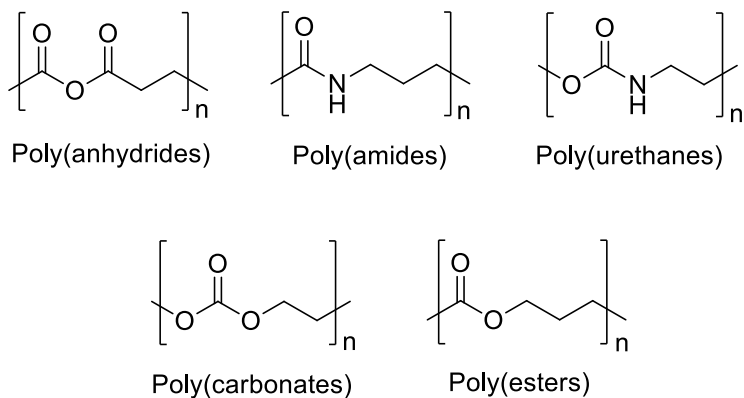


Chart 2. Various classes of bio-degradable polymers.

1.1. Poly(carbonates)

Carbon dioxide (CO₂) is one of the most abundant, non-flammable, and non-toxic C₁ waste-gas present in nature.^{9,10} It is released into environment from various sources including combustion of fossil fuels, emissions from industries, transportation- vehicles, as well as routine human activities.¹¹ In the event of well-developed large scale CO₂ gas capturing technologies, constructive utilization of the waste gas for the production of

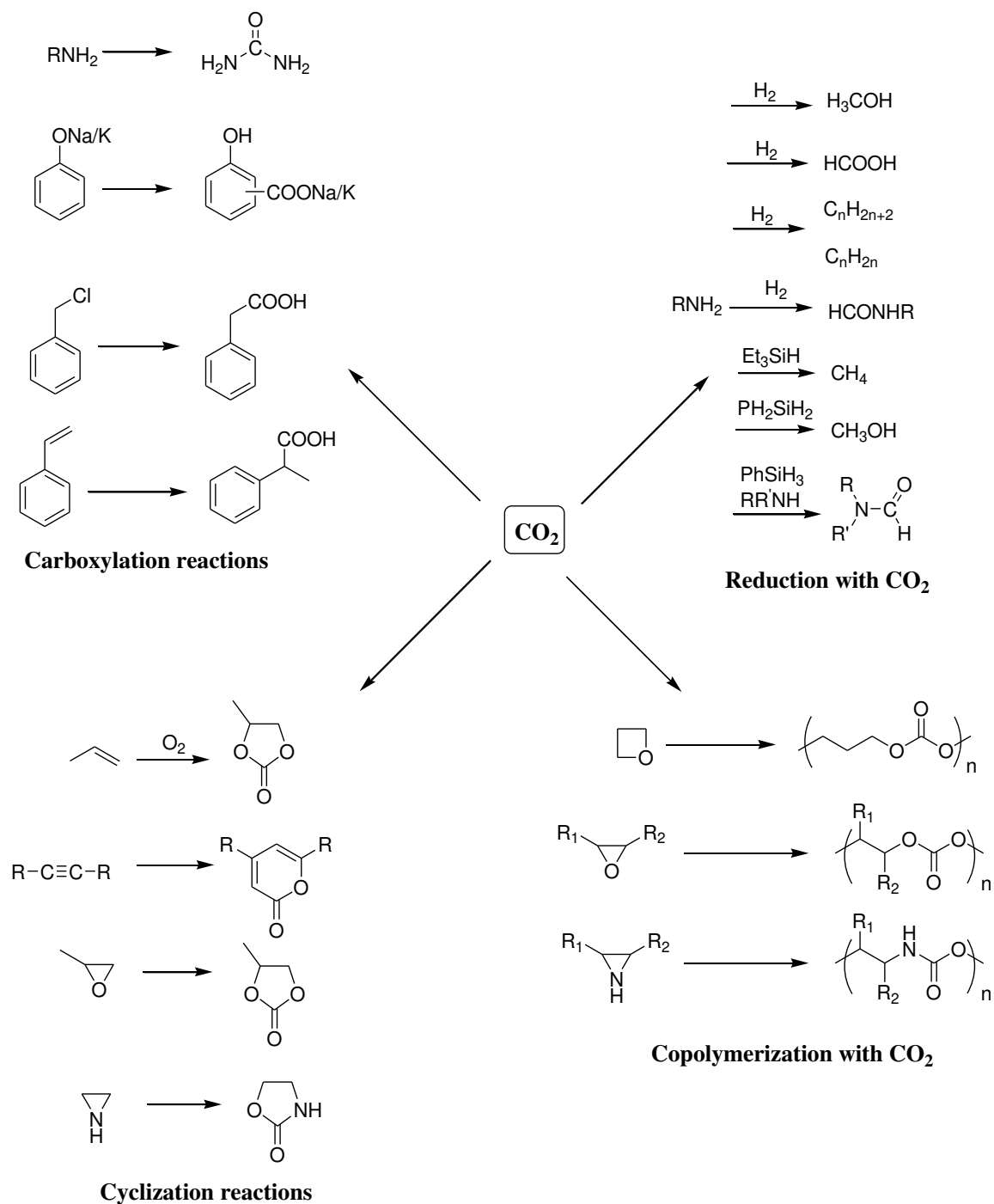
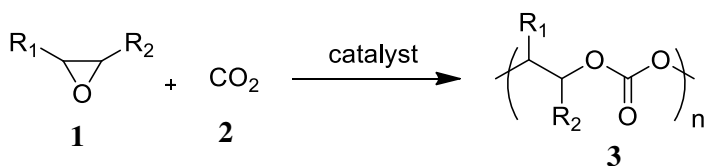


Figure 1. Selected applications of CO₂.

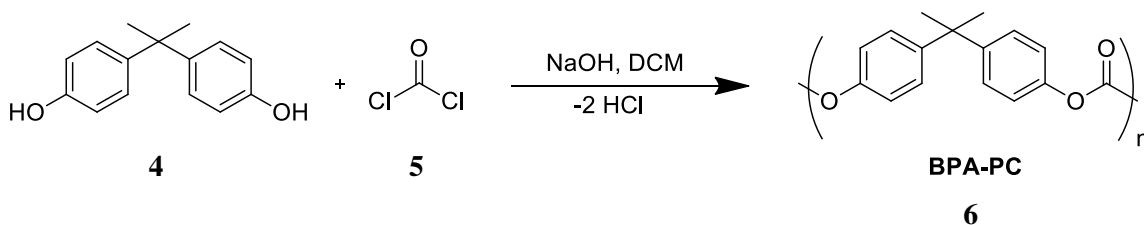
degradable polymers is a major area of present research (Figure 1).¹² However, thermodynamic stability of CO₂ limits its usage in the production of valuable products.¹³

New reaction strategies as well as development of organic and inorganic metal catalysts will aid for the conversions of CO₂.^{14,15} Various processes, as well as metal catalysts have been reported for this purpose.^{16,17,18} Some of them include the synthesis of polycarbonates and cyclic carbonates from ring-opening reactions of epoxides and CO₂ (Scheme 1).^{19,20,21,22,23} Especially, synthesis of polycarbonates from epoxides with CO₂ proved as an efficient pathway to degradable polymers with varied applications.^{24,25}



Scheme 1. General scheme for the ring-opening copolymerization of epoxide and CO₂

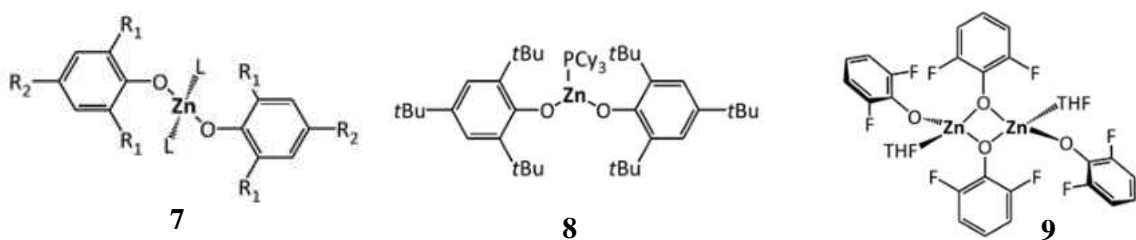
The excellent physical and thermal properties of initially discovered poly(bisphenol-A) polycarbonate (BPA-PC), led to its use for the production of plastics and epoxy resins since 1957.²⁶ Industrial production of BPA-PC involves the reaction of bisphenol-A (BPA) and phosgene under biphasic conditions using NaOH and DCM leaving HCl as a by-product (Scheme 2).²⁷ In another reaction, diphenyl carbonate is used instead of phosgene with the elimination of phenol as a by-product.²⁸ Phosgene is a toxic and corrosive gas and BPA used as a substrate is known to be carcinogenic.²⁹



Scheme 2. Synthesis of poly(bisphenol-A) polycarbonate.

Despite of their limitations, excellent glass-transition temperature (*T_g*) of BPA-PC makes it highly useful towards industrial applications. However, greener, and sustainable processes to produce polycarbonates alternate to conventional BPA-PC are highly required. In 1969, Inoue and co-workers reported the formation of poly(propylene

carbonate) (PPC) by using equimolar ratio of diethyl zinc and water.³⁰ Subsequently, they also reported several diethyl zinc complexes, either with resorcinol, dicarboxylic acids, or primary amines.³¹ Zinc-phenoxide complexes were reported to be active catalysts for ROCOP of epoxide with CO₂ affording 90% carbonate linkages, M_n of 38000 g/mol, and TOF of 2.4 h⁻¹ (Figure 2, **7a**). Similar result with TOF of 9.6 h⁻¹ was achieved with another complex varying in its substituents (Figure 2, **7b**).³² Further modifications in the catalyst yield 100% carbonate linkages (Figure 2, **8** and **9**).³³



7a R₁=Ph, R₂=H, L=Et₂O

7b R₁=R₂=Me, L=pyridine

Figure 2. Zinc-phenoxide catalysts for poly(carbonate) synthesis.

Complexes containing more than one active metal center proved to be efficient for poly(carbonates) compared to respective monometallic versions. Moreover, a cooperative mechanism between two metal centers in bimetallic complex seems to be the reason for its activity. In other words, the same bimetallic complex can activate both epoxide and CO₂ at the same time during copolymerization reaction. In 2005, Xiao and coworkers reported the bimetallic versions of dizinc and dimagnesium complexes and proved to be active catalysts for ROCOP of CHO and CO₂ (Figure 3, **10a** and **10b**).³⁴ A molecular weight M_n of 20 – 40,000 g/mol was achieved with TOF's of 142 h⁻¹ and 20 h⁻¹ respectively. However, varied substitutions at nitrogen in the phenolate lowered the catalytic activity.³⁵ More

details about zinc-based bimetallic catalysts for copolymerization of CHO and CO₂ are discussed in Chapter 2.

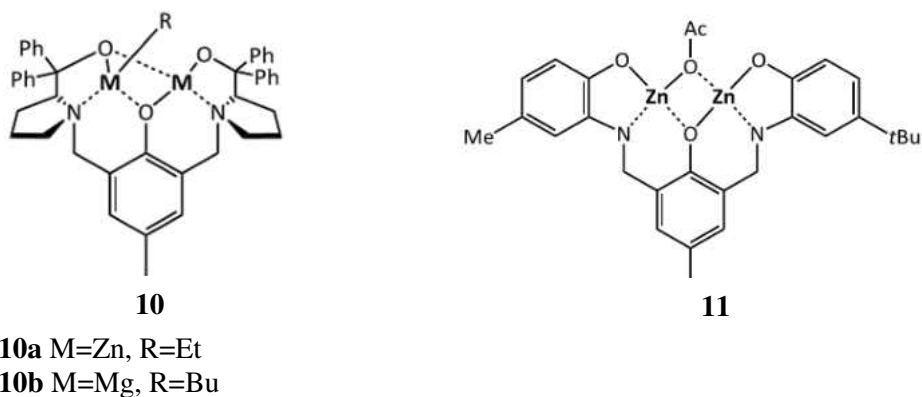
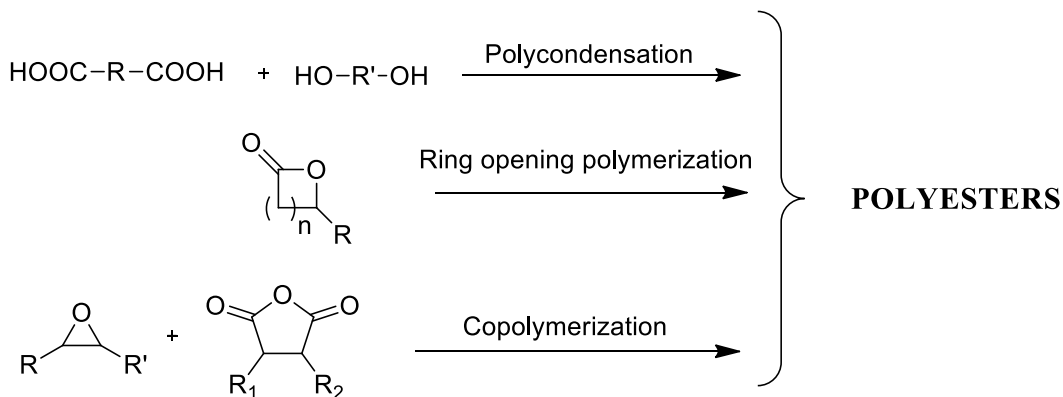


Figure 3. Bimetallic phenolate complexes for poly(carbonate) synthesis.

1.2. Poly(esters)

Poly(esters) are another important class of biodegradable polymers, produced at a rate of 50 million tons per year.³⁶ Poly(esters) have potential applications as drug carriers and are also used in the preparation of various medical supplies because of its biocompatibility.^{37,38} These polymers can be synthesized by polycondensation of diol and diacid or ring opening polymerization (ROP) of cyclic esters or ring opening copolymerization (ROCOP) of epoxides with cyclic anhydrides (Scheme 3).^{39,40,41} The step-growth polymerization from diols and diacids usually requires higher temperatures, longer reaction times, and often leads to side reactions and results in low molecular weight polymers. ROP of cyclic esters also effectively produces polyesters, but the availability of monomers is limited. ROCOP of epoxides and cyclic anhydrides is another alternative for the synthesis of polyesters. The polymer backbone can be easily modulated by changing

the functionalities on one of the monomer units to study the variations in thermal properties.



Scheme 3. General procedures for the synthesis of poly(esters).

The first reports on ROCOP of epoxides and anhydrides was published in 1960s using tertiary amines.⁴² Following the seminal work of Fischer and coworkers, several papers have been published about zinc and aluminum initiators. In 1985, Inoue and coworkers reported aluminum-porphyrin complexes in combination with phosphonium or ammonium salts as efficient catalysts for the copolymerization of styrene oxide (SO),

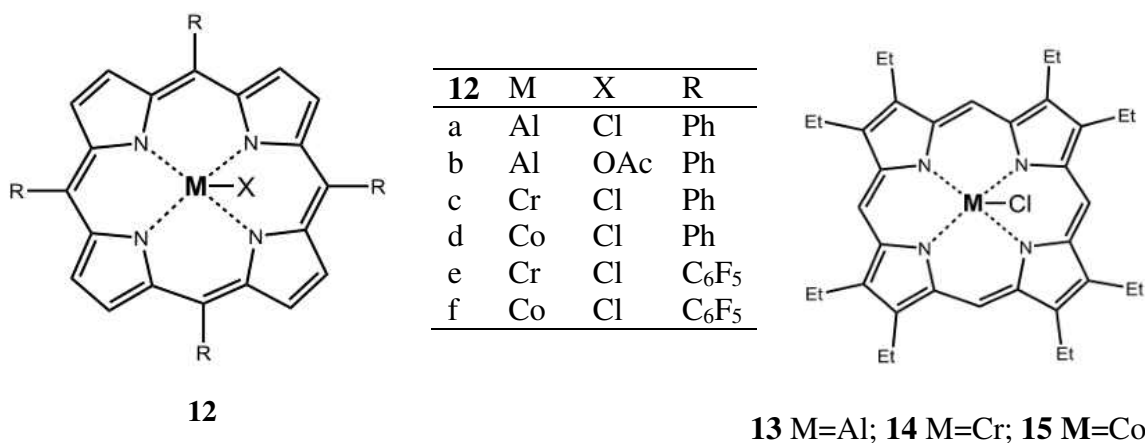


Figure 4. Porphyrin complexes for the ROCOP of epoxides with anhydrides.

propylene oxide (PO) with phthalic anhydride (PA), resulting in perfectly-alternating copolymers with TOF of 5 h^{-1} (Figure 4, **12a** & **b**).⁴³ Duchateau and co-workers reported

the similar porphyrin complex with chromium as a metal center for copolymerization of SO or cyclohexene oxide (CHO) with PA or succinic anhydride (SA). The resultant polymers were synthesized with high TOFs and molecular weights ranging from 1000 to 20,000 g/mol (Figure 4, complex **12c**).⁴⁴ Cobalt complex of the same set of ligand produced polymer with low TOF of 40 h⁻¹. Copolymerization of methyl succinic anhydride (MSA), maleic anhydride (MA), SA, or PA with PO have been reported using Co and Cr complexes (Figure 4, complexes **12c-f**, **13-15**).⁴⁵

Coates and coworkers also reported chromium salen complex for ROCOP of PO, phenyl glycidyl ether, epichlorohydrin, or allyl glycidyl ether with MA and achieved an M_n of 21–33 kg/mol (Figure 5, complex **17b**).⁴⁶ Duchateau and coworkers reported several aluminum, cobalt, and chromium complexes of salphen, salalen and salen complexes (Figure 5, complexes **16-18**).^{44,47} These complexes along with a cocatalyst DMAP were used to catalyze the ROCOP of CHO with PA, SA and CPrA to afford the poly(esters) with M_n of 2-15 kg/mol. High TOF of 150 h⁻¹ was achieved using chromium-salalen complexes (Figure 5, complexes **17a** & **17b**). They also reported the copolymerization of limonene oxide (LO), and PA with M_n of 4-7 kg/mol, Al and Cr salphen complexes were seen to have higher activity (Figure 5, complexes **16a** & **17a**).

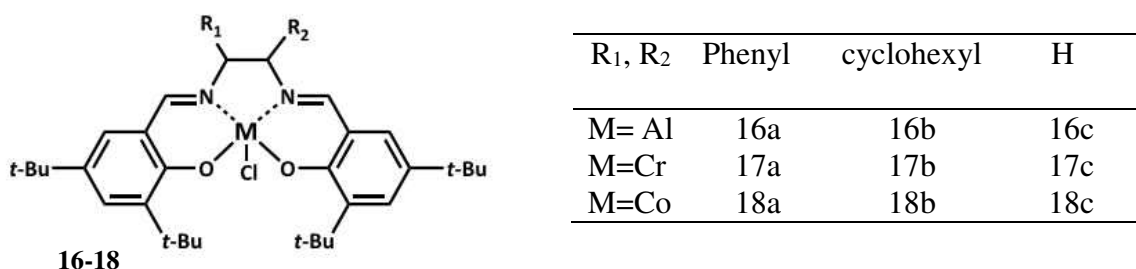


Figure 5. Series of chloro salen complexes for ROCOP of epoxides with anhydrides.

Coates and co-workers reported various β -diiminate zinc complexes, which proved to be

efficient catalysts for ROP of epoxides and ROCOP of epoxide and CO₂ (Figure 6, complexes **19a–c**). The same catalysts were used for ROCOP of LO, PO, isobutene oxide, or vinyl cyclohexene oxide with diglycolic anhydride.⁴⁸

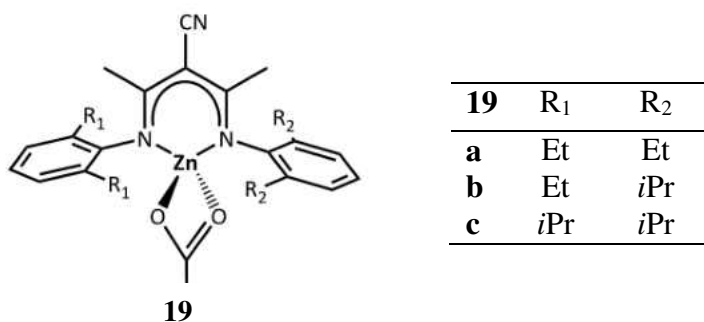


Figure 6. β -Diiminate zinc complexes for ROCOP of epoxides with anhydrides.

The general mechanism for ROCOP of an epoxide with an anhydride involves the activation of epoxide with a metal catalyst followed by a nucleophilic attack on either of the carbons of the oxirane. The ring opening takes place to attack the carbonyl carbon to form the first sequence in the repeating unit. The sequence of the growing polymer chain continues to form an alternating polymer chain (Figure 7).

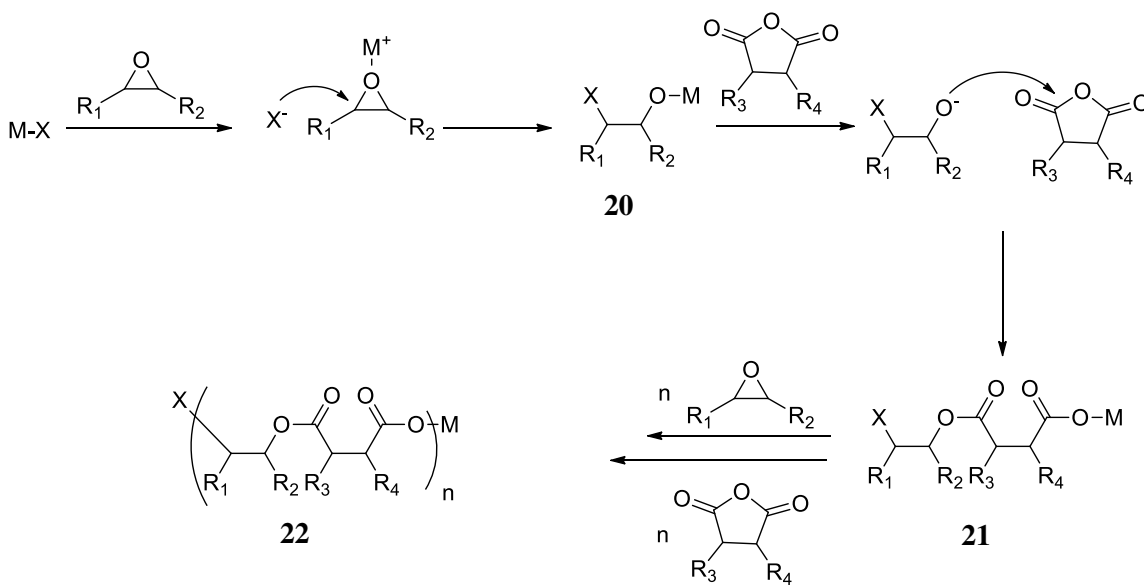


Figure 7. General mechanism for the ROCOP of epoxide with anhydride.

1.3. Silyl ethers

Reduction of unsaturated organic compounds, particularly carbonyl groups, represents an essential importance in organic transformations both in laboratory and in industrial research.⁴⁹ In 1957, Speier and coworkers reported the platinum catalyzed hydrosilylation of olefins.⁵⁰ The hydrosilylation of several other organic compounds including alkynes, carbonyl compounds, and imines have been investigated.⁴⁹

Some of the metal hydrides of the main group like boron, aluminum, can facilitate this reaction but they are required to be added in stoichiometric amounts, which makes researchers think for environmental, practical, and economical concerns. Transition-metal-based catalysts have been successfully implemented for these purposes via hydrogenation and hydrosilylation reactions.⁵¹ Even though hydrogenation reactions proceed in good yields; they require high pressures or high temperatures. In contrast, the hydrosilylation reaction require simple and mild conditions. Moreover, most of the silanes are inexpensive, less toxic, and easy to handle. A variety of transition metal catalysts based on molybdenum,⁵² platinum,⁵³ iridium, rhodium,⁵⁴ ruthenium,⁵⁵ are known to catalyze hydrosilylation, and a few papers also reported other metals, like iron,⁵⁶ copper, silver, and, gold.⁵⁷ Since the invention of the first Wilkinson's catalyst for hydrosilylation, this field has been dominated by low-valent metal based catalysts, such as rhodium, iridium, and, platinum.⁵⁸ However, high-valent metal based catalysts have received significant attention because of their effectiveness towards hydrosilylation of various substrates, particularly aldehydes and ketones.⁵⁹ Because of their high oxidation states, they are usually moisture stable and air stable complexes, which makes them easy to handle.

High-valent metal nitrides are of particular interest because of their involvement in industrial and biological nitrogen fixation processes⁶⁰ and also because of their applications in reductions and nitrogen atom transfer reactions.⁶¹ The most prominent metal nitrides among them are iron⁶² and manganese.⁶³ Nitridomanganese(V) complexes bearing a terminal Mn≡N were first reported in 1983 by two separate groups⁶⁴ and the use of such complexes as nitrogen atom transfer reagents was reported by Groves and co-workers.⁶⁵

Since then, several stable nitridomanganese(V) porphyrins and phthalocyanines were synthesized. Later, non-macrocyclic nitridomanganese(V) complexes were synthesized using tetradentate Schiff bases as ancillary ligands,⁶³ particularly, nitridomanganese(V) salen complex reported by Tai-Chu Lau and co-workers.⁶⁶

A significant effort was made to establish a mechanism for hydrosilylation. In 1965, Chalk and Harrod reported the first mechanism for hydrosilylation of alkenes.⁶⁷ The first step of the mechanism involves the oxidative addition of silane (R₃SiH) to a metal center leading to the formation of intermediate **23** followed by coordination of alkene to a metal center to form an intermediate **24**. Then the alkene insertion into the M–H bond to form **25** and finally a reductive elimination of Si forms product–C bond (Figure 8).⁶⁷

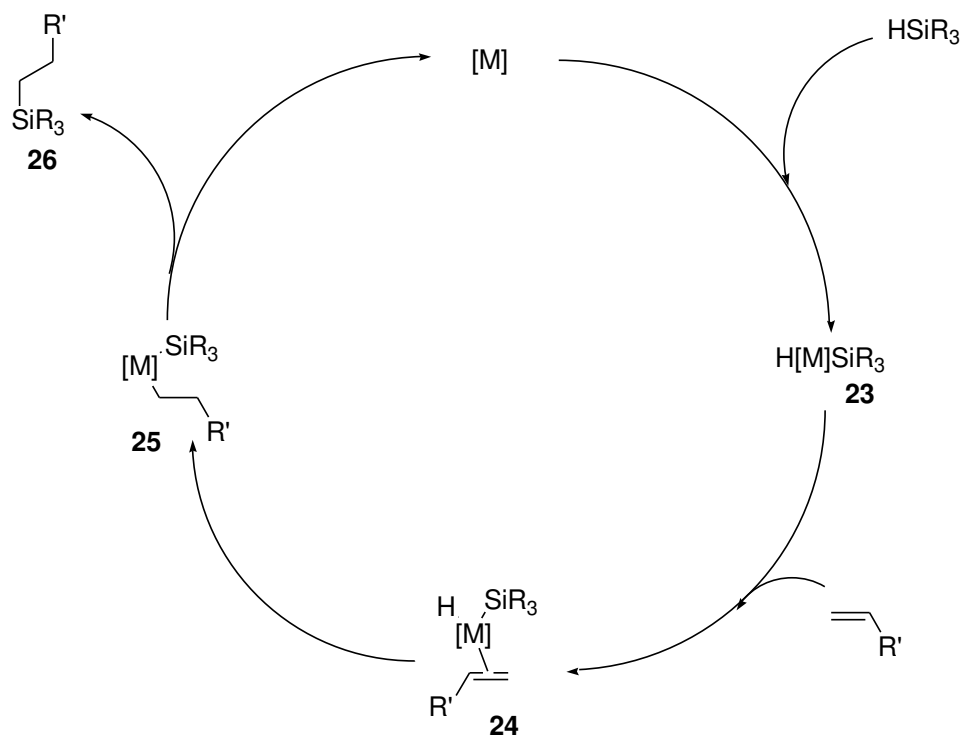


Figure 8. Chalk-Harrod mechanism for hydrosilylation of alkenes.

Several modified mechanisms were proposed for various types based on the type of substrate and metal complex used. Similarly, Ojima proposed a mechanism for hydrosilylation of carbonyl compounds.⁶⁸ The first step of the mechanism is like the previous, involves addition of Si-H across the metal center to form **23** that reacts with a carbonyl substrate to form intermediate **27** and further insertion into a M-H bond to form intermediate **28**, which, in turn undergoes reductive elimination to afford the corresponding silyl ether (Figure 9).

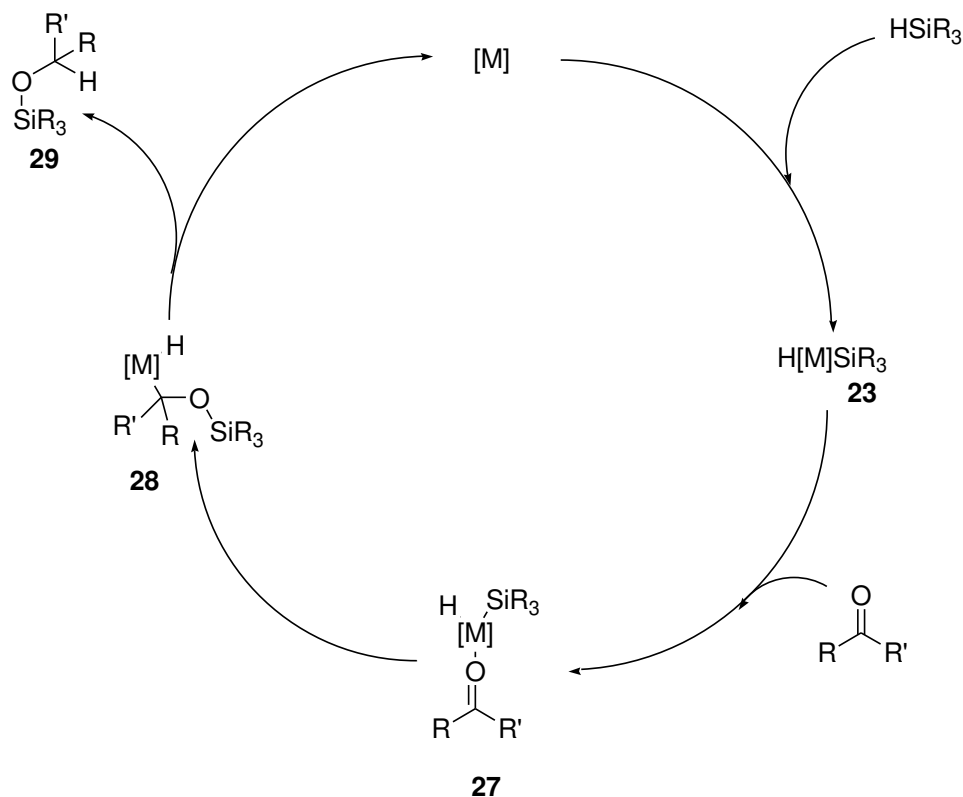


Figure 9. Ojima mechanism for hydrosilylation of carbonyl compounds

1.4. Value-added intermediates

Plant oils are readily available materials with triglycerides as their composition. A triglyceride is simply a glycerol with three hydroxyl groups substituted with fatty acid chains. The degree of unsaturation, usually expressed as iodine value (IV), of triglycerides varies among different plant oils. For example, castor and palm oils have IV under 100; soybean, corn, and sunflower oils have IV ranging between 100–150; and linseed oil have IV greater than 150. About 25% of global seed oil production is used for industrial purposes in various applications including plasticizers, coatings, and cosmetics.⁶⁹ The multiple C–C double bonds present on the fatty acid chains serves as the functional source to produce their derivatives.⁷⁰ Especially, epoxidation of these C–C double bonds generates more

reactive, three-membered cyclic ethers also known as, oxiranes. Epoxidized plant oils and their derivatives are industrially important thermoset resins used as plasticizers, stabilizers, and in coatings and paintings.⁷¹

In general, epoxidation of double bonds can be carried out in three different ways: (1) Acid or enzyme catalyzed epoxidation using percarboxylic acids (Prilezhaev epoxidation); (2) Transition-metal catalyzed epoxidation using organic and inorganic peroxides; (3) Epoxidation with metal supported activation of molecular oxygen.⁷²

Prilezhaev epoxidation is the most widely used procedure in industries. This is usually carried out by certain mineral acids like tungstic, molybdic, or sulfuric acids. These are used as catalysts in the transformation of carboxylic acids to their respective percarboxylic acids. Peracids by their nature adopt intramolecular hydrogen-bond conformation, and because of the degree of polarization, electrophilic oxygen is driven to be added to the double bonds. Stoichiometric amounts of the percarboxylic acids with double bonds produces the epoxides.⁷³ The usage of strong mineral acids leads to the corrosion of materials and therefore expensive non-corrosive materials are needed in large scale production plants. In addition, the final step involves the neutralization of acid produced with a base, which makes the process environment unfriendly. Improved results were obtained by the utilization of acid resins, however, 10–15 wt% of polystyrenesulfonicacid resin is usually required for the procedure based on the double bond. Hence, the other two procedures involving hydrogen peroxide and molecular oxygen are advantageous with more efficiency and environment friendly. More details regarding various metal-complexes catalyzed epoxidation of fatty acid chains using green oxidants were discussed in chapter 7.

1.5. References

1. Ross, M. L. *The Oil Curse: How Petroleum Wealth Shapes the Development of Nations*; Princeton University Press: Princeton, New Jersey, USA, **2012**.
2. www.eia.gov/todayinenergy/detail.cfm?id=21912 accessed on 11/29/2016.
3. www.census.gov/population/international/data/worldpop/graph_population.php accessed on 11/29/2016.
4. Ragauskas, A. J.; Williams, C. K.; Davison, B. H.; Britovsek, G.; Cairney, J.; Eckert, C. A.; Frederick Jr, W. J.; Hallett, J. P.; Leak, D. J.; Liotta, C. L.; Mielenz, J. R.; Murphy, R.; Templer, R.; Tschaplinski, T. *Science* **2006**, *311*, 484–489.
5. Yao, K.; Tang, C. *Macromolecules* **2013**, *46*, 1689–1712.
6. www.crudeoilpeak.com accessed on 11/29/2016.
7. www.indexmundi.com/energy/ accessed on 11/29/2016.
8. Mathers, R. T. *J. Polym. Sci. Part A: Polym. Chem.* **2012**, *50*, 1–15.
9. Kember, M. R.; Knight, P. D.; Reung, P. T. R.; Williams, C. K. *Angew. Chem. Int. Ed.* **2009**, *48*, 931–933.
10. Zhang, Z.; Hu, S.; Song, J.; Li, W.; Yang, G.; Han, B. *ChemSusChem* **2009**, *2*, 234–238.
11. Beer, C.; Reichstein, M.; Tomelleri, E.; Ciais, P.; Jung, M.; Carvalhais, N.; Rodenbeck, C.; Arain, M. A.; Baldocchi, D.; Bonan, G. B.; Bondeau, A.; Cescatti, A.; Lasslop, G.; Lindroth, A.; Lomas, M.; Luysaert, S.; Margolis, H.; Oleson, K. W.; Rouspard, O.; Elmar Veenendaal, E.; Viovy, N.; Christopher Williams, C.; Woodward, F. I.; Papale, D. *Science* **2010**, *329*, 834–839.
12. Xu, X.; Kan, Y.; Zhao, L.; Cao, X. *Environ. Pollut.* **2016**, *213*, 533–540.
13. Jessop, P. G.; Ikariya, T.; Noyori, R. *Chem. Rev.* **1999**, *99*, 475–493.
14. Schafer, D.-C. A.; Saak, D.-C. W.; Haase, D.; Muller, T. *Angew. Chem. Int. Ed.* **2012**, *51*, 2981–2984.
15. Darensbourg, D. J.; Holtcamp, M. W. *Coord. Chem. Rev.* **1996**, *153*, 155–174.
16. Sakakura, T.; Choi, J.-C.; Yasuda, H. *Chem. Rev.*, **2007**, *107*, 2365–2387.
17. Darensbourg, D. J. *Chem. Rev.* **2007**, *107*, 2388–2410.

-
18. Darensbourg, D. J.; Wilson, S. J. *Green Chem.* **2012**, *14*, 2665–2671.
19. Bai, D.; Wang, Q.; Song, Y.; Li, B.; Jing, H. *Catal. Commun.* **2011**, *12*, 684–688.
20. Aida, T.; Inoue, S. *J. Am. Chem. Soc.* **1983**, *105*, 1304–1309.
21. Nakano, K.; Hashimoto, S.; Nozaki, K. *Chem. Sci.* **2010**, *1*, 369–373.
22. Li, H.; Niu, Y. *Appl. Organomet. Chem.* **2011**, *25*, 424–428.
23. Wu, G.-P.; Wei, S.-H.; Ren, W.-M.; Lu, X.-B.; Xu, T.-Q.; Darensbourg, D. J. *J. Am. Chem. Soc.* **2011**, *133*, 15191–15199.
24. Nakano, K.; Kobayashi, K.; Nozaki, K. *J. Am. Chem. Soc.* **2011**, *133*, 10720–10723.
25. Kim, J. G.; Cowman, C. D.; LaPointe, C. D.; Wiesner, U.; Coates, G. W. *Macromolecules* **2011**, *44*, 1110–1113.
26. *Handbook of Polycarbonate Science and Technology*; Legrand, D. G.; Bendler, J.T., Eds.; Marcel Dekker, Inc.: New York, **2000**.
27. Kim, W. B.; Joshi, U. A.; Lee, J. S. *Ind. Eng. Chem. Res.* **2004**, *43*, 1897–1914.
28. Grause, G.; Tsukada, N.; Hall, W. J.; Kameda, T.; Williams, P. T.; Yoshioka, T. *Polym. J.* **2010**, *42*, 438–442.
29. Tsintzou, G. P.; Antonakou, E. V.; Achilias, D. S. *J. Hazard. Mater.* **2012**, *241*, 137–145.
30. Inoue, S.; Koinuma, H.; Tsuruta, T. *J. Polym. Sci. Part B* **1969**, *7*, 287–292.
31. (a) Kobayashi, M.; Inoue, S.; Tsuruta, T., *Macromolecules* **1971**, *4*, 658–659. (b) Kobayashi, M.; Inoue, S.; Tsuruta, T. *J. Polym. Sci. Polym. Chem. Ed.* **1973**, *11*, 2383–2385.
32. (a) Darensbourg, D. J.; Holtcamp, M. W. *Macromolecules* **1995**, *28*, 7577–7579. b) Darensbourg, D. J.; Holtcamp, M. W.; Struck, G. E.; Zimmer, M. S.; Niezgodna, S. A.; Rainey, P.; Robertson, J. B.; Draper, J. D.; Reibenspies, J. H. *J. Am. Chem. Soc.* **1999**, *121*, 107–116.
33. a) Darensbourg, D. J.; Wildeson, J. R.; Yarbrough, J. C.; Reibenspies, J. H. *J. Am. Chem. Soc.* **2000**, *122*, 12487–12496. b) Darensbourg, D. J.; Zimmer, M. S.; Rainey, P.; Larkins, D. L. *Inorg. Chem.* **2000**, *39*, 1578–1585.
34. (a) Xiao, Y.; Wang, Z.; Ding, K. *Chem. -Eur. J.* **2005**, *11*, 3668–3678. (b) Xiao, Y.; Wang, Z.; Ding, K. *Macromolecules* **2006**, *39*, 128–137.

-
35. Sugimoto, H.; Ogawa, A. *React. Funct. Polym.* **2007**, *67*, 1277–1283.
36. Okada, M. *Prog. Polym. Sci.* **2002**, *27*, 87–133.
37. Dadsetan, M.; Liu, Z.; Pumbeger, M.; Giraldo, C. V.; Ruesink, T.; Lu, L.; Yaszemski, M. J. *Biomaterials* **2010**, *31*, 8051–8062.
38. Lee, J. W.; Kang, K. S.; Lee, S. H.; Kim, J. Y.; Lee, B. K.; Cho, D. W. *Biomaterials* **2011**, *32*, 744–752.
39. Lutson, J.; Vass, F. *Adv. Polym. Sci.* **1984**, *56*, 91–133.
40. Mathieu, J. L.T.; Emilie, B.; Pierre, H.; Christophe, M. T. *Polym. Chem.* **2012**, *3*, 836–851.
41. Jeske, J. C.; DiCiccio, A. M.; Coates, G. W. *J. Am. Chem. Soc.* **2007**, *129*, 11330–11331.
42. Fischer, R. F. *J. Polym. Sci.* **1960**, *44*, 155–172.
43. (a) Aida, T.; Sanuki, K.; Inoue, S. *Macromolecules* **1985**, *18*, 1049–1055. (b) Aida, T.; Inoue, S. *J. Am. Chem. Soc.* **1985**, *107*, 1358–1364.
44. (a) Huijser, S.; HosseiniNejad, E.; Sablong, R.; de Jong, C.; Koning, C. E.; Duchateau, R. *Macromolecules* **2011**, *44*, 1132–1139. (b) Hosseini Nejad, E.; Paoniasari, A.; Koning, C. E.; Duchateau, R. *Polym. Chem.* **2012**, *3*, 1308–1313.
45. Bernard, A.; Chatterjee, C.; Chisholm, M. H. *Polymer* **2013**, *54*, 2639–2646.
46. DiCiccio, A. M.; Coates, G. W. *J. Am. Chem. Soc.* **2011**, *133*, 10724–10727.
47. Nejad, E. H.; van Melis, C. G. W.; Vermeer, T. J.; Koning, C. E.; Duchateau, R. *Macromolecules* **2012**, *45*, 1770–1776.
48. Jeske, R. C.; DiCiccio, A. M.; Coates, G. W. *J. Am. Chem. Soc.* **2007**, *129*, 11330–11331.
49. (a) Ojima, I.; Li, Z.; Zhu, J. *The Chemistry of Organic Silicon Compounds, Vol. 2*. Rappoport, Z.; Apeloig, Y. Ed. Wiley: New York, **1998**, pp 1687–1792. (b) Marciniak, B. M., H.; Pietraszuk, C.; Pawluc, P., *Hydrosilylation: A Comprehensive Review on Recent Advances*. Springer: London, **2008**.
50. Speier, J. L.; Webster, J. A.; Barnes, G. H. *J. Am. Chem. Soc.* **1957**, *79*, 974–979.
51. Riant, O.; Mostefai, N.; Courmarcel, J. *Synthesis* **2004**, *18*, 2943–2958.

-
52. Ziegler, J. E.; Du, G.; Fanwick, P. E.; Abu-Omar, M. M. *Inorg. Chem.* **2009**, *48*, 11290–11296.
53. Sabourault, N.; Mignani, G; Wagner, A.; Mioskowski, C. *Org. Lett.* **2002**, *13*, 2117–2119.
54. (a) Riener, K.; Hogerl, M. P.; Gigler, P.; Kühn, F. E. *ACS Catal.* **2012**, *2*, 613–621. (b) Chianese, A. R.; Crabtree, R. H. *Organometallics* **2005**, *24*, 4432–4436.
55. Abbina, S.; Bian, S; Oian, C.; Du, G. *ACS Catal.* **2013**, *3*, 678–684.
56. Tondreau, A. M.; Lobkovsky, E.; Chirik, P. J. *Org. Lett.* **2008**, Vol. 10, No. 13.
57. Gonzaleg, I. D.; Nolan, S. P. *Acc. Chem. Res.* **2008**, *41*, 349–358.
58. Noyori, R. *Asymmetric Catalysis in Organic Synthesis*, Wiley: New York, **1994**.
59. Du, G.; Fanwick, P. E.; Abu-Omar, M. M. *Inorg. Chim. Acta* **2008**, *361*, 3184–3192.
60. (a) Svastits, E. W.; Dawson, J. H.; Breslow, R.; Gellman, S. H. *J. Am. Chem. Soc.* **1985**, *107*, 6427–6428. (b) Hohenberger, J.; Ray, K.; Meyer, K. *Nat. Commun.* **2012**, *3*, 720–723.
61. Golubkov, G.; Gross, Z. *J. Am. Chem. Soc.* **2005**, *127*, 3258–3259.
62. Vogel, C.; Heinemann, F. W.; Sutter, J.; Anthon, C.; Meyer, K. *Angew. Chem. Int. Ed.* **2008**, *47*, 2681–2684.
63. Du Bois, J.; Hong, J.; Carreira, E. M.; Day, M. W. *J. Am. Chem. Soc.* **1996**, *118*, 915–916.
64. (a) Buchler, J. W.; Dreher, C.; Lay, K.-L.; Lee, Y. J. A.; Scheidt, W. R. *Inorg. Chem.* **1983**, *22*, 888–891. (b) Hill, C. L.; Hollander, F. J. *J. Am. Chem. Soc.* **1982**, *104*, 7318–7319.
65. Groves, J. T.; Takahashi, T. *J. Am. Chem. Soc.* **1983**, *105*, 2073–2074.
66. Yiu, S, –M.; Lam, W. W. Y.; Ho, C. –M.; Lau, T. –C. *J. Am. Chem. Soc.* **2007**, *129*, 803–809.
67. Chalk, A J.; Harrod, J. F. *J. Am. Chem. Soc.* **1965**, *87*, 16–18.
68. Ojima, I.; Kogure, T.; Kumagai, M.; Horiuchi, S.; Sato, T. *J. Organomet. Chem.* **1976**, *122*, 83–97.
69. Stevens, E. S. *Green Plastics: An Introduction to the New Science of Biodegradable Plastics*; Princeton University Press: Princeton, **2002**.

-
70. de Espinosa, L. M.; Meier, M. A. R. *Eur. Polym. J.* **2011**, *47*, 837–852.
71. (a) Pan, X.; Webster, D. C. *Macromol. Rapid Commun.* **2011**, *32*, 1324–1330. (b) Pan, X.; Webster, D.C. *Chem. Sus. Chem.* 2012, *5*, 419–429.
72. (a) Tong, K.-H.; Wong, K.-Y.; Chan, T. H. *Org. Lett.* **2003**, *5*, 3423–3425. (b) Mello, R.; Alcalde-Aragonés, A.; González Núñez, M. E.; Asensio, G. *J. Org. Chem.* **2012**, *77*, 6409–6413. (c) Schroder, K.; Join, B.; Amali, A. J.; Junge, K.; Ribas, X.; Costas, M.; Beller, M. *Angew. Chem. Int. Ed.* **2011**, *50*, 1425–1429.
73. Jana, N. K.; Verkade, J. G. *Org. Lett.* **2003**, *5*, 3787–3790.

CHAPTER 2

SYNTHESIS OF CHIRAL C₂-SYMMETRIC BIMETALLIC ZINC COMPLEXES OF AMIDO-OXAZOLINATES AND THEIR APPLICATION IN COPOLYMERIZATION OF CO₂ AND CYCLOHEXENE OXIDE

2.1. Introduction

With the depletion of petroleum based feedstocks and environmental concerns, production of biodegradable polymers from renewable resources has attracted much attention.^[74] Carbon dioxide (CO₂) is one of the leading renewable carbon resources because it is abundant, inexpensive, non-toxic, and non-flammable.^[75] Significant efforts have been directed towards the catalytic alternating copolymerization of aliphatic epoxides with carbon dioxide that generates aliphatic polycarbonates with a wide array of applications.^[76] Many mono-metallic complexes have been studied as initiators for the copolymerization, particularly of cyclohexene oxide (CHO) and CO₂, including zinc,^[77] aluminum,^[78] chromium,^[79] cobalt,^[80] cadmium,^[81] rare-earth metals,^[82] M(IV) metals,^[83] and most recently copper,^[84] supported by various ligand frameworks.

One of the recurring themes in polycarbonate catalysis has been the introduction of bimetallic catalysts that could potentially exhibit cooperative effects between two metal centers.^[85,86] In particular, a number of zinc based dinuclear complexes have been reported for alternating copolymerization of CO₂ with CHO.^[85d-1] Early examples typically featured bridging M–X bonds (X = OAc, OMe, OPh, etc), such as a well-defined, phenoxide-

bridged dimeric zinc complex that produced copolymer from CHO/CO₂ with high molecular weight of up to 252,000 g/mol (Figure 10, **I**),^[87] and a moderately stereoselective chiral dimeric zinc catalyst that achieved up to 80% enantioselectivity in poly(cyclohexene carbonate) (PCHC) (Figure 10, **III**).^[88] Following the seminal work by Coates et al that demonstrated a synergistic bimetallic enchainment process was operative in the copolymerization of CO₂ with CHO catalyzed by alkoxide-bridged bimetallic β -diketiminato zinc complexes (Figure 10, **II**), dizinc complexes incorporating dinucleating ligands connected by different linkers have been subsequently reported (Figure 10, **IV-VII**). Examples includes a series of zinc anilido-aldimine complexes (**IV**) that are highly active for the generation of PCHC with TONs of 670–2980,^[85h,89] dinuclear zinc Aze-Phenol complexes (**VII**) bearing chiral groups,^[85f,g,90] dizinc complexes of bis(β -diketiminato) ligands that are linked by different rigid frameworks such as xanthane (**VI**),^[91] *meta*-phenylene (**V**), *para*-phenylene, and 2, 6-pyridylene moieties.^[92] It is worth noting that copolymerization of CHO/CO₂ with **V** was extremely fast, while *para*-phenylene bridged complexes were less active, and 2, 6-pyridylene connected complexes were completely inactive.⁹² Obviously the choice of an appropriate linker/spacer is indispensable to achieve the maximum synergetic/cooperative effect between two metal centers. More recently, macrocyclic ligands with two coordination sites have been introduced in the zinc-catalyzed copolymerization. These include the dizinc complexes supported by reduced Robson-type ligands (**VIII**, Figure 10) that are highly active for copolymerization at reduced CO₂ pressure of 1 atm,^[93] and dinuclear β -diketiminato-zinc complexes with a flexible tether (**IX**, Figure 10) that shows high activity (TOF up to 9130 h⁻¹ for **IX-a** where R₁ = R₂ = Me,

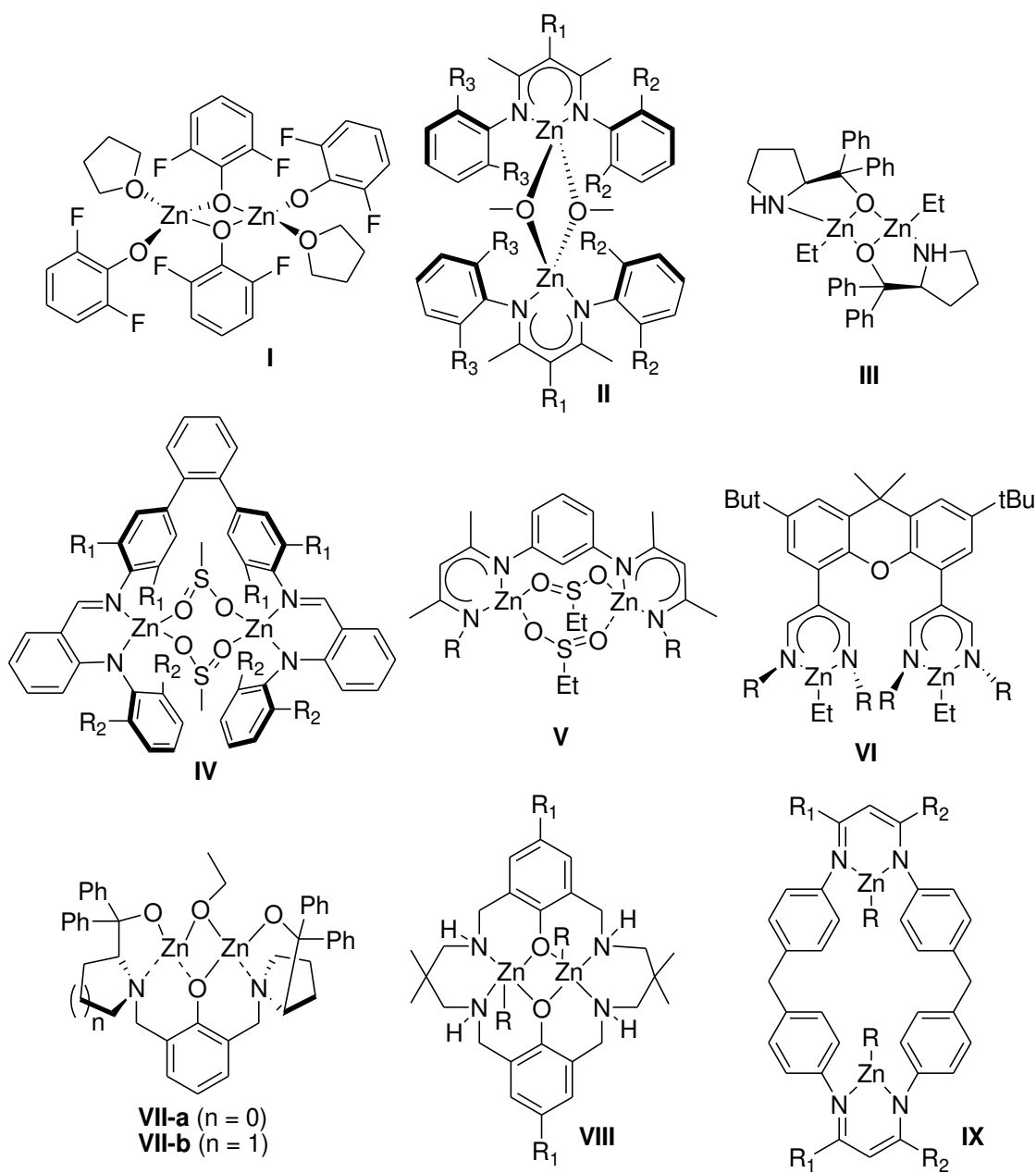


Figure 10. A set of dinuclear zinc complexes for CHO/CO₂ copolymerization.

and 155,000 h⁻¹ for **IX-b**, where R₁ = Ph, R₂ = CF₃).^[94] However, the stereoselectivity achieved by the zinc systems^[88] is lagging behind the cobalt and chromium-based catalysts. Because zinc is considered biocompatible and environmentally benign,^[94a] there is still strong interest in developing zinc-based catalysts with high activity and selectivity.

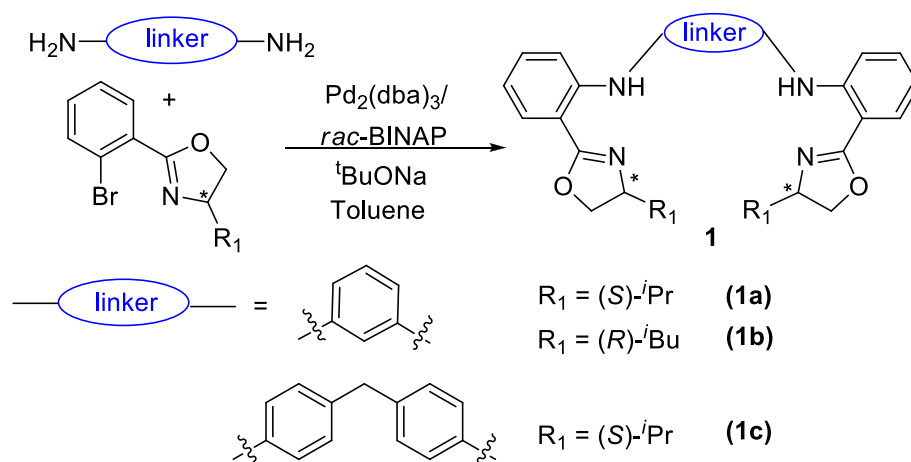
We have reported a series of mononuclear zinc complexes of chiral amido-oxazolate ligands for asymmetric alternating copolymerization of CO₂ and cyclohexene oxide, affording moderate isotactic PCHC with up to 90 % carbonate linkages. Since bimetallic complexes might have improved performances when compared to their mononuclear counterparts,^[85,86] we have sought to connect two bidentate amido-oxazolate chelating units with different linkers, affording a series of new binucleating ligands, and investigate the catalytic activity of the resulting dizinc complexes in CHO/CO₂ copolymerization. This also provides an opportunity to study the influence of rigidity of the linker on the efficiency of catalysts.

2.2. Results and discussion

2.2.1. Ligand design and synthesis

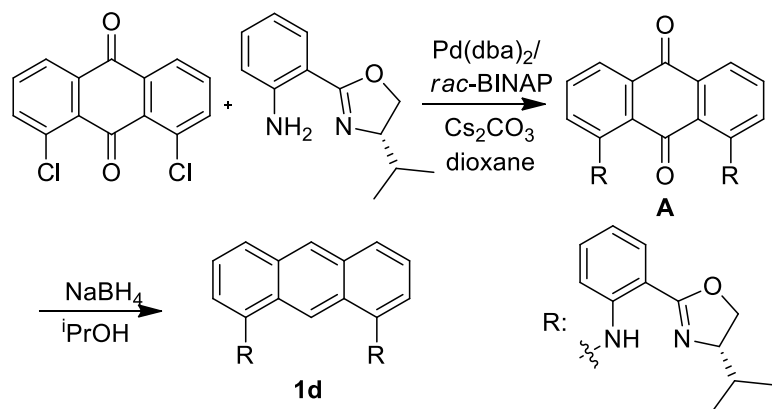
The structure of linkers has shown profound effect on the catalytic activity of bimetallic complexes in alternating copolymerization of CHO/CO₂.⁹² The linker in bimetallic complexes helps keep the two metal centers in an appropriate distance (3.70 Å to 6.10 Å) that facilitate cooperative interaction. Depending on the nature of the linkers, the two chelating systems can adopt different orientations, such as face-to-face (**IV** and **V**), in parallel (**VI**), and side-by-side (**VII** and **VIII** in Figure 10)^[85f,89,91,92,93] We initially selected three readily available diamines as linkers: *m*-phenylenediamine, 4-(4'-aminobenzyl)benzenamine, and 1,8-diaminoanthracene.^[95] It was envisioned that the ligand constructed with 1,8-diaminoanthracene linker provides the parallel arrangement while *m*-phenylenediamine incorporated ligand allows metal centers in a face-to-face orientation. The ligand with a more flexible linker, 4-(4'-aminobenzyl)benzenamine, may be amenable to either arrangement.

We have reported a family of bidentate amido-oxazolate ligands *via* modified Buchwald-Hartwig amination with the Pd(OAc)₂/BINAP system.^[96] The same protocol was first employed for the synthesis of dinucleating ligands, starting from bromophenyl substituted oxazolines and appropriate diamines; however, multiple products were obtained. To improve the yield and selectivity, the second-generation Buchwald-Hartwig catalytic system was employed.^[97] Thus, the coupling reactions were carried out using a combination of 3 mol% Pd₂(dba)₃, 6 mol% *rac*-BINAP and ^tBuONa in toluene at 120 °C (Scheme 4). The desired products **1a-1c** were obtained in high yields (85–90 %) after purification by column chromatography. The ¹H NMR spectra of **1a-1c** suggest the C₂-symmetry of these ligands, consistent with the ¹³C NMR spectra that have a single set of peaks. For instance, the ¹H NMR spectrum of **1a** has two up-field doublets (0.99 and 1.09 ppm), one septet (1.81 ppm), three resonances between 4–5 ppm, six peaks for aromatic protons at 6.80–7.85 ppm, corresponding to seven different protons with a total integration of 12, and a broad peak at 10.74 ppm for the –NH proton, consistent with the C₂-symmetric environment of the ligand. The resonance of the same –NH proton for the corresponding mono-nucleating amido-oxazolate ligands was typically around 9.00–10.0 ppm.^[76b] The two doublets in the up-field region indicate the non-equivalent nature of the methyl protons of the *iso*-propyl group. The ¹H NMR spectra of ligands **1b** and **1c** have similar features with **1a**. The distinction between two diastereotopic protons of –OCH₂ of the oxazoline ring was identified by ¹H-¹H COSY and HETCOR NMR spectroscopy. The coupling between two hydrogens and carbon (–OCH₂) can be observed on ¹H-DEPT-45 HETCOR NMR spectrum.



Scheme 4. Synthesis of dinucleating ligands **1a–c**.

When the above route was employed for the synthesis of ligand **1d** from 1,8-diaminoanthracene, formation of the C-N coupling product was very poor (~10%), despite of multiple attempts with different reaction conditions such as longer reaction times and excess amounts of catalyst and base. A copper(I) based catalytic system^[98] was also attempted without much improvement. We suspect that the low solubility of 1,8-diaminoanthracene in refluxing toluene might hamper the progress of the reaction. Inspired by a recent report on Pd(dba)₂-catalyzed diamination of 1,8-dichloroanthraquinones,^[99] we adopted an alternative synthetic route starting from 1,8-dichloroanthraquinone instead of 1,8-diaminoanthracene. Thus, the diamination of 1,8-dichloroanthraquinone was performed with 2-(*S*)-4,5-dihydro-4-isopropylloxazol-2-yl)benzenamine,^[100] giving the corresponding violet intermediate **A** in excellent yield (97 %) after purification by column chromatography (scheme 5). The characteristic –NH proton signal was observed in the low-field region of 12.05 ppm. Reduction of **A** with excess NaBH₄ in refluxing anhydrous 2-propanol^[101] yielded yellow compound **1d** in good yield (76 %).



Scheme 5. Synthesis of ligand **1d**.

In the ^1H NMR spectrum, two new sharp singlets appeared at 8.47 and 9.39 ppm, characteristic of protons at the 9 and 10 positions of the anthracene backbone. It is also noticed that the -NH proton and methine proton peaks in **1d** shifted to up-field in the ^1H NMR spectrum (11.58 ppm and 1.37 ppm respectively). The molecular structure of **1d** was determined by single-crystal X-ray diffraction techniques (Figure 11); the X-ray crystal data, data collection and refinement parameters are summarized in Appendix A.

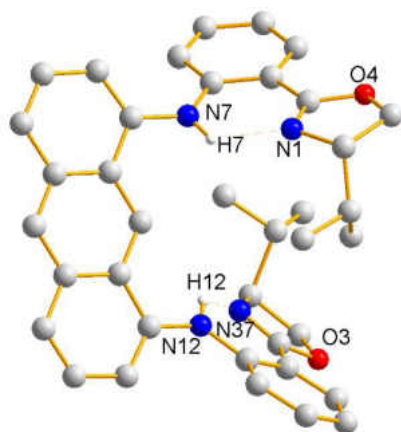


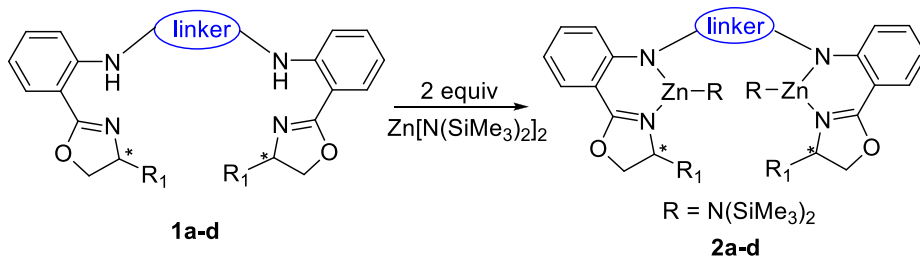
Figure 11. A ball and stick representation of complex **1d**. Hydrogen atoms, except when a hydrogen bond is present, are omitted for clarity.

The individual geometrical parameters of the amido-oxazoline moiety are very similar to mononucleating bidentate ligands.^[96b] The two NN-bidentate units adopt an anti parallel orientation and both are tilted from the plane of the anthracene linker, similar to

the arrangement of two coordinating units in compound **VI** (see Figure 10).^[91] Notably two isopropyl groups are oriented inward in spite of steric repulsion, perhaps due to crystal packing forces.

2.2.2. Synthesis of zinc complexes

The monomeric zinc complexes of bidentate amido-oxazolinato ligands have been prepared by reaction with $\text{Zn}[\text{N}(\text{SiMe}_3)_2]_2$.^[4b] With a similar procedure, dinucleating ligands (**1a-d**) were metallated with two equivalents of $\text{Zn}[\text{N}(\text{SiMe}_3)_2]_2$ in dry toluene at room temperature, affording the dizinc complexes (**2a-2d**) as yellow precipitates in excellent yields (Scheme 6). The disappearance of N–H signal of the ligand and the appearance of new broad peak for the 36 protons of the silylamido group in the up-field region at -0.04 ppm (**2a**), -0.03 ppm (**2b**), -0.17 ppm (**2c**) demonstrated the formation of expected complexes (**2a-2c**). For complex **2d**, two peaks that integrate to 18H each



Scheme 6. Synthesis of zinc complexes **2a-2d**.

appeared in the region of 0.25 and -0.30 ppm for the protons of $-\text{N}(\text{SiMe}_3)_2$ group, presumably due to the more restricted environment around the rigid anthracene backbone in **2d**. In all complexes, the resonances associated with the protons on the oxazoline ring shifted downfield in the ^1H NMR spectra. The same pattern of downfield shift was observed in the ^{13}C NMR spectroscopy as well. For instance, the signal for imine carbon in **2a** appeared at 169.45 ppm, in comparison to 163.00 ppm in **1a**. These observations support the coordination of the zinc metals to the nitrogen donors of ligands and revealed

that the C_2 symmetry of the ligands was retained upon the complex formation, at least in solution.

2.2.3. Copolymerization of CO₂ and CHO

We are interested in comparing the catalytic activity and selectivity of bimetallic complexes with their monometallic zinc analogues and probing the possible co-operative effect between the two metal centers in bimetallic complexes. In our previous report, we performed the alternating asymmetric copolymerization of CO₂ and CHO using monomeric zinc complexes of amido-oxazolinates at 500 psi of CO₂ and 75 °C, yielding poly(cyclohexene carbonate) with moderate isotacticity. Here the copolymerization reactions were carried out similar conditions with 0.5 mol% of catalyst loading,

Table 1. Screening the reaction conditions for copolymerization of CO₂ and CHO^[a]

entry	temp. (°C)	pressure (psi)	t/h	conv. (%) ^[b]	yield (%) ^[c]	M_n (kg/mol) ^[d]	M_w/M_n	carbonate linkages (%) ^[e]	ether linkages (%) ^[e]
1	75	500	20	72	30	10.6	1.4	78	22
2	50	100	48	72	41	8.6	1.4	37	63
3	100	500	20	84	17	305	1.5	3	97
4 ^[f]	75	500	20	54	25	4.5	1.3	71	29
5 ^[g]	75	500	24	60	28	148	1.6	8	92

[a] All the reactions were performed in neat CHO using catalyst **2a** unless otherwise mentioned. [b] Determined by ¹H NMR integration of methine protons (4.6 ppm for carbonate, 3.4 ppm for ether, and 3.1 ppm for CHO). Cyclic carbonates are not observed. [c] Isolated yields. [d] Determined by gel permeation chromatography calibrated with polystyrene standards in tetrahydrofuran. [e] Carbonate linkages were determined by the integration of the methine protons of PCHC at 4.6 ppm and ether linkages were determined by the integration of the methine protons of PCHE at 3.4 ppm. [f] ⁿBu₄NI (1 equiv. vs Zn) was added as cocatalyst. [g] Toluene (1:1 by volume relative to CHO) was used as solvent.

corresponding to 100 equiv of CHO per zinc (Table 1). Thus, **2a** generated the polymer with 78 % carbonate linkages, comparable with similar monomeric zinc complexes (~85 % polycarbonate linkage). The PCHC yielded by catalyst **2a** has molecular weight of 10.6 kg/mol and relatively narrow molecular weight distribution (M_w/M_n 1.4). However at reduced pressure and temperature, ether linkage became more prominent (entry **2**), and a

further increase in reaction temperature (100 °C) led to almost exclusive formation of polyethers (entry **3**).^[102,103] This behavior is quite similar to that observed in the case of monomeric zinc complexes of amido-oxazolate ligands. The combination of **2a** and a co-catalyst (ⁿBu₄NI) did not improve the content of carbonate linkages in the polymer backbone (entry **4**). To study the possible bimetallic effect in the present system, we also carried out the reaction under moderately dilute conditions, because such condition could lead to improved yields for CHO/CO₂ copolymers, given that the viscosity of the reaction mixture is decreased while the local concentration of active sites remains relatively high.^[92] However, dilution of the reaction mixture with toluene resulted in high percentage of ether linkages (entry **5**).^[102]

To investigate the influence of linker architecture in catalysis, complexes **2a–2d** were compared for alternating copolymerization of CHO and CO₂ under optimized conditions (Table 2). While complexes **2a** and **2c** showed good selectivity toward polycarbonate formation (carbonate linkages 78% for **2a** and 85% for **2c**), complexes **2b** and **2d** generated significant amounts of polyether linkage. Copolymerization with compound **2d** bearing a rigid 1,8-anthracene linker gave alternating copolymer with moderate (50%) carbonate linkages (Table 2, entry **4**), *M_n* of 7.8 kg/mol, and a narrow distribution (*M_w/M_n* 1.1). However, dilution of the reactants with toluene again led to preferred formation of polyether linkage (Table 2, entry **5**).

To facilitate the cooperative catalysis, the two zinc centers need to be in certain distances for the formation of bimetallic transition states.^[91,92] Unfortunately, no crystal structure was obtained for **2a–d**, despite of our repeated attempts. Nevertheless, the approximate distances between the two zinc centers can be estimated as in the order of **2a**,

2b < **2d** < **2c** on the basis of the nature of linkers. The observed activity and selectivity (see Table 2) painted a rather complicated picture. The flexible linker such as 4-(4'-aminobenzyl)benzenamine in compounds **IX** (see figure 1) has led to the highest reaction

Table 2. Asymmetric copolymerization of CO₂ and CHO with catalysts **2a-2d** and **3b**^[a]

entry	cat.	conv. (%) ^[b]	yield (%) ^[c]	M_n (kg/mol) ^[d]	M_w/M_n	carbonate linkage (%) ^[e]	ether linkage (%) ^[e]	m-centered tetrads ^[f]	SS/RR ^[g]
1	2a	72	30	10.6	1.4	78	22	75	48/52
2	2b	58	31	6.2	1.6	58	42	59	51/49
3	2c	39	12	8.6	5.0	85	15	61	50/50
4	2d	60	22	7.8	1.1	50	50	88	13/87
5	2d ^[h]	83	10	-	-	18	82	-	-
6	3b	83	72	39.8	2.1	6	94	-	-

[a] All the reactions were performed with [CHO]:[catalyst] = 100:1 at 500 psi of CO₂, 75 °C in neat CHO for 24 h. [b] Determined by ¹H NMR spectroscopy. [c] Isolated yields of polymeric products. [d] Determined by gel permeation chromatography calibrated with polystyrene standards in THF. [e] Carbonate linkages and ether linkages were determined by the relative intensity of methine protons of PCHC at 4.6 ppm and PCHE at 3.4 ppm, respectively. [f] Determined by ¹³C NMR spectroscopy in the carbonyl region (153–154 ppm). [g] Determined by chiral GC on 1,2-cyclohexane-diols after hydrolysis. [h] Reaction was performed in 1:1.2 CHO/toluene mixture (by volume).

rates for the copolymerization of CHO and CO₂,⁹⁴ but its presence in **2c** did not help as **2c** exhibited the lowest conversion among the series **2a–d**. Obviously, the macrocyclic structure in **IX** is also important in facilitating the catalysis. Despite featuring the same *meta*-phenylene linker, the selectivity of **2b** towards polycarbonates is substantially lower than **2a**. These results are in line with earlier observations both the distance and the orientation of active sites can greatly influences the formation of bimetallic transition states, thus the activity and selectivity of copolymerization.^[91,92]

The microstructure of the resulting PCHC was characterized by the ¹³C NMR spectroscopy, from which four prominent tetrad resonances ([*mmm*], [*mnr*], [*mrm*], and [*mrr*]) and two minor tetrad resonances ([*rrr*] and [*rmr*]) have been identified in the

carbonyl region (154.0-153.30 ppm).^[104] Thus, PCHC obtained from **2a** is moderately isotactic with 75% *m*-centered tetrads, slightly higher than that obtained with the monomeric analogues. Remarkably, the ¹³C NMR spectrum of PCHC generated by **2d** shows a dominant peak at 154.03 ppm corresponding to *m*-centered tetrads ([*mmm*] and [*mnr*]) and two small peaks at 153.49 and 153.40 ppm corresponding to *r*-centered tetrads ([*mrm*] and [*mrr*]) (Figure 12). This observation reveals that the obtained polycarbonate is highly isoenriched (86% *m*-centered tetrads), a result further corroborated by the almost negligible intensity of [*rr*] diads in the methylene region (29–30 ppm, 21–24 ppm).

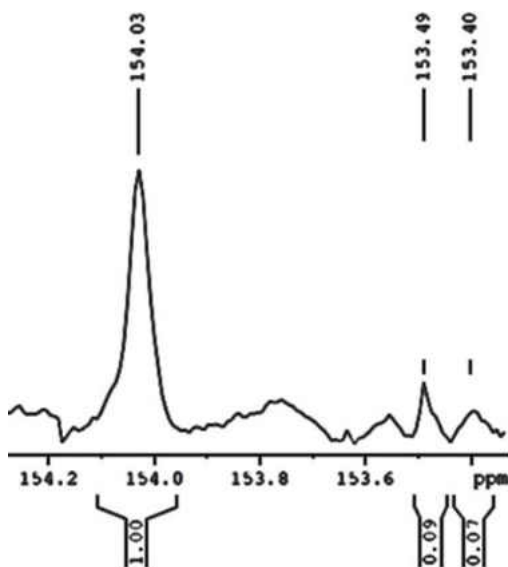
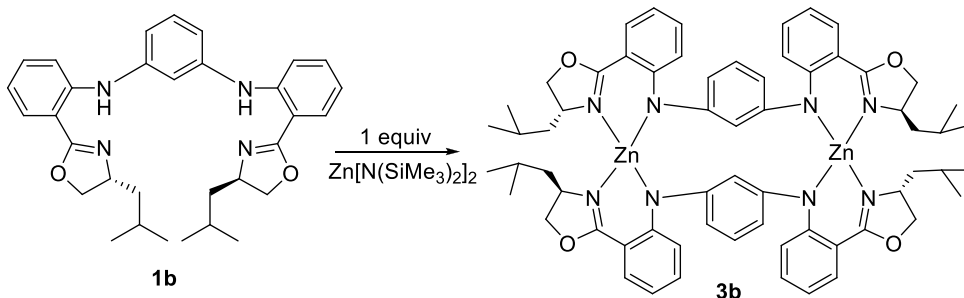


Figure 12. Carbonyl region of the ¹³C NMR spectrum of the poly(cyclohexene carbonate) generated by catalyst **2d**.

The stereoselectivity of the dinuclear catalysts were further evaluated by measuring the enantiomeric excess of 1,2-*trans*-cyclohexanediol produced from the alkaline hydrolysis of the copolymers. The measurements showed that chiral induction of catalyst **2a** was poor (*SS/RR*: 48/52), whereas catalyst **2d** showed good selectivity toward *R,R* configurations (*SS/RR*: 13/87) (Table 2). The sense of chiral induction is same as the mononuclear zinc catalysts, i.e. the *S* chiral center in the catalysts leads to preference in

opposite configuration in polycarbonates. Thus, dinuclear zinc complex **2d** was found to be more selective for the asymmetric alternating copolymerization of cyclohexene oxide and CO₂ than the monomeric counterparts. The high selectivity might be due to the involvement of intramolecular bimetallic pathway between the zinc metal centers in **2d**, or simply because of increased steric bulk of the rigid anthracene substituent.

To account for the observed differences among **2a–d** in selectivity, we further monitored the polymerization process by the NMR spectroscopy. Inspection of the ¹H NMR spectrum of the crude reaction mixture during the copolymerization with **2b** revealed **a**) a new set of signals in the regions of 3.50–4.50 and 6.00–7.80 ppm, **b**) different from that of complex **2b**, **c**) or the parent ligand **1b**. The new signals were assigned to a homoleptic dinuclear zinc complex **3b**, which was also prepared independently (Scheme 7). Treatment of ligand **1b** with exactly one equivalent of Zn[N(SiMe₃)₂]₂ in dry toluene at room temperature gave complex **3b**, which was isolated as a yellow solid in 76 % yield. The most notable feature is the absence of silylamide signals in the ¹H NMR spectrum, and two different sets of peaks were observed, indicating that two N,N-bidentate moieties in **3b** are in non-equivalent environment, in agreement with a tetrahedral arrangement around zinc. The structure of **3b** was confirmed by single-crystal X-ray diffraction analysis of crystals obtained from the reaction of **1b** and Zn[N(SiMe₃)₂]₂. The X-ray crystal data, data collection and refinement parameters are summarized in Appendix **B**. The structure of complex **3b** is depicted in Figure 13 with selected bond distances and bond angles. In agreement with the solution NMR data, **3b** is a dinuclear complex with two distorted tetrahedral zinc centers chelated by two equivalents of ligands, similar to the structure in the literature.^[92] The central linker aromatic rings are roughly parallel with each other. The



Scheme 7. Synthesis of zinc complex **3b**.

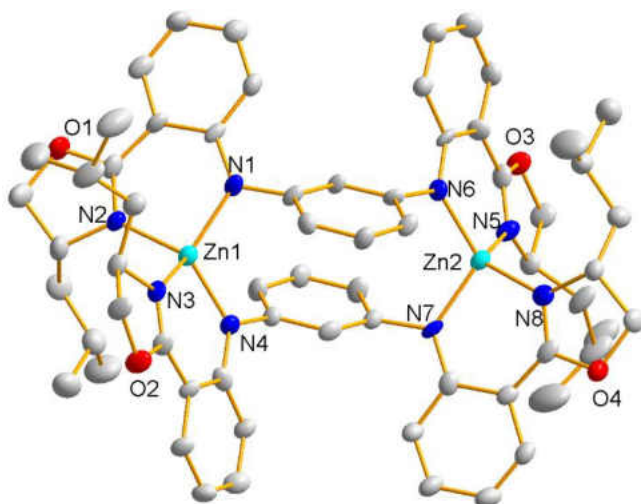


Figure 13. ORTEP drawing of complex **3b** with thermal ellipsoids drawn at the 50 % probability level. Selected bond distances (Å) and bond angles (°): Zn1–N1 1.957 (7), Zn1–N2 2.018 (8), Zn1–N3 1.998 (7), Zn1–N4 1.952 (7), Zn2–N5 2.002 (7), Zn2–N6 1.954 (7), Zn2–N7

bond distances around the metal centers are comparably longer than that in the mononuclear, three-coordinate analogues, a reflection of crowded environment here around the four-coordinate metal. The bond distance of Zn–N_{amido} (average 1.954 Å) is considerably shorter than that of Zn–N_{imino} (average 2.003 Å), which can be attributed to the stronger interaction with the anionic amido nitrogen. This difference (~0.05 Å) is similar with those mononuclear analogues and other unsymmetrical NN bidentate ligation.^[105]

Under catalytic conditions, the conversion of **2b** to **3b** turned out to be facile, within 30 min of reaction time. To further understand the nature of this conversion, a set of control experiments were performed in J. Young NMR tubes. When a solution of isolated complex **2b** in C₆D₆ (0.35 mL) was heated at 75 °C for 24 h, ¹H NMR analysis showed no formation of zinc complex **3b**. Addition of one equivalent of CHO led to no change after another 24 h of heating. In a separate experiment, after the introduction of ~1 atm of CO₂, the nearly quantitative conversion of **2b** to **3b** could be observed (along with a small amount of free ligand). Further introduction of one equivalent of CHO resulted in somewhat complicated spectrum that was not easily assignable. These observations indicate that the transformation from **2b** to **3b** might not be simply a ligand exchange reaction, and CO₂ is apparently involved in the process. In a possible reaction mechanism, CO₂ inserts into the Zn-N_{silyl} bond followed by the elimination of trimethylsilyl isocyanate. The generation of trimethylsilyl isocyanate was confirmed by the peak at 2280 cm⁻¹ in the FT-IR and the signal at -0.14 ppm in the ¹H NMR in C₆D₆.^[106] Ligand redistribution of the resulting zinc silyloxy furnishes the homoleptic **3b**. While the bis-chelating type zinc complexes such as **3b** were essentially inactive for copolymerization of CO₂ and CHO due to steric hindrance,^[107] **3b** can be active for the homopolymerization of CHO, as confirmed by experiments carried out with isolated **3b** under similar conditions (Table 2, entry 6). Experiments without CO₂ show diminished homopolymerization reactivity for CHO, suggesting CO₂ might be needed. Furthermore, the zinc containing byproduct, [Zn(OSiMe₃)₂]_n, an insoluble polymeric species,^[108] may serve as a catalyst for the homopolymerization of epoxide, leading to the formation of ether linkage in the polymer chain.

2.3. Conclusions

In summary, a series of new chiral bimetallic zinc complexes (**2a–2d**) has been synthesized *via* metathesis of C_2 -symmetric, dianionic, amido-oxazolate ligands (**1a–1d**) with $Zn[N(SiMe_3)_2]_2$ in dry toluene. The formation of these complexes was identified by different NMR spectroscopic techniques and elemental analysis. A homoleptic bis(amido-oxazolate) zinc complex, **3b**, was also synthesized to verify its catalytic activity for copolymerization of CO_2 and CHO. Although the transformation of bimetallic catalytic systems into bis-ligated complexes was observed, complexes **2a–2d** are shown to be viable initiators for copolymerization of CO_2 and CHO. Catalyst **2d**, with the two metal centers oriented parallel to each other, is moderately selective (yielding 50% polycarbonate content) and generates highly isotactic PCHC (86% *m*-centered tetrads). Future studies will be directed toward the improvement of analogous dinuclear catalysts and the mechanistic aspects of the copolymerization process.

2.4. Experimental section

General Procedures

All reactions involving air and/or moisture sensitive compounds were carried out using Schlenk line and glove box techniques. Toluene was distilled from Na/benzophenone. $CDCl_3$ and C_6D_6 were dried over CaH_2 and Na/benzophenone, respectively, and distilled and degassed prior to use. Isopropanol was distilled over activated Mg chunks under nitrogen and degasified three times before to use. Carbon dioxide (Airgas, high purity, 99.995%) was used as received. Cyclohexene oxide was distilled from CaH_2 following three freeze–pump–thaw cycles and stored in a glove box prior to use. Zinc bis(trimethylsilyl)amide was prepared according to the literature.

NMR spectra (^1H and ^{13}C) were recorded on a Bruker AVANCE-500 NMR spectrometer. Chiral GC analysis was carried out on an Agilent 7890 with FID detector using a chiral column (cyclodex-B, 30 m \times 0.25 mm \times 0.25 μm). The temperature program was as follows: injector temperature 250 $^\circ\text{C}$, detector 300 $^\circ\text{C}$, oven initial temperature 120 $^\circ\text{C}$, hold for 30 min, ramp at 30 $^\circ\text{C}/\text{min}$ to 200 $^\circ\text{C}$, hold for 10 min. Inlet flow: 85 mL/min (split mode, 68:1). Gel permeation chromatography (GPC) analysis was performed on a Varian Prostar, using a PLgel 5 μm Mixed-D column, a Prostar 355 RI detector, and THF as eluent at a flow rate of 1 mL/min (20 $^\circ\text{C}$). Polystyrene standards were used for calibration. The optical rotation was measured on a Jasco P-2000 polarimeter with 589 nm light source at 23 $^\circ\text{C}$.

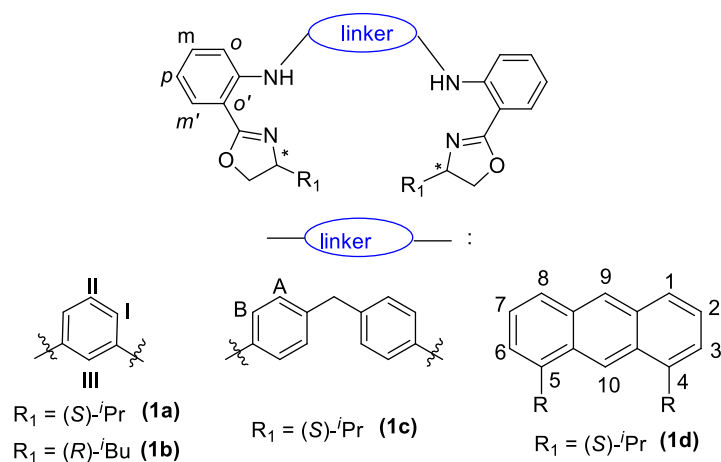


Chart 3. Schematic representation of protons of ligands **1a–d** for listing NMR data. (Similar protocol was used for listing the NMR data of the corresponding zinc complexes).

Synthesis of Ligand 1a. An oven dried round bottom flask was loaded with (*S*)-2-(2-bromophenyl)-4,5-dihydro-4-isoproploxazole (506 mg, 1.89 mmol), benzene-1,3-diamine (102 mg, 0.944 mmol), $\text{Pd}_2(\text{dba})_3$ (52 mg, 6.0 mol%), *rac*-BINAP (71 mg, 12 mol%), sodium *tert*-butoxide (363 mg, 3.77 mmol), and dry toluene (25 mL) in a glove box. The resulting solution was refluxed for 20 hr and reaction mixture was filtered through

a fritted funnel. The filtrate was concentrated and subjected to purification by silica gel chromatography (100:5 hexane/ethyl acetate) to afford the pure product as a yellow viscous liquid. Yellow-orange crystals were grown by slow evaporation of the diethylether solution of **1a** (401 mg, 88%). ^1H NMR (500.1 MHz; CDCl_3 ; 298 K, see the chart below for the labeling scheme): 0.99 (d, 6H, $J = 6.77$ Hz, $\text{CH}(\text{CH}_3)_2$), 1.09 (d, 6H, $J = 6.87$ Hz, $\text{CH}(\text{CH}_3)_2$), 1.81 (m, 2H, $\text{CH}(\text{CH}_3)_2$), 4.06 (t, 2H, $J = 8.18$ Hz, $\text{NCH}(\text{R})\text{CH}_2\text{O}$), 4.14 (m, 2H, $\text{NCH}(\text{R})\text{CH}_2\text{O}$), 4.40 (t, 2H, $J = 8.70$ Hz, $\text{NCH}(\text{R})\text{CH}_2\text{O}$), 6.80 (t, 2H, $J = 7.78$, *p-H*), 6.99 (d, 2H, $J = 8.18$ Hz, *I-H*), 7.23 (s, 1H, *III-H*), 7.35 (m, 3H, *m-H*, *II-H*), 7.52 (d, 2H, $J = 8.52$ Hz, *o-H*), 7.88 (d, 2H, $J = 8.69$ Hz, *m'-H*), 10.78 (br, 2H, NH). $^{13}\text{C}\{\text{H}\}$ NMR (125.8 MHz; CDCl_3 ; 298 K): 19.11 ((CH)*Me*₂), 19.28 ((CH)*Me*₂), 33.67 ((CH)*Me*₂), 69.50 (NCH(R)CH₂O), 73.23 (NCH(R)CH₂O), 110.80, 113.71, 113.86, 115.48, 117.33, 130.13, 130.22, 132.18 (CH_{arom}), 142.87, 145.59 (C_{quat}), 163.80 (C=N) (chart 3). HRMS (ESI-TOF) *m/z*: [M + H]⁺ Calcd for C₃₀H₃₅N₄O₂ 483.27; found 483.2714.

Synthesis of Ligand 1b. An oven dried round bottom flask was loaded with (*R*)-2-(2-bromophenyl)-4,5-dihydro-4-isobutyloxazole (120 mg, 0.425 mmol), benzene-1,3-diamine (23 mg, 0.21 mmol), Pd₂(dba)₃ (12 mg, 6.0 mol%), *rac*-BINAP (16 mg, 12 mol%), sodium *tert*-butoxide (82 mg, 0.85 mmol), and dry toluene (10 mL) in a glove box. The resulting solution was refluxed for 20 h and the reaction mixture was filtered through a fritted funnel. The filtrate was concentrated and subjected to purification by silica gel chromatography (100:5 hexanes/ethyl acetate) to afford the pure product as yellow viscous liquid (101 mg, 93%). ^1H NMR (500.1 MHz; CDCl_3 ; 298 K): 1.01 (d, 12H, $J = 5.36$ Hz, $\text{CH}_2\text{CH}(\text{CH}_3)_2$), 1.42 (m, 2H, $\text{CH}_2\text{CH}(\text{CH}_3)_2$), 1.68 (m, 2H, $\text{CH}_2\text{CH}(\text{CH}_3)_2$), 1.89 (m, 2H, $\text{CH}_2\text{CH}(\text{CH}_3)_2$), 3.90 (t, 2H, $J = 6.80$ Hz, $\text{NCH}(\text{R})\text{CH}_2\text{O}$), 4.43 (m, 4H, $\text{NCH}(\text{R})\text{CH}_2\text{O}$,

NCH(R)CH₂O), 6.76 (t, 2H, *J* = 7.37 Hz, *p*-H), 6.96 (d, 2H, *J* = 7.90, *l*-H), 7.17 (s, 1H, III-H), 7.29 (m, 3H, *m*-H, II-H), 7.41 (2H, d, *J* = 8.44 Hz, *o*-H), 7.80 (d, 2H, *J* = 7.89 Hz, *m*'-H), 10.58 (br, 2H, NH). ¹³C{H} NMR (125.8 MHz; CDCl₃; 298 K): 22.90 (CH₂CH(CH₃)₂), 23.21 (CH₂CH(CH₃)₂), 26.07(CH₂CH(CH₃)₂), 45.86 (CH₂CH(CH₃)₂), 65.36 (NCH(R)CH₂O), 71.73 (NCH(R)CH₂O), 110.77, 113.76, 114.22, 115.91, 117.25, 130.12 (CH_{arom}), 132.09, 142.79, 145.65 (C_{quat}), 163.68 (C=N). HRMS (ESI-TOF) *m/z*: [M + H]⁺ Calcd for C₃₂H₃₉N₄O₂ 511.30; found 511.2993.

Synthesis of Ligand 1c. An oven dried round bottom flask was loaded with (*R*)-2-(2-bromophenyl)-4,5-dihydro-4-isobutyloxazole (514 mg, 1.92 mmol), 4-(4-aminobenzyl)benzenamine (190 mg, 0.958 mmol), Pd₂(dba)₃ (53 mg, 6.0 mol%), rac-BINAP (72 mg, 12 mol%), sodium *tert*-butoxide (368 mg, 3.83 mmol), and dry toluene (26 mL) in a glove box. The resulting solution was refluxed for 20 hr and reaction mixture was filtered through a fritted funnel. The filtrate was concentrated and subjected to purification by silica gel chromatography (100:5 hexane/ethyl acetate) to afford the pure product as a yellow viscous liquid (480 mg, 87%). ¹H NMR (500.1 MHz; CDCl₃; 298 K): 0.91 (d, 6H, *J* = 6.71 Hz, CH(CH₃)₂), 0.96 (d, 6H, *J* = 6.62 Hz, CH(CH₃)₂), 1.81 (m, 2H, CH(CH₃)₂), 3.95 (s, 2H, -CH₂(C₆H₄)-), 4.03 (t, 2H, *J* = 8.07 Hz, NCH(R)CH₂O), 4.13 (m, 2H, NCH(R)CH₂O), 4.36 (t, 2H, *J* = 8.79 Hz, NCH(R)CH₂O), 6.73 (t, 2H, *J* = 7.44 Hz, *p*-H), 7.19 -7.26 (m, 10H, ArH), 7.32 (d, 2H, *J* = 8.44 Hz, *o*-H), 7.74 (d, 2H, *J* = 8.17 Hz, *m*'-H), 10.58 (br, 2H, NH). ¹³C{H} NMR (125.8 MHz; CDCl₃; 298 K): 18.98 ((CH)Me₂), 19.21 ((CH)Me₂), 31.78 ((CH)Me₂), 41.04 (CH₂(Ph)₂), 69.21 (NCH(R)CH₂O), 73.08 (NCH(R)CH₂O), 110.32, 113.19, 116.81, 122.13, 129.87, 130.11 (CH_{arom}), 132.07, 136.09, 139.70, 146.14 (C_{quat}),

163.82 (C=N). HRMS (ESI-TOF) m/z : $[M + H]^+$ Calcd for $C_{37}H_{41}N_4O_2$ 573.32; found 573.2993.

Synthesis of Ligand 1d. The precursor, 1,8-bis(2-(4,5-dihydro-4-isopropylloxazol-2-yl)phenylamino) anthracene -9,10-dione (**A**), was synthesized as follows: an oven dried Schlenk flask was loaded with 1,8-dichloroanthracene-9,10-dione (68 mg, 0.24 mmol), 2-(*S*)-4,5-dihydro-4-isopropylloxazol-2-yl)benzenamine (150 mg, 0.733 mmol), $Pd(dba)_2$ (11 mg, 8.0 mol%), *rac*-BINAP (18 mg, 12 mol%), Cs_2CO_3 (239 mg, 0.733 mmol), and freshly dried 1,4-dioxane (10 mL) in a glove box. After the reaction mixture was refluxed for 48 hr, the resulting solution was filtered and the filtrate was concentrated. The violet residue was purified by column chromatography (100:10 hexane/ethyl acetate) to give a violet product (145 mg, 97%). 1H NMR (500.1 MHz; $CDCl_3$; 298 K): 0.73 (d, 6H, $J = 6.84$ Hz, $CH(CH_3)_2$), 0.84 (d, 6H, $J = 6.66$ Hz, $CH(CH_3)_2$), 1.61 (m, 2H, $CH(CH_3)_2$), 4.00 (m, 2H, $NCH(R)CH_2O$), 4.12 (t, 2H, $J = 4.12$ Hz, $NCH(R)CH_2O$), 4.30 (t, 2H, $J = 8.37$ Hz, $NCH(R)CH_2O$), 7.07 (t, 2H, $J = 7.51$ Hz, *p*-H), 7.39 (t, 2H, $J = 8.18$ Hz, *m*-H), 7.47 (t, 2H, $J = 7.75$ Hz, 7-*ArH*, 2-*ArH*), 7.54 (d, 2H, $J = 8.32$ Hz, *o*-H), 7.73 (d, 2H, $J = 8.58$ Hz, 6-*ArH*, 3-*ArH*), 7.83 (d, 2H, $J = 7.36$ Hz, 8-*ArH*, 1-*ArH*), 7.89 (d, 2H, $J = 8.06$ Hz, *m'*-H), 12.05 (br, 2H, *NH*).

To a solution of 1,8-bis(2-(4,5-dihydro-4-isopropylloxazol-2-yl)phenylamino) anthracene-9,10-dione (96 mg, 0.16 mmol) (**A**) in freshly distilled isopropanol (10 mL), excess sodium borohydride (310 mg, 8.17 mmol) was added under nitrogen gas. The reaction progress was monitored with TLC (10:2 hexane/ethyl acetate). The mixture was refluxed for 12 h and transformed into a beaker containing ice water. The solution was treated with 12 N HCl at 0 °C until the pH of the solution was ~7 and the resulting solution was extracted

with CH₂Cl₂. The organic phase was washed with water and dried over MgSO₄. The volatiles were removed by rotavapor and the residue was purified by column chromatography (100:2 hexane/ethyl acetate system) to afford the yellow colored product **1d** (74 mg, 76 %). ¹H NMR (500.1 MHz; CDCl₃; 298 K): 0.52 (d, 6H, *J* = 6.83 Hz, CH(CH₃)₂), 0.53 (d, 6H, *J* = 6.53 Hz, CH(CH₃)₂), 1.37 (m, 2H, CH(CH₃)₂), 3.70 (m, 2H, NCH(R)CH₂O), 3.88 (t, 2H, *J* = 8.81 Hz, NCH(R)CH₂O), 4.32 (t, 2H, *J* = 8.50 Hz, NCH(R)CH₂O), 6.80 (t, 2H, *J* = 7.65 Hz, *p*-H), 7.33 (t, 1H, *J* = 8.21, *m*-H), 7.48 (t, 2H, *J* = 7.75 Hz, 7-ArH, 2-ArH), 7.64 (2H, d, *J* = 7.06 Hz, ArH), 7.67 (2H, d, *J* = 8.47 Hz, *o*-H), 7.76 (d, 2H, *J* = 8.73 Hz, ArH), 7.87 (d, 2H, *J* = 7.86 Hz, *m*'-H), 8.47 (s, 1H, 9-H), 9.39 (s, 1H, 10-H), 11.58 (br, 2H, NH). ¹³C{¹H} NMR (125.8 MHz; CDCl₃; 298 K): 18.79 ((CH)Me₂), 19.00 ((CH)Me₂), 33.43 ((CH)Me₂), 69.70 (NCH(R)CH₂O), 73.10 (NCH(R)CH₂O), 110.98, 113.41, 115.13, 116.34, 117.13, 122.88, 125.69, 127.04, 127.80 (CH_{arom}), 129.94, 132.16, 133.40, 138.08, 146.30 (C_{quat}), 163.72 (C=N). HRMS (ESI-TOF) *m/z*: [M + H]⁺ Calcd for C₃₈H₃₉N₄O₂ 583.30; found 583.3107.

Synthesis of Zinc Complex 2a. An oven dried Schlenk flask was loaded with ligand **1a** (150 mg, 0.311 mmol) and Zn[N(SiMe₃)₂] (0.250 ml, 0.622 mmol) in toluene (4 mL) in a glove box and the resulting yellow solution was stirred for 1 hr at room temperature. After the volatiles were removed *in vacuo*, the resultant residue was taken up with hexanes and passed through a pad of pre-dried celite 545. Removal of solvents afforded the product as a yellow powder. Yield: 225 mg (78%). ¹H NMR (500.1 MHz; CDCl₃; 298 K): -0.04 (br, 36H, N(Si(Me)₃)₂), 0.85 (d, 6H, *J* = 6.73 Hz, CH(CH₃)₂), 1.0 (d, 6H, *J* = 7.15 Hz, CH(CH₃)₂), 2.51 (m, 2H, CH(CH₃)₂), 4.38 (t, 2H, *J* = 7.16 Hz, NCH(R)CH₂O), 4.42 (t, 2H, *J* = 8.86 Hz, NCH(R)CH₂O), 4.51 (m, 2H, NCH(R)CH₂O), 6.44 (t, 2H, *J* = 7.61 Hz, *p*-H),

6.88 (br, 4H, *o*-H, I-H), 7.09 (t, 2H, $J = 8.34$ Hz, *m*-H), 7.28 (s, 1H, III-H), 7.41 (t, 1H, $J = 7.92$ Hz, II-H), 7.77 (d, 2H, $J = 8.18$ Hz, *m*'-H). $^{13}\text{C}\{\text{H}\}$ NMR (125.8 MHz; CDCl_3 ; 298 K): 5.10 (N(SiMe₃)₂), 14.67 ((CH)Me₂), 19.35 ((CH)Me₂), 30.80 ((CH)Me₂), 66.35 (NCH(R)CH₂O), 69.31 (NCH(R)CH₂O), 104.26, 113.24, 117.86, 122.66, 125.54, 128.47, 129.27 (CH_{arom}), 131.31, 134.00, 157.98 (C_{quat}), 169.45 (C=N). Anal. Calcd. for C₄₂H₆₈N₆O₂Si₄Zn₂.C₇H₈: C, 57.45; H, 7.48; N, 8.20. Found: C, 57.03; H, 6.93; N, 8.33.

Synthesis of Zinc Complex 2b. Complex **2b** was synthesized according to the same procedure as described for **2a**. Ligand **1b** (217 mg, 0.425 mmol), Zn[N(SiMe₃)₂]₂ (0.340 mL, 0.850 mmol), and toluene (10 mL) were used. The product was obtained as yellow powder (347 mg, 85%). ^1H NMR (500.1 MHz; CDCl_3 ; 298 K): -0.03 (br, 36H, N(Si(Me)₃)₂), 1.03 (d, 12H, $J = 7.03$ Hz, CH₂CH(CH₃)₂), 1.51 (m, 2H, CH₂CH(CH₃)₂), 1.68 (m, 2H, CH₂CH(CH₃)₂), 2.31 (m, 2H, CH₂CH(CH₃)₂), 4.15 (t, 2H, $J = 8.38$ Hz, NCH(R)CH₂O), 4.53 (m, 2H, NCH(R)CH₂O), 4.64 (t, 2H, $J = 8.98$ Hz, NCH(R)CH₂O), 6.43 (t, 2H, $J = 7.58$ Hz, *p*-H), 6.88 (br, 4H, *o*-H, I-H), 7.08 (t, 2H, $J = 7.61$ Hz, *m*-H), 7.28 (s, 1H, III-H), 7.40 (t, 1H, $J = 7.92$ Hz, II-H), 7.77 (d, 2H, $J = 8.07$ Hz, *m*'-H). $^{13}\text{C}\{\text{H}\}$ NMR (125.8 MHz; CDCl_3 ; 298 K): 5.18 (N(SiMe₃)₂), 21.93 (CH₂CH(CH₃)₂), 24.0 (CH₂CH(CH₃)₂), 25.94 (CH₂CH(CH₃)₂), 45.32 (CH₂CH(CH₃)₂), 63.64 (NCH(R)CH₂O), 71.81 (NCH(R)CH₂O), 104.51, 113.28, 117.90, 118.02, 122.54, 123.81 (CH_{arom}), 131.39, 133.39, 157.86 (C_{quat}), 169.38 (C=N). Anal. Calcd. for C₄₄H₇₂N₆O₂Si₄Zn₂: C, 55.04; H, 7.56; N, 8.75. Found: C, 54.79; H, 7.51; N, 8.65.

Synthesis of Zinc Complex 2c. Complex **2c** was synthesized similarly as **2a**: Ligand **1c** (88.0 mg, 0.153 mmol), Zn[N(SiMe₃)₂]₂ (0.130 mL, 0.307 mmol), and toluene (4 mL) were used. The product was isolated as yellow powder (128 mg, 82%). ^1H NMR (500.1 MHz;

CDCl₃; 298 K): -0.23 (br, 36H, N(Si(*Me*)₃)₂), 0.89 (d, 6H, *J* = 6.75 Hz, CH(CH₃)₂), 1.03 (d, 6H, *J* = 7.11 Hz, CH(CH₃)₂), 2.48 (m, 2H, CH(CH₃)₂), 4.04 (s, 2H, CH₂(Ph)₂), 4.37 (t, 2H, *J* = 6.91 Hz, NCH(R)CH₂O), 4.43 (t, 2H, *J* = 8.75 Hz, NCH(R)CH₂O), 4.51 (m, 2H, NCH(R)CH₂O), 6.41 (t, 2H, *J* = 7.34 Hz, *p*-H), 6.75 (d, 2H, *J* = 8.80 Hz, *o*-H), 6.96 (t, 4H, *J* = 8.07 Hz, ArH), 7.07 (t, 2H, *J* = 7.98 Hz, *m*-H), 7.14 (m, 4H, ArH), 7.80 (d, 2H, *J* = 8.25 Hz, *m'*-H). ¹³C{H} NMR (125.8 MHz; CDCl₃; 298 K): 4.93 (N(SiMe₃)₂), 14.89 ((CH)Me₂), 19.45 ((CH)Me₂), 30.89 ((CH)Me₂), 41.08 (CH₂(Ph)₂), 67.87 (NCH(R)CH₂O), 69.76 (NCH(R)CH₂O), 104.24, 113.19, 117.28, 125.54, 126.77, 130.48 (CH_{arom}), 131.52, 134.11, 148.24, 157.35 (C_{quat}), 168.10 (C=N). Anal. Calcd. for C₄₉H₇₄N₆O₂Si₄Zn₂: C, 57.57; H, 7.30; N, 8.22. Found: C, 57.51; H, 7.22; N, 8.18.

Synthesis of Zinc Complex 2d. This complex was prepared according to the procedure described for complex **2a**. Ligand **1d** (19.0 mg, 0.033 mmol), Zn[N(SiMe₃)₂]₂ (0.027 mL, 0.066 mmol), and toluene (3 mL) were used and **2d** was obtained as a yellow powder (30 mg, 87%). ¹H NMR (500.1 MHz; C₆D₆; 298 K): -0.30 (br, 18H, N(Si(*Me*)₃)₂), 0.29 (s, 18H, N(Si(*Me*)₃)₂), 0.67 (d, 12H, *J* = 6.83 Hz, CH(CH₃)₂), 2.45 (m, 2H, CH(CH₃)₂), 3.90 (t, 2H, *J* = 7.84 Hz, NCH(R)CH₂O), 4.04 (t, 2H, *J* = 9.27 Hz, NCH(R)CH₂O), 4.19 (m, 2H, NCH(R)CH₂O), 6.20 (t, 2H, *J* = 7.17 Hz, *p*-H), 6.67 (d, 2H, *J* = 8.75 Hz, ArH), 6.82 (t, 2H, *J* = 7.10 Hz, ArH), 7.40 (d, 2H, *J* = 6.67 Hz, ArH), 7.44 (t, 2H, *J* = 8.53 Hz, ArH), 7.73 (d, 2H, *J* = 8.43 Hz, ArH), 7.83 (d, 2H, *J* = 8.52 Hz, ArH), 8.31 (s, 2H, ArH). ¹³C{H} NMR (125.8 MHz; C₆D₆; 298 K): 5.47 (N(SiMe₃)₂), 14.41 ((CH)Me₂), 19.04 ((CH)Me₂), 30.41 ((CH)Me₂), 65.93 (NCH(R)CH₂O), 69.32 (NCH(R)CH₂O), 103.75, 112.31, 119.68, 121.02, 121.91, 125.44, 126.28, 128.58, 128.62 (CH_{arom}), 130.68, 133.79, 134.74, 146.90,

158.78 (Cquat), 169.50 (C=N). Anal. Calcd. for C₅₀H₇₂N₆O₂Si₄Zn₂: C, 58.18; H, 7.03; N, 8.14. Found: C, 57.76; H, 7.01; N, 8.16.

Synthesis of Zinc Complex 3b. A solution of ligand **1b** (180 mg, 0.352 mmol) and Zn[N(SiMe₃)₂]₂ (0.140 mL, 0.360 mmol) in dry toluene was stirred for 8 h at RT. All volatiles were removed *in vacuo* to afford a yellow solid (153 mg, 76%). ¹H NMR (500.1 MHz; CDCl₃; 298 K): 0.58 (d, 6H, *J* = 6.23, CH₂CH(CH₃)₂), 0.65 (d, 6H, *J* = 6.23, CH₂CH(CH₃)₂), 0.94 (br, 1H, CH₂CH(CH₃)₂), 1.29 (br, 1H, CH₂CH(CH₃)₂), 1.39 (br, 1H, CH₂CH(CH₃)₂), 1.63 (br, 2H, CH₂CH(CH₃)₂), 1.86 (br, 1H, CH₂CH(CH₃)₂), 3.85 (t, 1H, *J* = 9.11, NCH(R)CH₂O), 3.91 (t, 1H, *J* = 8.81, NCH(R)CH₂O), 4.11 (br, 1H, NCH(R)CH₂O), 4.38 (br, 1H, NCH(R)CH₂O), 4.53 (t, 1H, *J* = 8.64, NCH(R)CH₂O), 4.59 (t, 1H, *J* = 8.39, NCH(R)CH₂O), 6.05 (m, 1H, ArH), 6.14 (br, 3H, ArH), 6.27 (m, 1H, ArH), 6.73 (d, 1H, *J* = 8.96, ArH), 6.80 (d, 1H, *J* = 8.97, ArH), 6.89 (m, 3H, ArH), 7.59 (t, 2H, *J* = 8.90, ArH). ¹³C{¹H} NMR (125.8 MHz; CDCl₃; 298 K): 22.47, 22.49, 22.56, 22.66, 25.52, 25.72, 45.45, 45.54, 63.47, 63.98, 71.78, 72.71, 104.39, 104.97, 117.71, 118.09, 118.94, 119.08, 122.75, 125.53, 128.46, 129.29 (CH_{arom}), 129.88, 131.18, 133.04, 138.10, 158.12, 158.32 (Cquat), 168.35, 168.42 (C=N). Anal. Calcd. for C₃₂H₃₆N₄O₂Zn·CH₂Cl₂: C, 60.14; H, 5.81; N, 8.50. Found: C, 60.18; H, 5.81; N, 8.52.

Copolymerization of Cyclohexene Oxide/CO₂. In a glovebox, a 60 mL oven dried Teflon-lined Parr high-pressure reactor vessel was loaded with catalyst (1 mol%) and CHO (1 equiv). The vessel was loaded in the Parr reactor head and sealed tightly, and taken out of the glove box. The Parr reactor vessel was brought to desired temperature and CO₂ pressure. After the reaction mixture was treated with given conditions, it was allowed to cool to room temperature and a small fraction of the reaction mixture was taken for ¹H

NMR spectroscopy. The polymerization mixture was transferred into a round-bottom flask with CH₂Cl₂ (3–6 mL) and the polymer was precipitated from addition of methanol (15–30 mL). After separation, the polymer was dried in vacuo to constant weight to determine the yield. Molecular weight (M_n) and molecular weight distributions were determined by GPC using polystyrene standards.

Hydrolysis of Polymers and Chiral GC Analysis. In a general procedure, a small round-bottom flask was charged with polycarbonate (1 eq) and NaOH (2.1 eq) in MeOH (4–6 mL). The mixture was refluxed for 4 h and then neutralized with HCl (aq) (1 M). The crude mixture was then extracted with ether. After drying over anhydrous MgSO₄, a small aliquot was injected into a GC equipped with a Cyclodex-B column to determine the enantiomeric excess of the 1,2-*trans*-cyclohexanediol (t_R = 12.43 min for (*S,S*)-1,2-*trans* cyclohexanediol, t_R = 12.74 min for (*R,R*)-1,2-*trans* cyclohexanediol). Temperature program: initial temperature 110 °C for 30 min, temperature ramp: 30 °C/min, final temperature: 210 °C for 5 min.

X-ray Crystallography. Data for compounds **1d** and **3b** were collected on a Bruker APEX-II CCD diffractometer. The intensity data were corrected for absorption and decay (SADABS).¹⁰⁹ The data were integrated with SAINT¹¹⁰ and the structure was solved and refined using SHELXTL.¹¹¹ The factors for the determination of the absolute structure were refined according established procedures.¹¹² The data was mentioned in Appendices A and B.

2.5. References

74. a) J.-M. Raquez, Y. Habibi, M. Murariu, P. Dubois, *Prog. Polym. Sci.* **2013**, *38*, 1504–1542; b) K. Yao, C. Tang, *Macromolecules* **2013**, *46*, 1689–1712; c) S. A. Miller, *ACS Macro Lett.* **2013**, *2*, 550–554; d) M. J.-L. Tschan, E. Brule, P. Haquette, C. M. Thomas, *Polym. Chem.* **2012**, *3*, 836–851; e) K. Yao, J. Wang, W. Zhang, J. S. Lee, C. Wang, F. Chu, X. He, C. Tang, *Biomacromolecules* **2011**, *12*, 2171–2177; f) C. Robert, F. De Montigny, C. M. Thomas, *Nature Commun.* **2011**, *2*, 586–591; g) S. Klaus, S. I. Vagin, M. W. Lehenmeier, P. Deglmann, A. K. Brym, B. Rieger, *Macromolecules* **2011**, *44*, 9508–9516; h) L. Yu, *Biodegradable Polymer Blends and Composites from Renewable Resources*; John Wiley & Sons: Hoboken, New Jersey, USA, **2009**.
75. a) O. Vechorkin, N. Hirt, X. Hu, *Org. Lett.* **2010**, *12*, 3567–3569; b) T. Sakakura, K. Kohno, *Chem. Commun.* **2009**, 1312–1330; c) T. Sakakura, J.-C. Choi, H. Yasuda, *Chem. Rev.* **2007**, *107*, 2365–2387; d) M. Aresta, A. Dibenedetto, *Dalton Trans.* **2007**, 2975–2992.
76. a) K. Nakano, K. Kobayashi, T. Ohkawara, H. Imoto, K. Nozaki, *J. Am. Chem. Soc.* **2013**, *135*, 8456–8459; b) J. Geschwind, H. Frey, *Macromolecules* **2013**, *46*, 3280–3287; c) G. A. Luinstra, E. Borchardt, *Adv. Polym. Sci.* **2012**, *245*, 29–48; d) X.-B. Lu, D. J. Darensbourg, *Chem. Soc. Rev.* **2012**, *41*, 1462–1484; e) M. R. Kember, A. Buchard, C. K. Williams, *Chem. Commun.* **2011**, *47*, 141–163; f) S. Klaus, M. W. Lehenmeier, C. E. Anderson, B. Rieger, *Coord. Chem. Rev.* **2011**, *255*, 1460–1479; g) D. J. Darensbourg, *Inorg. Chem.* **2010**, *49*, 10765–10780; h) Y. Qin, X. Wang, *Biotechnol. J.* **2010**, *5*, 1164–1180; i) D. J. Darensbourg, *Chem. Rev.* **2007**, *107*, 2388–2410; j) G. W. Coates, D. R. Moore, *Angew. Chem. Int. Ed.* **2004**, *43*, 6618–6639; k) D. J. Darensbourg, R. M. Mackiewicz, A. L. Phelps, D. R. Billodeaux, *Acc. Chem. Res.* **2004**, *37*, 836–844; l) K. Nakano, N. Kosaka, T. Hiyama, K. Nozaki, *Dalton Trans.* **2003**, 4039–4050.
77. a) W. C. Ellis, Y. Jung, M. Mulzer, R. Di Girolamo, E. B. Lobkovsky, G. W. Coates, *Chem. Sci.* **2014**, *5*, 4004–4011; b) S. Abbina, G. Du, *Organometallics* **2012**, *31*, 7394–7403; c) K. L. Orchard, J. E. Harris, A. J. P. White, M. S. P. Shaffer, C. K. Williams, *Organometallics* **2011**, *30*, 2223–2229; d) M. Cheng, E. B. Lobkovsky, G. W. Coates, *J. Am. Chem. Soc.* **1998**, *120*, 11018–11019; e) M. Cheng, D. R. Moore, J. J. Reczek, B. M. Chamberlain, E. B. Lobkovsky, G. W. Coates, *J. Am. Chem. Soc.* **2001**, *123*, 8738–8749; f) S. D. Allen, D. R. Moore, E. B. Lobkovsky, G. W. Coates, *J. Am. Chem. Soc.* **2002**, *124*, 14284–14285; g) N. M. Rajendran, A. Haleel, N. D. Reddy, *Organometallics* **2014**, *33*, 217–224; h) D. R. Moore, M. Cheng, E. B. Lobkovsky, G. W. Coates, *J. Am. Chem. Soc.* **2003**, *125*, 11911–11924; i) C. M. Byrne, S. D. Allen, E. B. Lobkovsky, G. W. Coates, *J. Am. Chem. Soc.* **2004**, *126*, 11404–11405; j) S. Inoue, H. Koinuma, T. Tsuruta, *J. Polym. Sci. Part B* **1969**, *7*, 287–292; k) S. Inoue, H. Koinuma, T. Tsuruta, *Makromol. Chem.* **1969**, *130*, 210–220.
78. a) N. Ikpo, J. C. Flogeras, F. M. Kerton, *Dalton Trans.* **2013**, *42*, 8998–9006 and references therein; b) T. A. Zevaco, A. Janssen, J. Sypien, E. Dinjus, *Green Chem.* **2005**,

7, 659–666; c) D. J. Darensbourg, D. R. Billodeaux, *Inorg. Chem.* **2005**, *44*, 1433–1442; d) M. H. Chisholm, Z. Zhou, *J. Am. Chem. Soc.* **2004**, *126*, 11030–11039.

79. a) K. Nakano, M. Nakamura, K. Nozaki, *Macromolecules* **2009**, *42*, 6972–6980; b) D. J. Darensbourg, M. Ulusoy, O. Karroonnirum, R. R. Poland, J. H. Reibenspies, B. Çetinkaya, *Macromolecules* **2009**, *42*, 6992–6980; c) D. J. Darensbourg, S. B. Fitch, *Inorg. Chem.* **2009**, *48*, 8668–8677; d) D. J. Darensbourg, R. M. Mackiewicz, *J. Am. Chem. Soc.* **2005**, *127*, 14026–14038; e) D. J. Darensbourg, R. M. Mackiewicz, J. L. Rodgers, C. C. Fang, D. R. Billodeaux, J. H. Reibenspies, *Inorg. Chem.* **2004**, *43*, 6024–6034; f) D. J. Darensbourg, J. C. Yarbrough, C. Ortiz, C. C. Fang, *J. Am. Chem. Soc.* **2003**, *125*, 7586–7591; g) D. J. Darensbourg, J. C. Yarbrough, *J. Am. Chem. Soc.* **2002**, *124*, 6335–6342; h) W. J. Kruper, D. V. Dellar, *J. Org. Chem.* **1995**, *60*, 725–727.

80. a) J. Liu, W.-M. Ren, Y. Liu, X.-B. Lu, *Macromolecules* **2013**, *46*, 1343–1349; b) G.-P. Wu, W.-M. Ren, Y. Luo, B. Li, W.-Z. Zhang, X.-B. Lu, *J. Am. Chem. Soc.* **2012**, *134*, 5682–5688; c) W.-M. Ren, X. Zhang, Y. Liu, J.-F. Li, H. Wang, X.-B. Lu, *Macromolecules* **2010**, *43*, 1396–1402; d) W. M. Ren, Z. W. Liu, Y. Q. Wen, R. Zhang, X.-B. Lu, *J. Am. Chem. Soc.* **2009**, *131*, 11509–11518; e) H. Sugimoto, K. Kuroda, *Macromolecules* **2008**, *41*, 312–317; f) X.-B. Lu, Y. Wang, *Angew. Chem. Int. Ed.* **2004**, *43*, 3574–3577; g) Z. Qin, C. M. Thomas, S. Lee, G. W. Coates, *Angew. Chem. Int. Ed.* **2003**, *42*, 5484–5487.

81. a) D. J. Darensbourg, J. R. Wildeson, S. J. Lewis, J. C. Yarbrough, *J. Am. Chem. Soc.* **2002**, *124*, 7075–7083; b) D. J. Darensbourg, S. A. Niezgoda, J. D. Draper, J. H. Reibenspies, *J. Am. Chem. Soc.* **1998**, *120*, 4690–4698.

82. a) Z. Zhang, D. Cui, X. Liu, *J. Polym. Sci. Part A: Polym. Chem.* **2008**, *46*, 6810–6818; b) D. V. Vitanova, F. Hampel, K. C. Hultzsich, *J. Organomet. Chem.* **2005**, *690*, 5182–5197; c) D. Cui, M. Nishiura, Z. Hou, *Macromolecules* **2005**, *38*, 4089–4095; d) H. Sugimoto, H. Ohshima, S. Inoue, *J. Polym. Sci. Part A: Polym. Chem.* **2003**, *41*, 3549–3555.

83. a) C. C. Quadri, E. L. Roux, *Dalton Trans.* **2014**, *43*, 4242–4246; b) K. Nakano, K. Kobayashi, K. Nozaki, *J. Am. Chem. Soc.* **2011**, *133*, 10720–10723.

84. C.-Y. Tsai, B.-H. Huang, M.-W. Hsiao, C.-C. Lin, B.-T. Ko, *Inorg. Chem.* **2014**, *53*, 5109–5116.

85. For examples of M(II) (M = Zn, Mg) systems: a) P. K. Saini, C. Romain, C. K. Williams, *Chem. Commun.* **2014**, *50*, 4164–4167; b) P. D. Knight, A. J. P. White, C. K. Williams, *Inorg. Chem.* **2008**, *47*, 11711–11719; c) D. R. Moore, M. Cheng, E. B. Lobkovsky, G. W. Coates, *Angew. Chem. Int. Ed.* **2002**, *41*, 2599–2602; d) M. R. Kember, C. K. Williams, *J. Am. Chem. Soc.* **2012**, *134*, 15676–15679; e) K. Nakano, S. Hashimoto, M. Nakamura, T. Kamada, K. Nozaki, *Angew. Chem. Int. Ed.* **2011**, *50*, 4868–4871; f) Y. Xiao, Z. Wang, K. Ding, *Macromolecules* **2006**, *39*, 128–137; g) Y. Xiao, Z. Wang, K. Ding, *Chem. Eur. J.* **2005**, *11*, 3668–3678; h) T. Bok, H. Yun, B. Y. Lee, *Inorg. Chem.* **2006**, *45*, 4228–4237; i) M. Kroger, C. Folli, O. Walter, M. Doring,

Adv. Synth. Catal. **2006**, *348*, 1908–1918; j) S. D. Allen, D. R. Moore, E. B. Lobkovsky, G. W. Coates, *J. Organomet. Chem.* **2003**, *68*, 137–148.

86. For examples of M(III) (M = Fe, Cr, Co, Al) systems: a) S. M. Ahmed, A. Poater, M. I. Childers, P. C. B. Widger, A. M. LaPointe, E. B. Lobkovsky, G. W. Coates, L. Cavallo, *J. Am. Chem. Soc.* **2013**, *135*, 18901–18911; b) R. K. Dean, K. Devaine-Pressing, L. N. Dawe, C. M. Kozak, *Dalton Trans.* **2013**, *42*, 9233–9244; c) Y. Liu, W.-M. Ren, J. Liu, X.-B. Lu, *Angew. Chem. Int. Ed.* **2013**, *52*, 11594–11598; d) R. K. Dean, L. N. Dawe, C. M. Kozak, *Inorg. Chem.* **2012**, *51*, 9095–9103; e) K. Nishioka, H. Goto, H. Sugimoto, *Macromolecules* **2012**, *45*, 8172–8192; f) A. Buchard, M. R. Kember, K. G. Sandeman, C. K. Williams, *Chem. Commun.* **2011**, *47*, 212–214; g) S. I. Vagin, R. Reichardt, S. Klaus, B. Rieger, *J. Am. Chem. Soc.* **2010**, *132*, 14367–14369; h) K. Nakano, S. Hashimoto, K. Nozaki, *Chem. Sci.* **2010**, *1*, 369–373; i) M. R. Kember, A. J. P. White, C. K. Williams, *Macromolecules* **2010**, *43*, 2291–2298; j) E. K. Noh, S. J. Na, S. Sujith, S.-W. Kim, B. Y. Lee, *J. Am. Chem. Soc.* **2007**, *129*, 8082–8083.

87. D. J. Darensbourg, J. R. Wildeson, J. C. Yarbrough, J. H. Reibenspies. *J. Am. Chem. Soc.* **2000**, *122*, 12487–12496.

88. a) K. Nakano, T. Hiyama, K. Nozaki, *Chem. Commun.* **2005**, 1871–1873; b) K. Nakano, K. Nozaki, T. Hiyama, *J. Am. Chem. Soc.* **2003**, *125*, 5501–5510.

89. B. Y. Lee, H. Y. Kwon, S. Y. Lee, S. J. Na, S.-I. Han, H. Yun, H. Lee, Y.-W. Park, *J. Am. Chem. Soc.* **2005**, *127*, 3031–3037.

90. a) Y.-Z. Hua, L.-J. Lu, P.-J. Huang, D.-H. Wei, M.-S. Tang, M.-C. Wang, J.-B. Chang, *Chem. – Eur. J.* **2014**, *20*, 12394–12398; b) Y.-Z. Hua, X.-C. Yang, M.-M. Liu, X.-X. Song, M.-C. Wang, J.-B. Chang, *Macromolecules* **2015**, *48*, 1651–1657.

91. M. F. Pilz, C. Limberg, B. B. Lazarov, K. C. Hultsch, B. Ziemer, *Organometallics* **2007**, *26*, 3668–3676.

92. D. F.-J. Piesik, S. Range, S. Harder, *Organometallics* **2008**, *27*, 6178–6187.

93. a) M. R. Kember, P. D. Knight, P. T. R. Reung, C. K. Williams, *Angew. Chem. Int. Ed.* **2009**, *48*, 931–933; b) M. R. Kember, A. J. P. White, C. K. Williams, *Inorg. Chem.* **2009**, *48*, 9535–9542; c) F. Jutz, A. Buchard, M. R. Kember, S. B. Fredriksen, C. K. Williams, *J. Am. Chem. Soc.* **2011**, *133*, 17395–17405; d) M. W. Lehenmeier, C. Bruckmeier, S. Klaus, J. E. Dengler, P. Deglmann, A.-K. Ott, B. Rieger, *Chem. Eur. J.* **2011**, *17*, 8858–8869; e) A. Buchard, F. Jutz, M. R. Kember, A. J. P. White, H. S. Rzepa, C. K. Williams, *Macromolecules* **2012**, *45*, 6781–6795; f) M. Winkler, C. Romain, M. A. R. Meier, C. K. Williams, *Green Chem.* **2015**, *17*, 300–306; g) A. M. Chapman, C. Keyworth, M. R. Kember, A. J. J. Lennox, C. K. Williams, *ACS Catal.* **2015**, *5*, 1581–1588.

94. a) S. Kissling, M. W. Lehenmeier, P. T. Altenbuchner, A. Kronast, M. Reiter, P. Deglmann, U. B. Seemann, B. Rieger, *Chem. Commun.* **2015**, *51*, 4579–4582; b) S. Kissling, P. T. Altenbuchner, M. W. Lehenmeier, E. Herdtweck, P. Deglmann, U. B.

-
- Seemann, B. Rieger, *Chem. Eur. J.* **2015**, *21*, 8148–8157; c) M. W. Lehenmeier, S. Kissling, P. T. Altenbuchner, C. Bruckmeier, P. Deglmann, A.-K. Brym, B. Rieger, *Angew. Chem. Int. Ed.* **2013**, *52*, 9821–9826.
95. A. Dahan, T. Ashkenazi, V. Kuznetsov, S. Makievski, E. Drug, L. Fadeev, M. Bramson, S. Schokoroy, E. Rozenshine-Kemelmakher, M. Gozin, *J. Org. Chem.* **2007**, *72*, 2289–2296.
96. a) P. I. Binda, S. Abbina, G. Du, *Synthesis* **2011**, 2609–2618; b) Z. Lu, S. Abbina, J. R. Sabin, V. N. Nemykin, G. Du, *Inorg. Chem.* **2013**, *52*, 1454–1465; c) S. Bian, S. Abbina, Z. Lu, E. Kolodka, G. Du, *Organometallics* **2014**, *33*, 2489–2495; d) S. Abbina, G. Du, *ACS Macro Lett.* **2014**, *3*, 689–692.
97. a) S. Doherty, J. G. Knight, C. H. Smyth, N. T. Sore, R. K. Rath, W. McFarlane, R. W. Harrington, W. Clegg, *Organometallics* **2006**, *25*, 4341–4350; b) J. P. Wolfe, S. Wagaw, S. L. Buchwald, *J. Am. Chem. Soc.* **1996**, *118*, 7215–7216; c) M. S.; Driver, J. F. Hartwig, *J. Am. Chem. Soc.* **1996**, *118*, 7217–7223.
98. A. Shafir, S. L. Buchwald, *J. Am. Chem. Soc.* **2006**, *128*, 8742–8743.
99. I. P. Beletskaya, A. G. Bessmertnykh, A. D. Averin, F. Denat, R. Guilard, *Eur. J. Org. Chem.* **2005**, 281–305.
100. S. Doherty, J. G. Knight, A. Mcrae, R. W. Harrington, W. Clegg, *Eur. J. Org. Chem.* **2008**, 1759–1766.
101. M. A. Tius, J. Gomez-Galeno, X.-Q. Gu, J. H. Zaidi, *J. Am. Chem. Soc.* **1991**, *113*, 5775–5183.
102. The formation of high molecular weight polyether is likely due to the presence of side products or trace impurities under these conditions.
103. M. I. Childers, J. M. Longo, N. J. Van Zee, A. M. LaPointe, G. W. Coates, *Chem. Rev.* **2014**, *114*, 8129–8152.
104. a) B. Li, G.-P. Wu, W.-M. Ren, Y.-M.; Wang, D.-Y. Rao, X.-B. Lu, *J. Polym. Sci. Part A: Polym. Chem.* **2008**, *46*, 6102–6113; b) C. T. Cohen, C. M. Thomas, K. L. Peretti, E. B. Lobkovsky, G. W. Coates, *Dalton Trans.* **2006**, 237–249; c) L. Shi, X.-B. Lu, R. Zhang, X.-J. Peng, C.-Q. Zhang, J.-F. Li, X.-M. Peng, *Macromolecules* **2006**, *39*, 5679–5685; d) C. T. Cohen, T. Chu, G. W. Coates, *J. Am. Chem. Soc.* **2005**, *127*, 10869–10878; e) M. Cheng, N. A. Darling, E. B. Lobkovsky, G. W. Coates, *Chem. Commun.* **2000**, 2007–2008.
105. L.-C. Liang, T.-L. Tsai, C.-W. Li, Y.-L. Hsu, T.-Y. Lee, *Eur. J. Inorg. Chem.* **2011**, 2948–2957.
106. M. T. Whited, A. J. Kosanovich, D. E. Janzen, *Organometallics* **2014**, *33*, 1416–1422.

-
107. S. Range, D. F.-J. Piesik, S. Harder, *Eur. J. Inorg. Chem.* **2008**, 3442–3451.
108. M. Driess, K. Merz, R. Schoenen, S. Rabe, F. E. Kruis, A. Roy, A. Birkner, *Comptes Rendus Chim.* **2003**, *6*, 273–281.
109. R. Blessing, *Acta Crystallogr.*, **1995**, *A51*, 33–38.
110. Bruker Analytical X-Ray Systems, SAINT: *Program for Reduction of Area Detector Data*; Bruker-AXS, Inc.: Madison, WI, 2003.
111. G. M. Sheldrick, *Acta. Crystallogr. Sect. A.*, **2008**, *64*, 112–122.
112. S. Parsons, H. D. Flack, T. Wagner, *Acta Crystallogr. Sect. B.* **2013**, *B69*, 249–259.

CHAPTER 3

RING OPENING COPOLYMERIZATION OF STYRENE OXIDE AND CYCLIC ANHYDRIDES CATALYZED BY CHIRAL ZINC AMIDO-OXAZOLINATE COMPLEXES

3.1. Introduction

Until today, the most commonly consumed polymers are derived from oil-based feedstocks and this production causes severe problems i.e. dwindling of fossil fuel resources and thus causes increase in the price of petroleum based feedstock as well as other environmental issues.^{113,114} To overcome the issues with conventional polymers, spectacular improvements have been made in synthesis of biodegradable and environmentally adaptable polymers using renewable resources during the last three decades.^{115,116,117} Among the explored polymers, polyesters are an important class of polymers as they are widely used in a variety of applications, including drug delivery systems, artificial tissues, and commodity materials and moreover, most of the polyesters are biodegradable and biocompatible.^{118,119,120,121} In general, most of the polyesters can be synthesized from either polycondensation of diols and diacids or by ring-opening polymerization (ROP) of cyclic esters. Although these methods have been used for some time, they have suffered from several problems, such as drastic reaction conditions, side reactions, and limited choices of monomer units.^{122,123,124,125}

To establish a more efficient synthetic route for the generation of ABABABAB type polyesters, more attention has been turned onto ring opening copolymerization of epoxides with cyclic anhydrides^{126,127,128,129,130} since the ring opening copolymerization has become a popular route for the synthesis of polycarbonates *via* copolymerization of CO₂ and epoxides.¹³¹ The initial discovery by Inoue and coworkers showed that (porphyrin)Al(III)

catalysts can copolymerize cyclic anhydrides with epoxides and CO₂, however, activity of these catalysts is very low (TOFs).^{132,15a} Subsequent reports by Inoue *et al*^{15b} and Maeda *et al*¹²⁶ also described the copolymerization of anhydrides with epoxides, but these systems suffered with obtaining low molecular weight copolymers and homopolymerization of epoxides. The reports by Coates and coworkers illustrates that zinc complexes of β-diketiminate ligands catalyze the copolymerization of aliphatic anhydrides and a variety of epoxides, yielding copolymers with high molecular weight (up to 55, 000 g/mol) and narrow molecular weight distributions.^{133,134} Duchateau and co-workers vigorously studied the ring opening copolymerization of various epoxides and anhydrides using salen-based metal (Co, Cr, Al, and Mn) complexes.^{12,135}

We have previously reported zinc complexes (Chart 4, **1–4**) of amido-oxazolate ligands as viable initiators for asymmetric alternating copolymerization of epoxides and CO₂.¹³⁶ In addition, we have also confirmed that the same zinc complexes can act as catalysts for ring opening polymerization of *rac*-lactides.¹³⁷ Based on these results, we anticipated that our catalytic systems might serve as active catalytic systems for the ring-opening copolymerization of oxiranes and cyclic anhydrides. Herein, we report the highly-active catalytic systems, zinc complexes of amido-oxazolate ligands, for the synthesis of polyesters *via* alternating copolymerization of styrene oxide (SO) and cyclic anhydrides (succinic anhydride (SA), maleic anhydride (MA), and phthalic anhydride (PA)) and its mechanistic aspects.

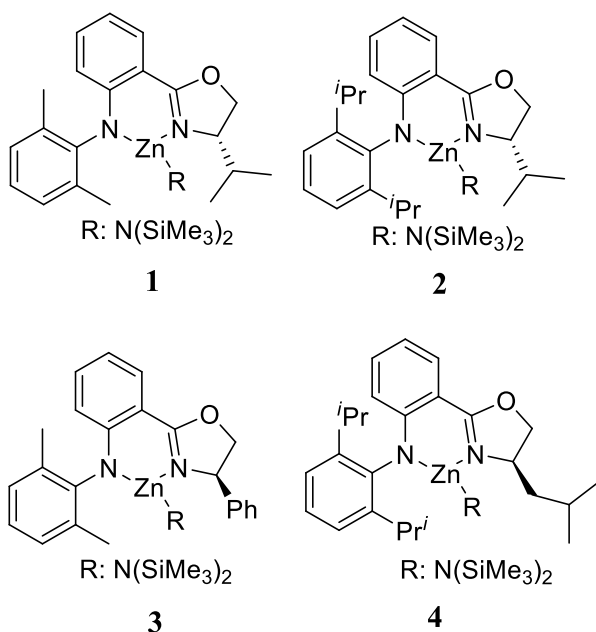
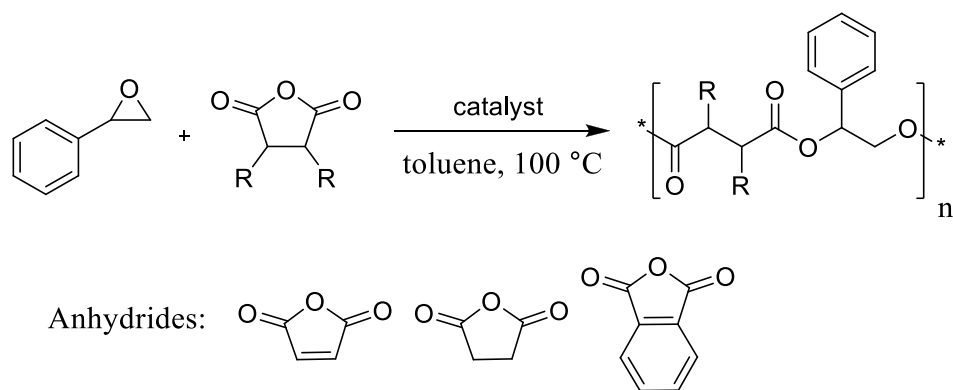


Chart 4. Structures of amido-oxazolinato zinc complexes.

3.2. Results and discussion

3.2.1. Screening of the polymerization reaction conditions

Initially, to screen the ring opening copolymerization reaction conditions, polymerization of styrene oxide (SO) with maleic anhydride (MA) was carried at 100 °C using zinc complexes **1** in toluene (Scheme 8). The copolymerization of SO and MA was performed without catalyst; it did not produce any copolymer even at prolonged reaction times (Table 3, entry **1**). This emphasizes the need of catalyst for this copolymerization reaction. Catalyst **1a**, produced moderate TOFs at 303 h⁻¹ at 100 °C in toluene, generated perfectly alternating copolymers (Table 3, entry **2**). The formation of polymer was confirmed by NMR spectroscopy (¹H and ¹³C). The olefinic protons in the polymer are observed at 6.27 ppm and the protons from the styrene oxide monomer are found at 6.25 (methine proton) and 4.40–4.60 ppm (methylene proton). The formation of the side product, phenyl ethanal (PE), was also confirmed by the proton resonances at 3.80 and 9.80–9.85 ppm in the ¹H NMR spectrum.



Scheme 8. Copolymerization of styrene oxide with cyclic anhydrides

At similar conditions, polymerization reactions were performed involving SO to [Zn] ratios of 200:1, 500:1, 1000:1, 2500:1, and 4000:1. Catalyst **1a** exhibits very high TOF of 8000 h⁻¹ at 100 °C (Table 3, entry **6**), which is among the highest TOFs for ring opening copolymerization of maleic anhydride and styrene oxide. In all cases, phenyl ethanal was observed in significant amounts of the SO:Zn ratios. The formation of phenyl ethanal, an isomerized product of styrene oxide, has been reported in the literature. Chisholm and co-workers studied the formation of phenyl ethanal and its influence on the copolymerization

Table 3. Screening the reaction conditions of ring opening co-polymerization process of styrene oxide and maleic anhydride.^a

entry	epoxide	anhydride	[cat]/ [monomer]	time (h)	ratio of polyester/PE ^b	M_n (g/mol)	PDI
1	SO	MA	-	24	-	-	-
1	SO	MA	1:100	20	75/25	1477	1.33
2	SO	MA	1:200	20	76/24	2644	1.13
3	SO	MA	1:500	20	76/24	1712	1.24
4	SO	MA	1:1000	20	76/24	2328	1.41
5	SO	MA	1:2500	30	75/25	1870	1.22
6	SO	MA	1:4000	30	76/24	1388	1.28

PE: phenyl ethanal, MA: maleic anhydride, SO: styrene oxide. ^aAll reactions were performed using catalyst **1** in toluene (1-4 mL) at 100 °C. ^bDetermined by measuring the intensities of peaks on ¹H NMR spectroscopy. In all cases, 100 % conversion was achieved with respect to SO.

process.¹³⁸ Per this study, adventitious water trapped in anhydrides might help the formation of phenyl ethanol (PE). Even after three times of careful sublimation of anhydrides, the moisture was still not eliminated completely. The trace amounts water produces corresponding acids that can help the transformation of styrene oxide into phenyl ethanal.

3.2.2. Effect of catalyst structure on catalytic behavior

To study the influence of the steric and electronic features of the catalyst on their polymerization behavior, we decided to use the catalysts (**1–4**) for ring opening polymerization of SO with different anhydrides (MA, PA, SA, and MCHA) with an oxirane:anhydride:catalyst ratio of 200:200:1 in toluene at 100 °C (Table 4). Evidently, catalyst **1**, with *i*Pr group and 2,6-DMP on amido-oxazolate ligand framework, afforded perfectly alternating polymer chains with a significantly higher degree of polymerization than the remaining catalysts **2–4**. Catalyst **3**, with (*R*)-Ph group and 2,6-DMP on amido-oxazolate ligand framework, showed low TOFs for all conversions except the conversion of SO and SA (Table 4). From the data, it can be believed that the substitution on amido nitrogen can alter the activity of the catalyst. In case of catalyst **2** and **4**, the conversion of MA and SO is faster than SO and PA while catalysts **1** and **3** gave faster degree of polymerization for SO and PA. Except the coupling of SO and SA, catalysts **1–4** exhibit the following order **1>2>4>3** for all remaining polymerization reactions.

Polystyrene succinate (PSS), obtained from ring opening of copolymerization of SO and SA ((SO-SA)_n), possesses three different types of microstructures (Figure 14). The microstructures of the PSS (HT, HH, and TT junctions) can be easily identified by ¹³C-

Table 4. Results of copolymerization of styrene oxide with different anhydrides.^a

entry	catalyst	anhydride	time (h)	ratio of polyester/PE ^b	M_n (g/mol)	PDI
1	1	PA	0.5	76/24	1619	1.1
2	1	MA	0.58	78/22	2560	1.2
3	1	SA	4	85/15	1890	1.3
5	2	PA	1.5	79/12	1802	1.2
6	2	MA	2	80/20	3769	1.0
7	2	SA	12	87/13	2221	1.3
9	3	PA	2.5	76/24	2023	1.1
10	3	MA	3.25	76/24	2995	1.2
11	3	SA	9.5	82/18	2344	1.3
13	4	PA	2	80/20	2221	1.1
14	4	MA	1.75	77/23	2042	1.3
15	4	SA	11	79/21	2427	1.3

PE: phenyl ethanol, MA: maleic anhydride, SA: succinic anhydride. PA: phthalic anhydride. MCA: 4-methylcyclohexane anhydride. ^aAll reaction were performed using catalyst **1** in toluene (2 mL) at 100 °C. ^bDetermined by measuring the intensities of peaks on ¹H NMR spectroscopy. In all cases, 100 % conversion was achieved with respective SO, determined by ¹H NMR spectroscopy.

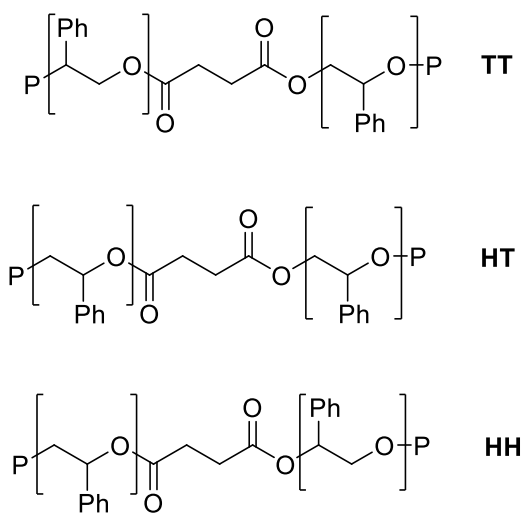


Figure 14. Regiostructures of polystyrene succinate: Tail-Tail (TT), Head-Tail (HT), and Head-Head (HH) junctions.

NMR spectroscopy. As per previous assignments, the peaks at 171.82 and 171.28 ppm correspond to HT junctions.¹³⁸ The two chemical shifts at 171.60 and 171.20, respectively, relate to TT and HH junctions. The split in HH junction relates *iso*, *syn* diads of the HH junctions of the PSS. ¹³C NMR spectrum of the carbonyl region of PSS, obtained by catalyst 3, is shown in Figure 15 and clearly indicates the presence of four resonances that correlate to four microstructures of PSS. The peaks at 171.20 ppm and 171.16 ppm correspond to *i* and *s* HH-junctions.

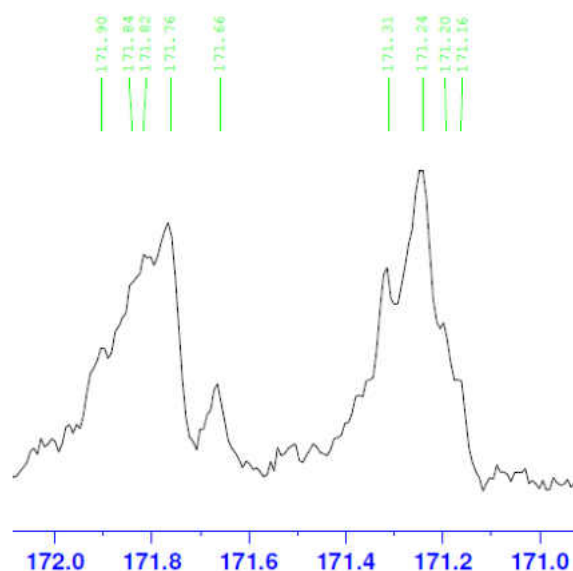


Figure 15. Carbonate region of the PSS of ¹³C NMR spectrum generated from SO and SA by catalyst 3.

3.2.3. Effect of anhydrides

To investigate the influence of anhydride on copolymerization process, three anhydrides (PA, MA, and SA) were chosen. All polymerization reactions catalyzed by complexes 1–4 yielded 100% conversions in term of styrene oxide concentration and gave perfectly alternating copolymers without any ether linkages. The ring strain can dramatically influence the polymerization behavior. The relative rate of hetero coupling of

styrene oxide with anhydrides was found in the following order, PA>MA>SA (Figure 16). The conversion of SA and SO with all catalysts **1–4** was rather low due to the less ring strain of SA.

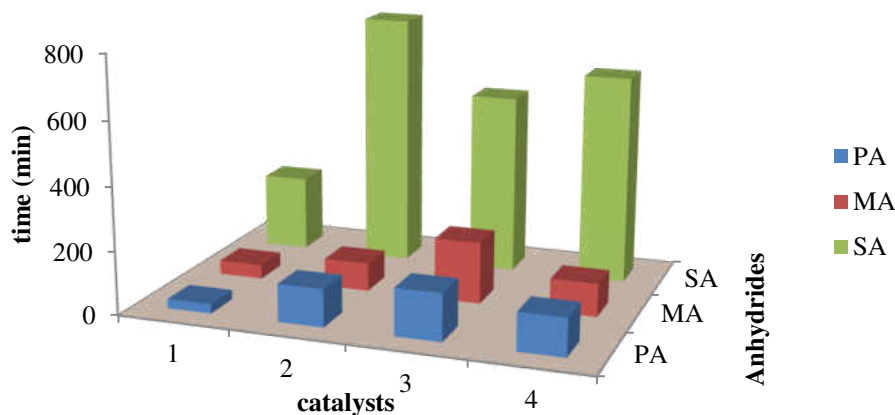


Figure 16. copolymerization of SO and anhydrides catalyzed by **1–4**.

3.3. Conclusions

In conclusion, we have demonstrated the catalytic activity of zinc complexes of amido-oxazolate ligands for ring-opening copolymerization of anhydrides and styrene oxide. Among the four catalysts, catalyst **1** proved to be the most active catalyst. A study on the copolymerization of styrene oxide and anhydrides, different anhydrides exhibited a trend following in the order of PA>MA>SA. The catalytic system appeared to be well suited for ring opening copolymerization of anhydrides and styrene oxide.

3.4. Experimental section

General Conditions

All reactions were performed by exclusion of air using standard Schlenk line and dry box techniques. All chemicals were purchased from Sigma Aldrich unless otherwise noted. Deuterated solvents were purchased from Cambridge Isotope Laboratories. Analytical grade THF was purchased from Fisher Scientific and used as received. Purified materials were stored under nitrogen in glove box prior to use. Styrene oxide (SO) was distilled from CaH_2 following three freeze–pump–thaw cycles. Synthesis of zinc bis(trimethylsilyl)amide¹³⁹ and catalysts **1**–**4**¹³⁶ were prepared as per the reported literature methods. Maleic anhydride, phthalic anhydride, and succinic anhydride were sublimed three times under nitrogen. Toluene was distilled from Na/benzophenone under nitrogen. CDCl_3 and CD_3CN were distilled from CaH_2 and degassed prior to use. All 1D and 2D NMR experiments were recorded on a Bruker Avance-500 NMR spectrometer and referenced to the residual peaks in CDCl_3 or CD_3CN at 298 K. Gel permeation chromatography (GPC) analysis was performed on a Varian Prostar with autosampler model 400, using a PLgel 5 μm Mixed-D column, a Prostar 355 RI detector, and THF as eluent at a flow rate of 1 mL/min (20 °C). Polystyrene standards purchased from Agilent technologies were used for calibration. Galaxie software was used to operate the instrument and Cirrus software was used for data processing. High-resolution mass spectrometry (HRMS) analysis was performed using an Agilent G1969A TOF-MS system with an electrospray ionization (ESI) source (Agilent, Santa Clara, CA, USA). The analyte-containing solution was introduced into the instrument via direct infusion using a syringe drive (5 $\mu\text{L}/\text{min}$). The electrospray ionization (e.g., capillary) and collision-induced dissociation (e.g., fragmentor) potentials were set to 4500 V and 200 V, respectively.

Ammonium acetate was used as an electrolyte at $2.5 \text{ mmol}\cdot\text{L}^{-1}$. Mass Hunter Qualitative Analysis software was used for data processing.

General Procedure for Copolymerization reactions

An oven dried 10 mL schlenk flask equipped with a stir bar was loaded with 0.5 mol% catalyst (usually around 10 mG), 1 eq. anhydride and dissolved in 1 eq. SO followed by 2 mL toluene in a glove box. The mixture was stirred and heated in a preheated oil bath at $100 \text{ }^\circ\text{C}$ till complete conversion in SO was observed by ^1H NMR spectroscopy. The unreacted monomers, catalyst, and phenyl acetaldehyde were separated from polymers by dissolving the crude reaction mixture in 5-6 mL methanol followed by filtration and drying at reduced pressure. Purified polymers were characterized by various NMR techniques, ESI-MS and molecular weight was determined by GPC.

Characterization of compounds in table 4.

Copolymer of styrene oxide and maleic anhydride (entry 2). ^1H NMR (500MHz, CDCl_3): 4.10–4.60 (br, $-\text{PhCHCH}_2\text{COO}-$, 2H), 5.90-6.50 (br, $-\text{PhCHCH}_2\text{COO}$, 1H), 5.90 6.50 (br, $-\text{COOHC}=\text{CHCOO}$, 2H).

Copolymer of styrene oxide and succinic anhydride (entry 3). ^1H NMR (500MHz, CDCl_3): 4.30–4.65 (br, $-\text{PhCHCH}_2\text{COO}-$, 2H), 6.10-6.40 (br, $-\text{PhCHCH}_2\text{COO}$, 1H), 6.10 6.40 (br, $-\text{COOPhHCOO}-$, 4H).

Copolymer of styrene oxide and phthalic anhydride (entry 1). ^1H NMR (500MHz, CDCl_3): 2.50–2.80 (br, $-\text{COOCH}_2\text{CH}_2\text{COO}-$, 4H), 4.29 (br, $-\text{PhCHCH}_2\text{COO}$, 2H), 6.08 (br, $-\text{PhCHCH}_2\text{COO}$, 1H).

3.5. References

113. Dechy-Cabaret, O.; Martin-Vaca, B.; Bourissou, D. *Chem. Rev.* **2004**, *104*, 6147–6176.
114. Gandini, A. *Macromolecules* **2008**, *41*, 9492-9504.
115. Okada, M. *Prog. Polym. Sci.* **2002**, *27*, 87–133.
116. Dechy-Cabaret, O.; Martin-Vaca, B.; Bourissou, D. *Chem. Rev.* **2004**, *104*, 6147–6176.
117. Pilla, S. *Handbook of Bioplastics and Biocomposites Engineering Applications*; John Wiley & Sons, Inc: Hoboken, New Jersey, 2011.
118. Coulembier, O.; Degee, P.; Hedrick, J. L.; Dubois, P. *Prog. Polym. Sci.* **2006**, *31*, 723–747.
119. Ikada, Y.; Tsuj, H. *Macromol. Rapid Commun.* **2000**, *21*, 117–132.
120. Vink, E. T. H.; Rabago, K. R.; Glassner, D. A.; Springs, B.; O'Connor, R. P.; Kolstad, J.; Gruber, P. R. *Macromol. Biosci.* **2004**, *4*, 551-564.
121. Chasin, M.; Langer, R. *Biodegradable Polymers as Drug Delivery Systems*; Marcel Dekker Inc: New York, **1990**.
122. (a) Thomas, C. M. *Chem. Soc. Rev.* **2010**, *39*, 165–173. (b) Robert, C.; de Montigny, F.; Thomas, C. T. *Nature Commun.* **2011**, *2*, 586–592.
123. Kricheldorf, H. R. *Chem. Rev.* **2009**, *109*, 5579–5594.
124. Huijser, S.; Nejad, E. H.; Sablong, R.; Jong, C. D.; Koning, C. E.; Duchateau, R. *Macromolecules* **2011**, *44*, 1132–1139.
125. Yoneyama, M.; Kakimoto, M.; Imai, Y. *Macromolecules* **1989**, *22*, 2593–2596.
126. Maeda, Y.; Nakayama, A.; Kawasaki, N.; Hayashi, K.; Aiba, S.; Yamamoto, N. *Polymer* **1997**, *38*, 4719–4725.
127. Aida, T.; Inoue, S. *J. Am. Chem. Soc.* **1985**, *107*, 1358–1364. (b) Aida, T.; Sanuki, K.; Inoue, S. *Macromolecules* **1985**, *18*, 1049–1055.
128. Eberhardt, R.; Allmendinger, M.; Rieger, B. *Macromol. Rapid Commun.* **2003**, *24*, 194–196.
129. Darensbourg, D. J.; Poland, R. P.; Escobedo, C. *Macromolecules* **2012**, *45*, 2242–2248.

-
130. Maeda, Y. *Polymer* **1997**, *38*, 4719–4725.
131. Nakano, K.; Kobayashi, K.; Ohkawara, T.; Imoto, H.; Nozaki, K. *J. Am. Chem. Soc.* **2013**, *135*, 8456–8459. (b) Geschwind, J.; Frey, H. *Macromolecules* **2013**, *46*, 3280–3287. (c) Lu, X.-B.; Darensbourg, D. J. *Chem. Soc. Rev.* **2012**, *41*, 1462–1484.
132. Inoue, S.; Koinuma, H.; Tsuruta, T. *J. Polym. Sci. Polym. Lett.* **1969**, *7*, 287–292.
133. Jeske, R. C.; DiCiccio, A. M.; Coates, G. W. *J. Am. Chem. Soc.* **2007**, *129*, 11330–11331.
134. Jeske, R.; Rowley, J.; Coates, G. *Angew. Chem., Int. Ed.* **2008**, *47*, 6041–6044.
135. (a) Nejad, E. H.; Melis, C. G. W.; Vermeer, T. J.; Koning, C. E.; Duchateau, R. *Macromolecules* **2012**, *45*, 1770–1776. (b) Nejad, E. H.; Paoniasari, A.; Melis, C. G. W.; Koning, C. E.; Duchateau, R. *Macromolecules* **2013**, *46*, 631–637.
136. Abbina, S.; Du, G. *Organometallics* **2012**, *31*, 7394–7403.
137. Abbina, S.; Du, G. *ACS Macro Lett.* **2014**, *3*, 689–692.
138. Harrold, N. D.; Li, Y.; Chisholm, M. H. *Macromolecules* **2013**, *46*, 692–698.
139. Darensbourg, D. J.; Holtcamp, M. W.; Struck, G. E.; Zimmer, M. S.; Niezgoda, S. A.; Rainey, P.; Robertson, J. B.; Draper, J. D.; Reibenspies, J. H. *J. Am. Chem. Soc.* **1999**, *121*, 107–116.

CHAPTER 4

RING OPENING COPOLYMERIZATION OF CYCLOHEXENE OXIDE AND CYCLIC ANHYDRIDES CATALYZED BY CHIRAL ZINC AMIDO-OXAZOLINATE COMPLEXES

4.1. Introduction

Poly(esters) are another important class of biodegradable and biocompatible polymers and they possess various applications in drug delivery, orthopedic implants, artificial tissues, and commodity materials.^{140,141,142} Traditional synthetic methods of polyesters involve step growth co-polymerization of diols and diacids or by ring-opening polymerization of cyclic esters.^{143,144,145} The step-growth polymerization from diols and diacids usually requires high temperatures, long reaction times, and often leads to side reactions and results in low molecular weight polymers.^{146,147,148,149} ROP of cyclic esters also effectively produce polyesters but the availability of monomers is limited. Catalytic chain growth polymerization of epoxides and anhydrides is another technique to produce polyesters that could possibly circumvent the limitations posed by step growth polymerization.¹⁵⁰

In contrast to the catalysts needed for step-growth co-polymerization, various metal complexes were reported to catalyze the ring-opening copolymerization of epoxides and anhydrides. Haieh et al. reported the first examples for co-polymerization of propylene oxide (PO) and MA, using AlR_3 as metal catalysts, resulted in low monomer conversions, low molecular weights of polymers, and often homopolymerization of PO is a side product.¹⁵¹ Several other metal catalysts were reported such as rare earth metal-complexes,¹⁵² $Mg(OEt)_2$,¹⁵³ and $Zn_3[Co(CN)_6]_2$.¹⁵⁴ Duchateau and co-workers reported the chromium-porphyrin complexes for copolymerization of CHO with PA or SA. The

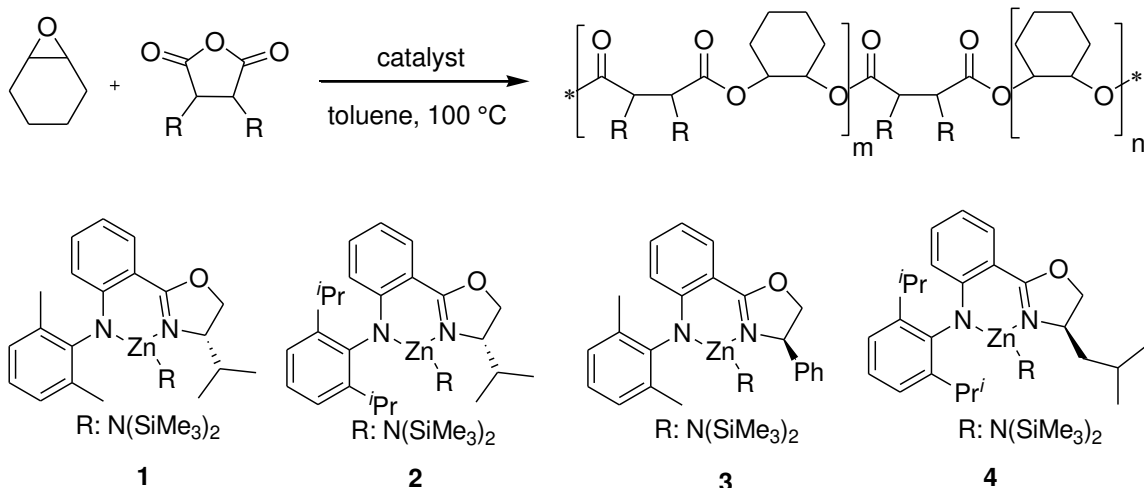
resultant polymers are formed with high TOFs and molecular weights, ranging from 1000 to 20,000 g/mol.¹⁵⁵ The analogous cobalt-porphyrin complex produced polymer with low TOF of 40 h⁻¹. They also reported several aluminum, cobalt, and chromium complexes of salphen, salalen and salen complexes.^{44,156} These complexes along with a cocatalyst DMAP were used to catalyze the ROCOP of CHO with PA, SA and CPrA and afforded the poly(esters) with M_n of 2–15 kg/mol. High TOF of 150 h⁻¹ was achieved using chromium-salalen complexes. Zinc-based alkoxides were promising, but low yields and a considerable amount of polyethers are still the limitations. Various reports by Coates and co-workers illustrated that zinc complexes of β -diketiminato ligands are good initiators for copolymers with high molecular weight (up to 55,000 g/mol) and narrow molecular weight distributions.^{157,158}

4.2. Results and discussion

4.2.1. Screening of reaction conditions

Four different zinc complexes **1–4** that are used for the ROCOP of SO with anhydrides (SA, MA, PA) from chapter 3 were also used for the ROCOP of CHO with anhydrides (Scheme 9). CHO can easily undergo homopolymerization at elevated temperatures in presence of catalyst to form poly(cyclohexene ether) as a by-product along with poly(cyclohexene-*co*-anhydride) using zinc complexes **1–4**. Hence, the initial reactions were focused to minimize the formation of poly(ether). The copolymerization of CHO with MA without catalyst didn't afford the formation of either poly(ester) or poly(ether) at 100 °C even at elongated reaction time. This emphasizes the importance of catalyst in the formation of polymer (Table 5, entry **1**). A reaction was performed in toluene

at 100 °C with an CHO:MA:cat-1 ratio of 100:100:1, complete conversion of CHO was achieved in 16 h with 53% poly(ester) formation with M_n of 5917 g/mol and PDI of 1.29.



Scheme 9. Amido-oxazolinone zinc complexes for ROCOP of CHO with anhydrides.

In spite of moderate molecular weight, 47% poly(ether) was formed using this condition (Table 5, entry 2). In a different run, a solution of CHO in toluene was slowly added to a solution of catalyst-1, and CHO in toluene over a period of 30 min to see if it minimizes the formation of poly(ether). 73% poly(ester) linkages were formed, however, the reaction took longer for 100% conversion with respect to CHO and low molecular-weight polymer was observed. By diluting the reaction mixture, the reaction needed longer time and resulting in low molecular weight polymers (Table 5, entry 2). Using CHO:MA:cat-1 ratio of 200:200:1, reaction afforded 61% poly(ester) formation in 9 h with M_n of 2269 and PDI of 1.2 (Table 5, entry 4). To see the effect of dilution, the same reaction was repeated with 10 mL toluene instead of the previously used 2 mL. As expected, reaction took longer time and M_n was decreased to 1200 g/mol with not much change in the selectivity towards poly(ester) (Table 5, entry 5). Having observed the effect of concentration on rate of

reaction as well as molecular weight of the polymer, a bulk reaction was performed using the same quantities as entry-**2**. Homopolymerization of CHO was predominant in this case

Table 5. Optimization of reaction conditions.^a

entry	[cat]: [CHO]:[MA]	time (h)	conversion (%) ^b	ratio of polyester/PE ^b	M_n (g/mol) ^f	PDI ^f
1	0:1:1	24	0	-	-	-
3	1:100:100	16	100	53/47	5917	1.29
2 ^c	1:100:100	24	100	73/27	2726	1.43
4	1:200:200	9	100	61/39	2269	1.20
5 ^d	1:200:200	16	96	62/34	1200	1.19
6 ^e	1:200:200	0.92	88	12/76	3811	1.82
7	1:200:400	1	100	46/54	781	1.12
8	1:1000:1000	1.5	100	34/66	1197	1.28

^aAll reaction were performed using catalyst **1** in toluene (2 mL) at 100 °C. ^bDetermined by measuring the intensities of peaks on ¹H NMR spectroscopy. In all cases, 100 % conversion was achieved with respective CHO, determined by ¹H NMR spectroscopy. ^c CHO in toluene was added slowly to a solution of catalyst and maleic anhydride. ^d 5 times the normal volume of toluene was used. ^e Bulk reaction. ^f Determined by GPC using THF as solvent with a flow rate of 1 mL/min.

leading to the highest 76% poly(ether) content (Table 5, entry **6**). This may be due to the viscous nature of the reaction mixture that limited the reactivity between two comonomers in the reaction. Using excess MA in the reaction afforded low molecular weight polymers (Table 5, entry **7**). The trace amount of maleic acid present in MA even after multiple sublimations may have acted as chain transfer agents to form low molecular weight polymers. The same result was observed in the last run, where excess comonomers resulted in low molecular weight polymers (Table 5, entry **8**).

4.2.2. Effect of catalyst structure on catalytic activity

Based on the optimized conditions, CHO:anhydride:catalyst ratio of 200:200:1 was used for further runs in Table 6. MA was reactive with CHO compared to the other anhydrides and ROCOP of CHO with MA afforded 100% conversion with respect to CHO. This may be attributed toward the solubility of MA in toluene. As observed in the table, as poly(ether) was formed in all the entries, MA cannot be completely consumed in the reaction. Catalyst 1 was active with MA with the formation of 61% poly(ester) selectivity (Table 6, entry 1). Complete conversion can be achieved with catalysts 2-4, however, selectivity towards poly(ester) was drastically decreased (Table 6, entries 2-4). Moderate molecular weight can be achieved using catalyst-3 but the selectivity was very low (Table 6, entry 3). Good selectivity was not observed with PA, the highest poly(ester) content achieved was only 43% (Table 6, entry 8). The reaction times was comparatively longer but moderate. Cat-1 was not active for PA affording to the formation of only 34% poly(ester) (Table 6, entry 5). Pheyl substitution on the oxazoline ring (cat-3) or isopropyl substituent on anilido ring (cat-2) didn't have much change towards the ROCOP of CHO with MA (Table 6, entries 6 & 7). Copolymer formed from SA was superior with high molecular weight as well as selectivities towards poly(ester). Eventhough, catalysts have different substitutions, their behavior was same with SA. 50-60% poly(ester) was formed in these cases. Cat-2 bearing isopropyl substituent on the anilido moiety as well as on the oxazoline ring afforded 58% selectivity and M_n of 4226 g/mol and PDI of 1.3, however, 100% conversion was not achieved in this case even after longer time (Table 6, entry 10). Cat-3 bearing phenyl substituent also produced with 50% selectivity and M_n of 4204 g/mol

with 91% conversion (Table 6, entry **11**). 98% conversion was achieved with catalysts 1 and 4 with 59% and 66% selectivities respectively (Table 6, entries **9** & **12**).

Table 6. Results of ROCOP of CHO with anhydrides.^a

entry	catalyst	anhydride	time (h)	conversion (%) ^b	ratio of polyester/PE _b	M_n (g/mol) ^c	PDI ^c
1	1	MA	9	100	61/39	2269	1.29
2	2	MA	3.5	100	44/56	2565	1.3
3	3	MA	2	100	37/63	5304	1.30
4	4	MA	2	100	40/60	2864	1.34
5	1	PA	3	93	34/59	1545	1.17
6	2	PA	5.5	97	39/58	1776	1.24
7	3	PA	3	100	41/59	1937	1.15
8	4	PA	4.5	97	43/54	1757	1.20
9	1	SA	9	98	59/39	3706	1.24
10	2	SA	5.5	78	58/20	4226	1.3
11	3	SA	9	91	50/41	4204	1.15
12	4	SA	11	98	66/32	3269	1.14

PE: polyester ^aAll reaction were performed using catalyst **1** in toluene (2 mL) at 100 °C. ^b Determined by measuring the intensities of peaks on ¹H NMR spectroscopy. In all cases, 100 % conversion was achieved with respective CHO, determined by ¹H NMR spectroscopy. ^c Determined by GPC using THF as solvent with a flow rate of 1 mL/min.

4.3. Conclusions

Amido-oxazolate zinc complexes **1–4** are active towards ROCOP of CHO with MA, PA, or SA. The substitutions on the catalyst has less effect on the poly(ester) formations. This emphasizes the reactivity of the amido-oxazolate frame work along with the initiator. Reactions with MA have higher rate of reaction with good selectivities and moderate molecular weights affording 61% selectivity and M_n of 2269 g/mol with catalyst-1. Reactions with SA are more active, high selectivities and molecular weights were observed in all the runs, but cannot lead to complete conversions. PA was less selective

compared to MA and SA. More than 50% ether linkages were formed with all catalysts. Overall, these zinc complexes can catalyze the ring-opening reactions to afford poly(ester).

4.4. Experimental section

General Conditions

All reactions were performed by exclusion of air using standard Schlenk line and dry box techniques. All chemicals were purchased from Sigma Aldrich unless otherwise noted. Deuterated solvents were purchased from Cambridge Isotope Laboratories. Analytical grade THF was purchased from Fisher Scientific and used as received. Purified materials were stored under nitrogen in glove box prior to use. CHO was distilled from CaH₂ following three freeze-pump-thaw cycles. Synthesis of zinc bis(trimethylsilyl)amide¹⁵⁹ and catalysts **1–4**¹³⁶ were prepared according to the reported literature methods. Maleic anhydride, phthalic anhydride, and succinic anhydride were sublimed three times under nitrogen. Toluene was distilled from Na/benzophenone under nitrogen. CDCl₃ and CD₃CN were distilled from CaH₂ and degassed prior to use. All 1D and 2D NMR experiments were recorded on a Bruker Avance-500 NMR spectrometer and referenced to the residual peaks in CDCl₃ or CD₃CN at 298 K. Gel permeation chromatography (GPC) analysis was performed on a Varian Prostar with autosampler model 400, using a PLgel 5 μm Mixed-D column, a Prostar 355 RI detector, and THF as eluent at a flow rate of 1 mL/min (20 °C). Polystyrene standards purchased from Agilent technologies were used for calibration. Galaxie software was used to operate the instrument and Cirrus software was used for data processing.

General Procedure for Copolymerization reactions

An oven dried 10 mL schlenk flask equipped with a stir bar was loaded with 0.5 mol% catalyst (usually around 10 mg), 1 eq. anhydride and dissolved in 1 eq. CHO followed by

2 mL toluene were added in a glove box. The mixture was stirred and heated in a preheated oil bath at 100 °C till complete conversion in CHO was achieved, the conversion was monitored by ^1H NMR spectroscopy. Polymer was precipitated in toluene by adding excess MeOH followed by filtration and drying at reduced pressure. Purified polymers were characterized by 1D and 2D NMR techniques, molecular weight was determined by GPC.

4.5. References

140. Okada, M. *Prog. Polym. Sci.* **2002**, *27*, 87–133.
141. Dadsetan, M.; Liu, Z.; Pumbeger, M.; Giraldo, C. V.; Ruesink, T.; Lu, L.; Yaszemski, M. J. *Biomaterials* **2010**, *31*, 8051–8062.
142. Lee, J. W.; Kang, K. S.; Lee, S. H.; Kim, J. Y.; Lee, B. K.; Cho, D. W. *Biomaterials* **2011**, *32*, 744–752.
143. Lutson, J.; Vass, F. *Adv. Polym. Sci.* **1984**, *56*, 91–133.
144. Mathieu, J. L.T.; Emilie, B.; Pierre, H.; Christophe, M. T. *Polym. Chem.* **2012**, *3*, 836–851.
145. Jeske, J. C.; DiCiccio, A. M.; Coates, G. W. *J. Am. Chem. Soc.* **2007**, *129*, 11330–11331.
146. (a) Thomas, C. M. *Chem. Soc. Rev.* **2010**, *39*, 165–173. (b) Robert, C.; de Montigny, F.; Thomas, C. T. *Nature Commun.* **2011**, *2*, 586–592.
147. Kricheldorf, H. R. *Chem. Rev.* **2009**, *109*, 5579–5594.
148. Huijser, S.; Nejad, E. H.; Sablong, R.; Jong, C. D.; Koning, C. E.; Duchateau, R. *Macromolecules* **2011**, *44*, 1132–1139.
149. Yoneyama, M.; Kakimoto, M.; Imai, Y. *Macromolecules* **1989**, *22*, 2593–2596.
150. Mathieu, J. L. T.; Emilie, B.; Pierre, H.; Christophe, M. T. *Polym. Chem.* **2012**, *3*, 836–851.
151. Haieh, H. L. *J. Macromol. Sci. Chem.* **1973**, *7*, 1525–1535.
152. Fang, J. H.; Chen, X. H.; Zhang, Y. F.; Shen, Z. Q. *Chin. J. Catal.* **1994**, *15*, 45–49.
153. Takenouchi, S.; Takasu, A.; Inai, Y.; Hirabayashi, T. *Polym. J.* **2002**, *34*, 36–42.
154. Hua, Z. J.; Qi, G. R.; Chen, S. *J. Appl. Polym. Sci.* **2004**, *93*, 1788–1792.
155. (a) Huijser, S.; HosseiniNejad, E.; Sablong, R.; de Jong, C.; Koning, C. E.; Duchateau, R. *Macromolecules* **2011**, *44*, 1132–1139. b) Hosseini Nejad, E.; Paoniasari, A.; Koning, C. E.; Duchateau, R. *Polym. Chem.* **2012**, *3*, 1308–1313.
156. Nejad, E. H.; van Melis, C. G. W.; Vermeer, T. J.; Koning, C. E.; Duchateau, R. *Macromolecules* **2012**, *45*, 1770–1776.

157. Jeske, R. C.; DiCiccio, A. M.; Coates, G. W. *J. Am. Chem. Soc.* **2007**, *129*, 11330–11331.

158. Jeske, R.; Rowley, J.; Coates, G. *Angew. Chem., Int. Ed.* **2008**, *47*, 6041–6044.

159. Darensbourg, D. J.; Holtcamp, M. W.; Struck, G. E.; Zimmer, M. S.; Niezgoda, S. A.; Rainey, P.; Robertson, J. B.; Draper, J. D.; Reibenspies, J. H. *J. Am. Chem. Soc.* **1999**, *121*, 107–116.

CHAPTER 5

AN EFFICIENT CATALYST BASED ON MANGANESE SALEN FOR HYDROSILYLATION OF CARBONYL COMPOUNDS

5.1. Introduction

Recently search for catalysts based on earth-abundant, inexpensive, and non-toxic metals has seen rapid growth, partly prompted by the rising cost of the commonly used precious metals in catalysis and concerns over their toxicity in the final products.¹⁶⁰ In particular, catalysis based on iron, one of the most abundant and readily available metals,¹⁶¹ has been extremely appealing.¹⁶² For example, a number of efficient iron-based catalysts have been reported for the reduction of carbonyl compounds by hydrosilanes, or hydrosilylation, an important transformation carried out conventionally with precious-metals.¹⁶³ The hydrosilylation reaction is atom economical, generating silylether protected alcohols in a single step, and can be employed as a convenient alternative to hydrogenation due to the mild nature and ease of handling of liquid hydrosilanes.¹⁶⁴ Therefore, a wide variety of efficient catalysts have appeared.¹⁶⁵ Besides iron, notable examples of reduction catalysts based on non-precious metals include titanium,¹⁶⁶ nickel,¹⁶⁷ copper,¹⁶⁸ zinc,¹⁶⁹ molybdenum and tungsten,¹⁷⁰ calcium¹⁷¹ and aluminum.¹⁷² Curiously, manganese, with the third largest global reserve (behind only iron and copper) at ~630 million metric tons,¹⁶¹ has received much less attention in these developments. It should be mentioned that manganese plays an essential role in biological systems as it is involved in several

Reproduced with the permission of Chidara *et al.* *Organometallics*, **2013**, 32, 5034–5037.
Copyright 2013 American Chemical Society.

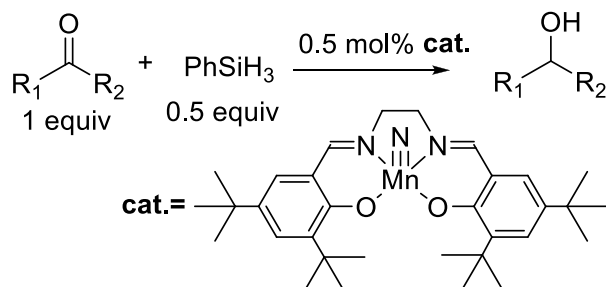
important oxidation reactions such as oxygen evolution.¹⁷³ Perhaps because of this, research on Mn has focused on its application in oxidation reactions such as alkene epoxidation.¹⁷⁴ However, its application in catalytic reduction is much less studied. Only a few low valent Mn(I) complexes bearing carbonyl ligands¹⁷⁵ and a Mn(III) complex¹⁷⁶ have been reported to catalyze hydrosilylation,¹⁷⁷ but they offer little opportunity for ligand modification and fine tuning.

Our interest in Mn-catalyzed reduction originates from the report that a high valent compound ($\text{ReO}_2\text{I}(\text{PPh}_3)_2$) of rhenium(V), a heavier congener of Mn, catalyzes the hydrosilylation of aldehydes and ketones.¹⁷⁸ This opens up a new venue for reduction catalysis,¹⁷⁹ and various rhenium and molybdenum complexes bearing multiply bonded oxo or imido groups have been shown to be effective in a number of reduction reactions,^{180,181,182} Although the mechanistic pathways may vary, catalytic reduction by high valent transition metal complexes has been extended to include ruthenium(VI)¹⁸³ and vanadium(V)¹⁸⁴ complexes. We became interested to see if high valent manganese compounds can catalyze such reductions given that manganese is abundant and inexpensive, and high valent manganese compounds are readily available as other neighbouring metals in groups 6–8.¹⁸⁵

5.2. Results and discussion

We focus on Mn^{V} that is isoelectronic with Mo^{IV} , Re^{V} , and Ru^{VI} , featuring a diamagnetic d^2 electron configuration. $[\text{MnN}(\text{salen-3,5-}^t\text{Bu}_2)]$ (**1**)¹⁸⁶ (catalyst in scheme **10**) is chosen as a model complex on the consideration that it is easily prepared and soluble in common organic solvents. The catalytic activity of **1** has been examined using

benzaldehyde and acetophenone as representative substrates under various reaction conditions (Table 7). Initial screening was carried out at ambient temperature without exclusion of air in a sealed



Scheme 10. General scheme representing the hydrosilylation of carbonyl compounds catalyzed by manganese salen complex.

NMR tube. Reduction of PhCOMe by PhSiH₃ was clearly observed; however, a somewhat capricious induction period marred the reaction. When the reaction was run under nitrogen and at elevated temperature, the reduction went smoothly. When PhCHO was employed, an induction period, albeit much shorter (~10–20 min), was still notable. The reaction seems to proceed similarly in either polar (CH₃CN) or non-polar (benzene) solvents, and can be conducted under neat conditions without solvent. The catalyst loading at 0.5 mol% level works well for both PhCHO and acetophenone.

We started the runs with excess PhSiH₃ (1.5 equivalents vs carbonyl substrate), but noted that even with 1.0 equivalent there was still unreacted PhSiH₃ after the complete consumption of PhCHO. Half equivalents of PhSiH₃ seem to be sufficient for the reduction (Table 7, entry 4). Further decrease in PhSiH₃ revealed that even 1/3 equivalent of PhSiH₃ was able to reduce most of PhCHO (Table 7, entry 6), at longer reaction times. Obviously, all of the three Si-H bonds in PhSiH₃ are being used for reduction. These observations prompted us to investigate other hydrosilanes. Indeed, a secondary silane, Ph₂SiH₂, and a tertiary silane, (EtO)₃SiH, are both effective in the reaction (Table 7, entries 7 & 8), and

the reduction was complete in less than 4 h for PhCHO. As expected, they are less reactive than the primary silane. However, when Et₃SiH was employed, no hydrosilylation was detected after 48 h (Table 7, entry **9**), though a color change of the reaction mixture can still be observed.

Table 7. Hydrosilylation of benzaldehyde and acetophenone.^a

Entry	Substrate	Silane (equiv)	Solvent	Temp (°C)	Time (h)	Conv. ^b (%)
1	PhCHO	PhSiH ₃ (1.0)	C ₆ D ₆	rt	47	>9
2	PhCHO	PhSiH ₃ (1.0)	C ₆ D ₆	80	0.33	>97
3	PhCHO	PhSiH ₃ (1.0)	CDCl ₃	rt	22	>97
4	PhCHO	PhSiH ₃ (0.5)	CDCl ₃	60	1.0	>97
5	PhCHO	PhSiH ₃ (0.5)	CD ₃ CN	80	0.33	>97
6	PhCHO	PhSiH ₃ (0.33)	CD ₃ CN	80	3.3	95
7	PhCHO	Ph ₂ SiH ₂ (0.5)	CD ₃ CN	80	3.3	>97
8	PhCHO	(EtO) ₃ SiH(1.0)	CD ₃ CN	80	2.5	>97
9	PhCHO	Et ₃ SiH(1.0)	CD ₃ CN	80	48	NR
10	PhCHO	PhSiH ₃ (0.5)	neat	80	5.0	70
11	PhCOMe	PhSiH ₃ (0.5)	CD ₃ CN	80	2.0	>97

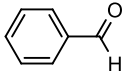
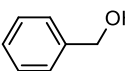
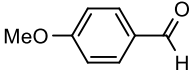
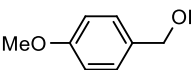
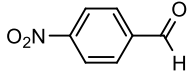
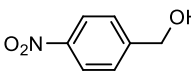
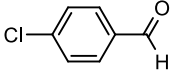
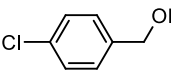
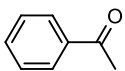
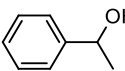
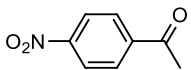
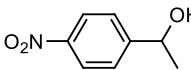
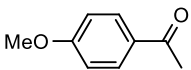
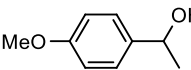
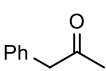
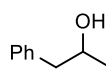
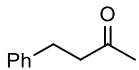
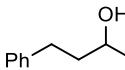
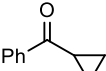
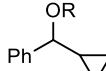
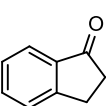
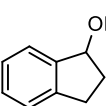
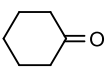
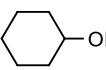
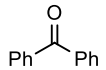
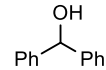
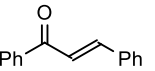
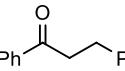
^aReaction conditions: substrate (0.4–1.0 mmol), silane, and MnN catalyst (0.5 mol %), under N₂ in J-Young NMR tube. ^bDetermined by ¹H NMR based on the consumption of PhCHO and PhCOMe.

Product analysis of the crude reaction mixture resulting from PhSiH₃ showed that the dialkoxy silanes were the major product. A small amount of the corresponding alcohols, mono- and trialkoxy silanes were also detected, based on the NMR and GC-MS analysis. With longer reaction time or higher temperature, the portion of trialkoxy silanes can be prevalent. In one experiment, the reduction of acetophenone was allowed to run for a prolonged period of time and the trialkoxy silane, (PhCH(Me)O)₃SiPh, was isolated as the major product (84%).

Having established the activity of a MnN catalyst in hydrosilylation, we chose 0.5 equivalents PhSiH₃ as the reducing reagent with 0.5 mol% of **1** as catalyst, to further investigate the scope and possible limitations of the present system. Several aliphatic and aryl carbonyl compounds including a series of benzaldehyde and acetophenone derivatives (Table 8) are readily reduced under standard conditions. The conversions were generally complete within 20 min for aldehydes and less than 3 h for ketones, and high yields of corresponding alcohols were obtained after workup. Functional groups such as halides, nitro, and methoxy are tolerated. Cyclopropyl phenyl ketone is reduced cleanly without formation of ring opening products (Table 8, entry **10**). Benzaldehydes with electron withdrawing groups at *para* positions are more readily reduced than those with electron donating groups. Particularly, it is observed that reduction of *p*-NO₂ benzaldehyde was extremely fast, even without heating. In comparison, the reduction of *p*-NO₂ acetophenone was very sluggish, taking up to two days without achieving full conversion (Table 8, entry **6**). It should be noted that reduction of an α,β -unsaturated ketone, chalcone (Table 8, entry **14**), leads to the isolation of 1,3-diphenyl-propan-1-one, apparently via a silyl enol ether intermediate formed by 1,4 addition of silane.

Various reaction pathways have been proposed for the high-valent transition metal based reduction catalysts, which may feature silane activation via 3+2 addition toward metal-oxo bond or η^2 -silane σ -adduct,^{180,187} and carbonyl activation by the Lewis acidic metal center.¹⁸⁸ Low valent rhenium may also be responsible for hydrosilylation with the oxorhenium(V) catalysts.¹⁸⁹ We are thus interested in gaining more insight on the reaction mechanisms of the present system. The absence of any ring opening product in the reduction of cyclopropyl phenyl ketone suggests that a radical mechanism is unlikely.¹⁹⁰

Table 8. Hydrosilylation of carbonyl compounds catalyzed by **1**.^a

Entry	Substrate	Product	Time (h)	Yield (%) ^b
1			0.33	>98 (95)
2			2.8	>98 (90)
3			1min	>98 (73)
4			0.3	>98 (87)
5			1.0 2.0	93 98 (91)
6			3.0	64 (58)
7			2.3	>98 (86)
8			1.5	97 (78)
9			3.3	98 (80)
10			2.0	>98 ^c
11			1.5	>98 (64 ^d)
12			2.0	>98 (75 ^e)
13			2.0	80 (73)
14			3.0	>98 (45 ^f)

^aReaction conditions: 0.40-1.0 mmol substrate, 0.5 equiv of PhSiH₃, catalyst **1** (0.5 mol%), under N₂, in heated acetonitrile (~80 °C). ^bThe conversions are based on NMR integration; isolated yields are in parenthesis. ^cMostly (PhCH(C₃H₅)O)₂SiHPh based on ¹H NMR. ^dA small amount of 1-indene is also detected after workup. ^eIsolated yield of trialkoxysilane PhSi(OCy)₃. ^fYield of isolated 1,3-diphenylpropan-1-one. Other products, 1, 3-diphenylprop-2-en-1-ol and 1,3-diphenylprop-2-ene, are observed in small amounts.

No reaction was noted between PhCHO and **1**, while stoichiometric reaction between **1** and PhSiH₃ shows a broadening of the NMR signal, accompanied by the color change from green of **1**, to reddish brown and then yellow, parallel to the observation under catalytic conditions. Moreover, a broad singlet peak between -1 and -3 ppm can be detected, with its position shifting upfield up to -2.8 ppm over time. The exact nature of such species is unclear at the moment; we tentatively assign it to a Mn-H species or a Mn-SiH adduct that is apparently in equilibrium with silane.¹⁹¹ Its appearance seems to correlate with the induction period, the reduction typically occurs after the color changed to yellow.

We explored the effect of electronics on rate of reduction by competition kinetics with a series of *para*-X-C₆H₄CHO derivatives (X = NO₂, COOMe, Cl, H, Me, and OMe) using the tertiary silane (EtO)₃SiH as the reductant. The Hammett plot (Figure 17) thus obtained shows a positive slope ($\rho = 0.46$), in agreement with the observation that electron withdrawing groups accelerate the reaction in the *para*-X-C₆H₄CHO series.

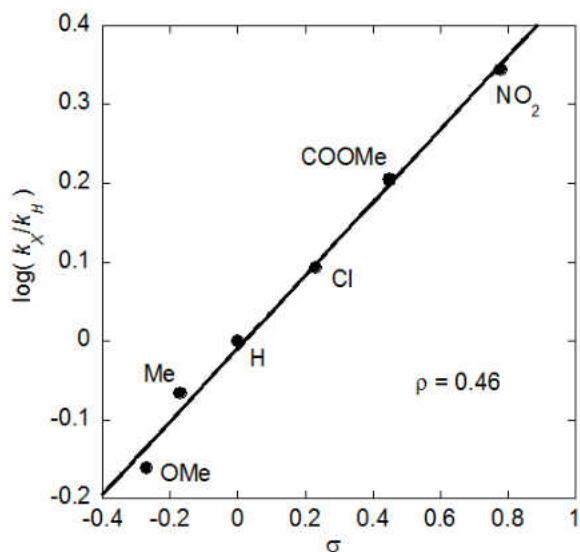


Figure 17. Hammett plot for benzaldehyde derivatives.

Based on these findings, we postulate that the catalytically active species is reduced Mn, possibly a Mn (III) hydride (or a silane adduct), that undergoes electrophilic attack by the carbonyl substrates (Scheme 10). The ρ value is similar to that observed for a low valent Re catalyzed hydrosilylation in which a Re hydride is identified as the key intermediate.¹⁸⁹ However, the nature of the active catalyst has not been identified, and a few questions remain to be addressed. Undoubtedly, more specific studies are required to reveal the mechanistic details.

5.3. Conclusions

In summary, we have described a manganese-salen based system that is effective for hydrosilylation of carbonyl substrates at low catalyst loadings (0.5 mol%) and tolerates functionalities such as halide, cyclopropyl, and nitro groups. Remarkably, the present catalyst features an earth abundant and inexpensive first-row transition metal, and a salen ligand framework that is readily tunable. Studies focusing on the development of this type of Mn based reduction catalysts, particularly for asymmetric reductions, and the mechanistic understanding are underway.

5.4. Experimental section

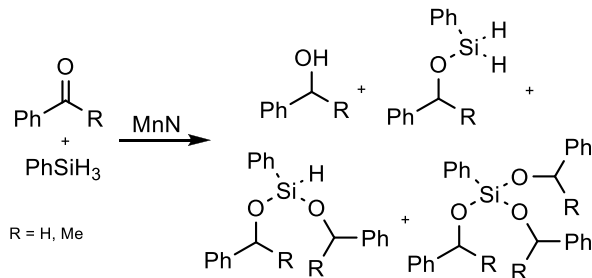
General. Manganese salen complexes were prepared according to the literature reports. All the substrates and reagents were obtained commercially and were degasified and dried over molecular sieves prior to the reaction. The ¹H and ¹³C NMR spectra were recorded on a Bruker AVANCE-500 NMR spectrometer and referenced to the residue peaks in CDCl₃ (7.26), CD₃CN (1.94), or C₆D₆ (7.16). GC-MS analyses were performed on an HP 5890 GC/HP 5971/B MSD system with electron impact ionization (70 eV) and a DB5 column

(30m x 0.53 mm ID, 0.25 μm thick; initial temperature 50 $^{\circ}\text{C}$, initial time 1 min; ramp rate 10 $^{\circ}\text{C}/\text{min}$; final temperature 310 $^{\circ}\text{C}$, final time 5 min or 20 min). High resolution mass spectrometry (HRMS) was performed using high-resolution time of flight G1969A instrumentation (Agilent, Santa Clara, CA, USA). UV-vis measurement was performed on a PerkinElmer Lambda 35 spectrophotometer.

Catalytic hydrosilylation. In a typical procedure, MnN catalyst-1 (2–3 mg, 0.5 mol%), substrate (~1 mmol, 2.0 equivalents), CD_3CN (0.30–0.35 mL), and PhSiH_3 (1 equivalent) were added to a J Young NMR tube, usually in that order. Trimethylphenylsilane was used as an internal standard (5–10 mol%). This was then heated in an oil bath at ~80 $^{\circ}\text{C}$ and the reaction progress was monitored by ^1H NMR at preset times. After the reaction was complete or nearly complete, the mixture was transferred to a round bottom flask with diethylether, and hydrolyzed with aqueous HCl or TBAF (tetrabutylammonium fluoride). A small aliquot of sample was taken and analyzed by GC-MS before and after the hydrolysis. After hydrolysis, the organic layer was extracted with ether and subjected to column chromatography using silica with hexane-EtOAc as eluent. The resultant products were characterized by ^1H NMR and GC-MS analysis in comparison with literature data or authentic samples.

Synthesis and Characterization of Manganese salen complex [MnN(salen-3,5- $^t\text{Bu}_2$)]

(1): The complex was prepared according to the literature.¹⁹² The data here were obtained to verify its identity. ^1H NMR (500 MHz, CDCl_3 , 298 K): δ 1.28 (s, 18H), 1.46 (s, 18H), 3.63 (d, $J=6.42$, 2H), 3.65 (d, $J=6.78$, 2H), 6.95 (br, 2H), 7.47 (s, 2H), 8.03 (s, 2H). ^1H NMR (500 MHz, C_6D_6 , 298 K): δ 1.38 (s, 18H, ^tBu), 1.81 (s, 18H, ^tBu), 2.55 (s, 4H, CH_2CH_2), 6.85 (s, 2H, ArH), 7.05 (s, 2H, ArH), 7.74 (s, 2H, N=CH).



Scheme 11. Initial products in Mn-catalyzed hydrosilylation.

Product Identification in Scheme 11:

Reduction of PhCHO: (PhCH₂O)₃SiPh: ¹H NMR (500MHz, CD₃CN, 298 K): δ 7.94 (d, J = 5.44, *ArH*, 2H), 7.54–7.32 (m, *ArH*, 18H), 5.03 (s, OCH₂Ph, 6H). GC/MS: t_R = 28.98 min; m/z 426 (M⁺), 335, 319, 257, 229, 167, 91(100), 65.

(PhCH₂O)₂SiHPh: GC/MS: t_R = 23.65 min; m/z 319 (M⁺), 243, 227, 211, 167, 137, 105, 91(100), 65, 51.

PhCH₂OH: GC/MS: t_R = 7.32 min; m/z 108 (M⁺), 91, 79 (100), 63, 51.

Reduction of PhCOMe: PhHSi(OCH(Me)Ph)₂:¹⁹³ It appears that all three possible diastereomers of PhHSi(OCH(Me)Ph)₂ are formed during the reaction, based on the apparent triplet of Si-H signals at around 5.3–5.5 ppm. The rough 1:2:1 ratio agrees with the statistical distribution of these diastereomers. ¹H NMR (500 MHz, C₆D₆, 298K) mixture of three diastereomers: δ = 7.82 (m, 2H, *ArH*), 7.40–7.10 (m, 12 H, *ArH*), 5.44 (s, 1H, *SiH*), 5.38 (s, 1H, *SiH*), 5.31 (s, 1H, *SiH*), 5.08 (m, 2H, OCH(Me)Ph), 1.51–1.44 (a few overlapping doublets, 3H, OCH(Me)Ph). GC/MS (70 eV): t_R = 22.97 min; m/z: 348 (M⁺), 333, 255, 243, 227, 199, 165, 139 (100), 123, 105, 91, 77.

(PhCH(Me)O)₃SiPh: ¹H NMR (500 MHz, CDCl₃, 298K) δ 7.48 (m, 3H, *ArH*), 7.40–7.10 (m, 17 H, *ArH*), 5.08–4.90 (m, 3H, OCH(Me)Ph), 1.40–1.20 (m, 9H, OCH(Me)Ph). ¹³C

NMR (125 MHz, CDCl₃, 298K): δ 144.75, 144.71, 144.65, 144.61, 133.90, 132.25, 130.38, 129.15, 127.06, 126.99, 126.60, 125.87, 125.78, 124.36, 124.34, 124.31, 124.29, 70.09 (OCH(Me)Ph), 25.57, 25.53, 25.43, 25.41 ((OCH(Me)Ph). GC/MS (70 eV): t_R = 27.64 min; m/z: 468 (M⁺), 453, 363, 333, 285, 270, 241, 227, 199, 165, 139 (100), 105 (100), 91, 77.

PhH₂Si(OCH(Me)Ph): t_R = 15.58 min; GC/MS (70 eV) m/z (%): 228 (M⁺), 213, 183, 167, 150, 135, 123 (100), 105, 91, 77, 51.

Characterization of products in Table 8:

Benzyl alcohol (entry 1): ¹H NMR (500 MHz, CDCl₃): δ 7.41–7.29 (m, 5H, ArH), 4.69 (s, PhCH₂OH, 2H), 1.60 (br, PhCH₂OH, 1H). GC/MS: t_R = 7.32 min; m/z 108 (M⁺), 91, 79 (100), 51.

4-Methoxybenzyl alcohol (entry 2): ¹H NMR (500MHz, CDCl₃; 298 K): δ 7.30 (d, J = 8.55, ArH, 2H), 6.91 (d, J = 8.55, ArH, 2H), 4.60 (s, -CH₂OH, 2H), 3.82 (s, -OMe, 3H), 2.04 (br, -CH₂OH, 1H). GC/MS: t_R = 11.01 min; m/z 138 (M⁺), 109.

4-Nitrobenzyl alcohol (entry 3): ¹H NMR (500MHz, CDCl₃, 298 K): δ 8.23 (d, J = 8.41, ArH, 2H), δ 7.55 (d, J = 8.41, ArH, 2H), δ 4.84 (s, -CH₂OH, 2H), δ 1.74 (br, -CH₂OH, 1H). GC/MS: t_R = 14.87 min; m/z 153 (M⁺), 136, 107, 94, 89, 77 (100).

4-Chlorobenzyl alcohol (entry 4): ¹H NMR (500 MHz, CDCl₃, 298 K): δ 7.57 (d, J = 8.62, Cl-C₆H₄-CH₂OH, 2H), 7.53 (d, J = 8.22, Cl-C₆H₄-CH₂OH, 2H), 4.88 (s, Cl-C₆H₄-CH₂OH, 2H), 2.72 (br, Cl-C₆H₄-CH₂OH, 1H). GC/MS: t_R = 11.0 min; m/z 142 (M⁺), 125, 107, 89, 79 (100).

4-Chlorobenzyl alcohol (entry 4): ^1H NMR (500MHz, CDCl_3 , 298 K): δ 7.57 (d, $J = 8.62$, ArH, 2H), 7.53 (d, $J = 8.22$, ArH, 2H), 4.88 (s, $-\text{CH}_2\text{OH}$, 2H), 2.72 (br, $-\text{CH}_2\text{OH}$, 1H). GC/MS: $t_R = 11.0$ min; m/z 142 (M^+), 125, 107, 89, 79 (100).

1-Phenyl ethanol (entry 5): ^1H NMR (500MHz, CDCl_3 , 298 K): δ 7.16-7.36 (m, ArH, 5H), 4.91 (q, $J = 6.6$, $-\text{CH}(\text{OH})\text{CH}_3$, 1H), 1.62 (br, $-\text{CH}(\text{OH})\text{CH}_3$, 1H), 1.29 (d, $J = 6.37$, $-\text{CH}(\text{OH})\text{CH}_3$, 3H). GC/MS: $t_R = 7.78$ min, m/z 122 (M^+), 107, 91, 79 (100), 51.

1-(4-Nitrophenyl)ethanol (entry 6): ^1H NMR (500MHz, CDCl_3 , 298 K): δ 8.33 (d, $J = 7.85$, ArH, 2H), δ 8.13 (d, $J = 7.85$, ArH, 2H), δ 5.30 (s, $-\text{CH}(\text{OH})\text{CH}_3$, 1H), δ 2.69 (s, $-\text{CH}(\text{OH})\text{CH}_3$, 3H). GC/MS: $t_R = 14.09$ min, m/z 167 (M^+), 150 (100), 120, 104, 76, 51.

1-(4-Methoxyphenyl)ethanol (entry 7): ^1H NMR (500MHz, CDCl_3 , 298 K): δ 7.30 (d, $J = 8.82$, ArH, 2H), 6.87 (d, $J = 8.81$, ArH, 2H), 4.85 (q, $J = 6.48$, $-\text{CH}(\text{OH})\text{CH}_3$, 1H), 3.81 (s, $-\text{OMe}$, 3H), 1.75 (br, $-\text{CH}(\text{OH})\text{CH}_3$, 1H), 1.48 (d, $J = 6.30$, $-\text{CH}(\text{OH})\text{CH}_3$, 3H). GC/MS: $t_R = 13.1$ min, m/z 152 (M^+), 137 (100), 119, 109, 94, 77, 65, 51.

1-Phenylpropan-2-ol (entry 8): ^1H NMR (500MHz, CDCl_3 , 298 K): δ 7.34 (t, $J = 8.82$, ArH, 2H), 7.25 (m, ArH, 3H), 4.05 (sex, $J = 6.33$, $-\text{CH}(\text{OH})\text{CH}_3$, 1H), 2.82 (dd, $J = 4.85$, $-\text{CH}_2\text{CH}(\text{OH})\text{CH}_3$, 1H), 2.74 (dd, $J = 4.70$, $-\text{CH}_2\text{CH}(\text{OH})\text{CH}_3$, 1H), 1.28 (d, $-\text{CH}_2\text{CH}(\text{OH})\text{CH}_3$, 3H). GC/MS: $t_R = 9.12$ min, m/z 136 (M^+), 121, 103, 92 (100), 77, 65, 51. The reaction mixture before hydrolysis mostly contains dialkoxysilane product with all three diastereomers: ^1H NMR (500MHz, CD_3CN , 298 K): δ 7.4-7.2 (m, ArH, 15H), 4.87 (s, SiH), 4.74 (s, SiH), 4.66 (s, SiH), 4.19 (m, OCH, 2 H), 2.75 (m, CH_2 , 4 H), 1.16 (m, CH_3 , 6H).

4-Phenyl-butan-2-ol (entry 9): ^1H NMR (500MHz, CDCl_3 , 298 K): δ 7.1-7.3 (m, ArH, 5H), 3.83 (m, $-\text{CH}_2\text{CH}_2\text{CH}(\text{OH})\text{CH}_3$, 1H), 2.75 (m, $-\text{CH}_2\text{CH}_2\text{CH}(\text{OH})\text{CH}_3$, 1H), 2.69 (m,

-CH₂CH₂CH(OH)CH₃, 1H), 1.78 (m, -CH₂CH₂CH(OH)CH₃, 2H), 1.26 (br, -CH₂CH₂CH(OH)CH₃, 1H), 1.22 (d, J = 6.30, -CH₂CH₂CH(OH)CH₃, 3H). GC/MS: t_R = 11.02 min; m/z 150 (M⁺), 132, 117 (100), 105, 91, 78

(PhCH(C₃H₅)O)₂SiHPh (entry 10). All three possible diastereomers of (PhCH(C₃H₅)O)₂SiHPh are observed as the major product for the reaction, based on the apparent triplet of Si-H signals at around 5.1–5.4 ppm. The rough 1:2:1 ratio is in agreement with the statistical distribution of these diastereomers. ¹H NMR (500 MHz, CD₃CN, 298K): δ = 7.82 (m, 2H, ArH), 7.60–7.20 (m, 13 H, ArH), 5.33 (s, 1H, SiH), 5.23 (s, 1H, SiH), 5.11 (s, 1H, SiH), 4.38 (m, 2H, OCH(C₃H₅)Ph), 1.29 (m, 2H, C₃H₅), 0.53 (m, 8H, C₃H₅). GC-MS (EI, 70 eV): t_R = 26.19 min; m/z = 399 ([M-1]⁺), 359, 269, 253, 223, 191, 165, 147, 131, 91(100), 77, 51. The reaction appears to be clean, with minimum amount of additional NMR signals. However, isolation of the products has been difficult, as it appears that they would decompose on the column. We were only able to isolate cyclopropyl phenyl methanol¹⁹⁴ in small amount (~21%) so far. ¹H-NMR (500 MHz, CDCl₃): 7.43 (d, 2H, ArH), 7.35 (t, 2H, ArH), 7.28 (t, 1H, ArH), 4.02 (d, 1H, OCH), 1.24 (m, 1H, CH in C₃H₅ ring), 0.65 (m, 1H, CH₂ in C₃H₅ ring), 0.56 (m, 1H, CH₂ in C₃H₅ ring), 0.49 (m, 1H, CH₂ in C₃H₅ ring), 0.39 (m, 1H, CH₂ in C₃H₅ ring). GC-MS (EI, 70 eV): t_R = 11.55 min; m/z = 148 (M⁺), 120 (100), 105, 91, 77. In any case, no ring opening product was noticed.

1-Indanol (entry 11): ¹H NMR (500MHz, CDCl₃, 298 K): δ 7.84 (m, 1H), 7.15–7.46 (m, ArH, 3H), 5.66 (s, ArCH(OH)-, 1H), 3.07 (br, ArCH₂, 1H), 2.81 (br, ArCH₂, 1H), 2.48 (br, ArCH(OH)CH₂-, 1H), 2.18 (br, ArCH(OH)CH₂, 1H). GC/MS: t_R = 10.49 min, m/z 134 (M⁺), 133 (100), 115, 105, 91, 77, 51. After hydrolysis and column, a small portion of

mixture of 1-indanol and 1-indene can be isolated. GC/MS for **1-Indene**: $t_R = 7.45$ min, m/z 116 (M^+), 89, 74, 63, 51.

PhSi(OCy)₃ (entry 12): 1H NMR (500MHz, $CDCl_3$, 298 K): δ 7.68 (d, $J = 6.56$, C_6H_5 , 2H), 7.35 (m, C_6H_5 , 3H), 3.90 (m, OCH, 3H), 1.83 (br, $C_6H_{11}O$, 6H), 1.71 (br, $C_6H_{11}O$, 6H), 1.48 (br, $C_6H_{11}O$, 6H), 1.40 (br, $C_6H_{11}O$, 6H), 1.21 (br, $C_6H_{11}O$, 6H).

1, 1-Diphenylmethanol (entry 13): 1H NMR (500MHz, $CDCl_3$, 298 K): δ 7.18–7.32 (m, ArH, 10H), 5.78 (s, -CH(OH)- C_6H_5 , 1H), 2.16 (br, -CH(OH)- C_6H_5 , 1H).

1, 3-Diphenylpropan-1-one (entry 14)¹⁹⁵: 1H NMR (500MHz, $CDCl_3$, 298 K): δ 7.96 (m, *o*-PhCO, 2H), 7.54 (m, ArH, 1H), 7.43 (m, ArH, 2H), 7.30-7.18 (m, ArH, 5H), 3.29 (t, $J = 7.28$, $PhCH_2CH_2C(O)Ph$, 2 H), 3.06 (t, $J = 7.28$, $C_6H_5CH_2CH_2C(O)C_6H_5$, 2 H). GC/MS: $t_R = 18.75$ min, m/z 210 (M^+), 115, 105 (100), 91, 77, 51. After hydrolysis and column, a small portion of mixture of 1, 3-diphenylprop-2-en-1-ol and 1, 3-diphenylprop-2-ene was isolated. **1, 3-Diphenylprop-2-en-1-ol (entry 14)**: GC/MS: $t_R = 19.7$ min, 210 (M^+), 181, 165, 131, 105(100), 77. **1, 3-Diphenylprop-2-ene (entry 14)**: GC/MS: $t_R = 21.39$ min, m/z 194 (M^+), 131, 116 (100), 105, 91, 77, 51.

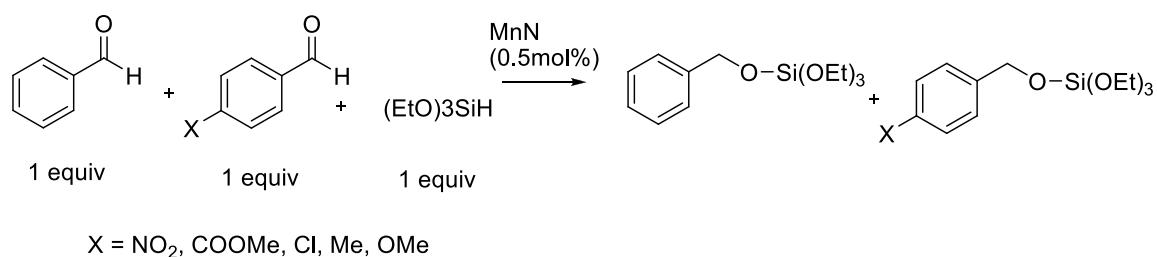
Table 9. Initial screening experiments of catalytic hydrosilylation of benzaldehyde and acetophenone.

entr y	substrate	catalyst (mol%)	silane (equiv)	solvent	N ₂ /air	temp (°C)	time	conv.
1	PhCOMe	1.0	PhSiH ₃ (1.5)	C ₆ D ₆	air	r. t.	4 d	>97%
2	PhCOMe	1.0	PhSiH ₃ (1.0)	C ₆ D ₆	air	r. t.	4 d	>97%
3	PhCOMe	0.5	PhSiH ₃ (0.5)	CD ₃ CN	air	80	5.6 h	94%
4	PhCHO	0.5	PhSiH ₃ (0.5)	CD ₃ CN	air	80	28 h	>97%

Competition reactions.¹⁹⁶ Following the general catalytic hydrosilylation procedure described above, 1 equivalent of *p*-X- C_6H_4CHO , 1 equivalent of parent PhCHO, 1 equivalent of (EtO)₃SiH in the presence of 0.5 mol% catalyst **1**, and 5 mol % PhSiMe₃, an

internal standard, were charged into a J-Young NMR tube under nitrogen with CD₃CN (0.30–0.35 mL). The tube was heated in an oil-bath preset at 80 °C. (EtO)₃SiH, instead of PhSiH₃, was used for the competition reaction because it gives only one hydrosilylation product. The reaction progress was monitored periodically by ¹H NMR until (EtO)₃SiH was consumed. The relative rates (k_X/k_H) were calculated based on the relative consumption of *p*-X-C₆H₄CHO vs PhCHO, which was determined by the integrations of the characteristic aldehydic peaks (*CHO*) at around 10 ppm. The results are summarized in Table 10.

Table 10. Data for competition reactions of benzaldehydes.



X	σ	k_X/k_H	$\log k_X/k_H$
NO ₂	0.78	2.21	0.34427435
MeOOC	0.45	1.60	0.204499824
Cl	0.23	1.24	0.093421685
Me	-0.17	0.86	-0.065956281
MeO	-0.27	0.69	-0.161780778

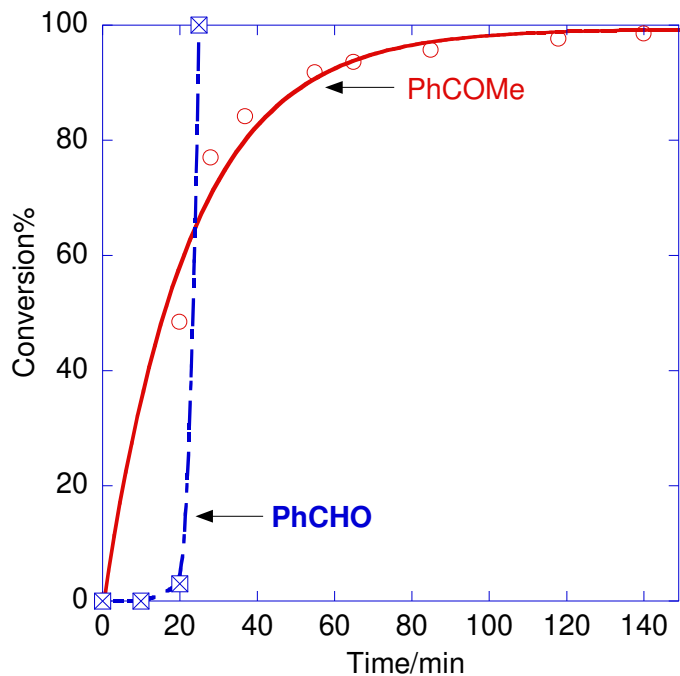


Figure 18. The conversion-time profile of PhCHO (blue hashed square) and PhCOMe (red circle) under standard conditions. The line for PhCHO is a smoothing function whereas the line for PhCOMe is an exponential fit. It appears that PhCHO has a clear induction period.

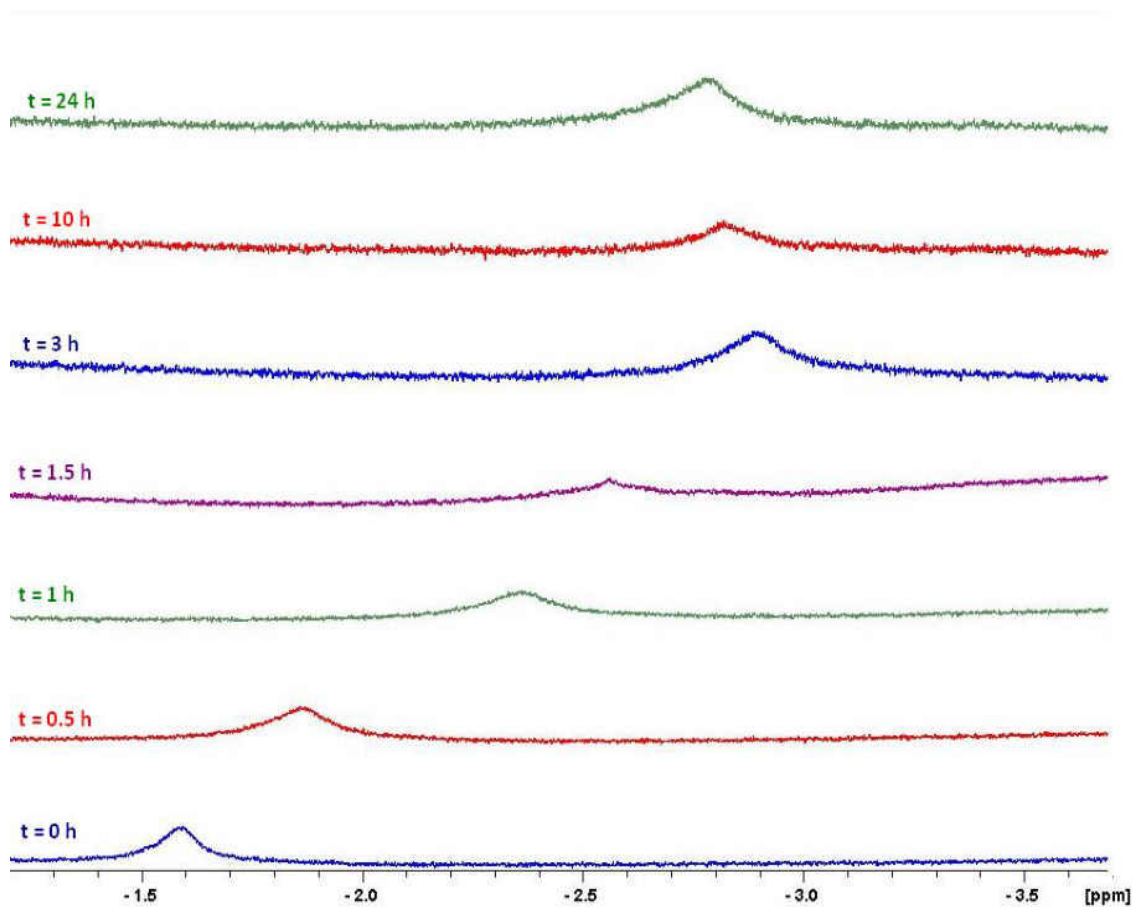


Figure 19. NMR for observed upfield peak. Conditions: 15 mg [MnN(salen-3,5-tBu₂)], 1.0 equivalent of PhSiH₃ in 0.55 mL CD₃CN at 80 °C.

5.5. References

160. (a) Bullock, R. M., Ed. *Catalysis without Precious Metals*, Wiley-VCH: Weinheim, Germany, **2010**. (b) Chirik, P. J.; Wieghardt, K. *Science*, **2010**, *327*, 794–795.
161. Ritter, S. K. *Chem. Eng. News* **2012**, *90*, 12–18.
162. (a) Gopalaiah, K. *Chem. Rev.* **2013**, *113*, 3248–3296. (b) Mancheno, O. G. *Angew. Chem. Int. Ed.* **2011**, *50*, 2216–2218. (c) Sun, C. -L.; Li, B. -J.; Shi, Z. -J. *Chem. Rev.* **2011**, *111*, 1293–1314. (d) Buchwald, S. L.; Bolm, C. *Angew. Chem. Int. Ed.* **2009**, *48*, 5586–5587. (e) Sherry, B. D.; Furstner, A. *Acc. Chem. Res.* **2008**, *41*, 1500–1511. (f) Tondreau, A. M.; Atienza, C. C. H.; Weller, K. J.; Nye, S. A.; Lewis, K. M.; Delis, G. P.; Chirik, P. J. *Science* **2012**, *335*, 567–570. (g) Casey, C. P.; Guan, H. *J. Am. Chem. Soc.* **2007**, *129*, 5816–5817.
163. (a) Yang, J.; Tilley, T. D. *Angew. Chem. Int. Ed.* **2010**, *49*, 10186–10188. (b) Warratz, S.; Postigo, L.; Royo, B. *Organometallics*, **2013**, *32*, 893–897. (c) Tondreau, A. M.; Lobkovsky, E.; Chirik, P. J. *Org. Lett.* **2008**, *10*, 2789–2792. (d) Langlotz, B. K.; Wadepohl, H.; Gade, L. H. *Angew. Chem. Int. Ed.* **2008**, *47*, 4670–4674. (e) Shaikh, N. S.; Enthaler, S.; Junge, K.; Beller, M. *Angew. Chem. Int. Ed.* **2008**, *47*, 2497–2501.
164. (a) Marciniak, B., Ed. *Hydrosilylation: A Comprehensive Review on Recent Advances*, Springer: The Netherlands, **2010**. (b) Ojima, I.; Li, Z.; Zhu, J. in *The Chemistry of Organic Silicon Compounds, Vol. 2*. (Eds.: Z. Rappoport, Y. Apeloig), Wiley: New York, **1998**, pp 1687–1792. (c) de Vries, J. G.; Elsevier, C. J., Ed. *The Handbook of Homogeneous Hydrogenation*, Wiley-VCH: Weinheim, Germany, **2007**, Vol. 1–3.
165. (a) Chakraborty, S.; Guan, H. *Dalton Trans.* **2010**, *39*, 7427–7439. (b) Riant, O.; Mostefai, N.; Courmarcel, J. *Synthesis*, **2004**, *18*, 2943–2958. (c) Carpentier, J. F.; Bette, V. *Curr. Org. Chem.* **2002**, *6*, 913–936.
166. Yun, J.; Buchwald, S. J. *J. Am. Chem. Soc.* **1999**, *121*, 5640–5644.
167. (a) Zheng, J.; Darcel, C.; Sortais, J.-B. *Catal. Sci. Technol.* **2013**, *3*, 81–84. (b) Tran, B. L.; Pink, M.; Mindiola, D. J. *Organometallics* **2009**, *28*, 2234–2243.
168. Diez-Gonzalez, S.; Nolan, S. P. *Acc. Chem. Res.* **2008**, *41*, 349–358.
169. (a) Das, S.; Wendt, B.; Moller, K.; Junge, K.; Beller, M. *Angew. Chem. Int. Ed.* **2012**, *51*, 1662–1666. (b) Das, S.; Addis, D.; Zhou, S.; Junge, K.; Beller, M. *J. Am. Chem. Soc.* **2010**, *132*, 1770–1771.
170. Bullock, R. M. *Chem. Eur. J.* **2004**, *10*, 2366–2374.
171. Spielmann, J.; Harder, S. *Eur. J. Inorg. Chem.* **2008**, 1480–1486.
172. Koller, J.; Bergman, R. G. *Organometallics* **2012**, *31*, 2530–2533.

-
173. (a) Ferreira, K. N.; Iverson, T. M.; Maghlaoui, K.; Barber, J.; Iwata, S. *Science* **2004**, *303*, 1831–1838. (b) Wu, A. J.; Penner-Hahn, J. E.; Pecoraro, V. L. *Chem. Rev.* **2004**, *104*, 903–938.
174. Jacobsen, E. N.; Zhang, W.; Muci, A. R.; Ecker, J. R.; Deng, L. *J. Am. Chem. Soc.* **1991**, *113*, 7063.
175. (a) Gregg, B. T.; Hanna, P. K.; Crawford, E. J.; Cutler, A. R. *J. Am. Chem. Soc.* **1991**, *113*, 384–385. (b) Mao, Z.; Gregg, B. T.; Cutler, A. R. *J. Am. Chem. Soc.* **1995**, *117*, 10139–10140. (c) Gregg, B. T.; Cutler, A. R. *J. Am. Chem. Soc.* **1996**, *118*, 10069–84. (d) Hanna, P. K.; Gregg, B. T.; Cutler, A. R. *Organometallics* **1991**, *10*, 31–33. (e) Mao, Z.; Gregg, B. T.; Cutler, A. R. *Organometallics* **1998**, *17*, 1993–2002. (f) Cavanaugh, M. D.; Gregg, B. T.; Cutler, A. R. *Organometallics* **1996**, *15*, 2764–2769. (g) Son, S. U.; Paik, S.-J.; Lee, I. S.; Lee, Y. -A.; Chung, Y. K.; Seok, W. K.; Lee, H. N. *Organometallics* **1999**, *18*, 4114–4118. (h) Son, S. U.; Paik, S.-J.; Chung, Y. K. *J. Mol. Cat. A: Chem.* **2000**, *151*, 87–90. (i) Hilal, H. S.; Suleiman, M. A.; Jondi, W. J.; Khalaf, S.; Masoud, M. M.; *J. Mol. Cat. A: Chem.* **1999**, *144*, 47–59.
176. Magnus, P.; Fielding, M. R. *Tetrahedron Lett.* **2001**, *42*, 6633–6636.
177. It should be mentioned that reports of Mn based hydrosilylation catalysts have appeared very recently in patent literature. (a) Tondreau, A. M.; Chirik, P. J.; Delis, J. G. P.; Weller, K. J.; Lewis, K. M.; Nye, S. A. U.S. Pat. Appl. Publ. **2012**, US 20120130021 A1 20120524. (b) Delis, J. G. P.; Nye, S. A.; Lewis, K. M.; Weller, K. J.; Chirik, P. J.; Tondreau, A. M.; Russell, S. K. U.S. Pat. Appl. Publ. **2011**, US 20110009573 A1 20110113.
178. Kennedy-Smith, J. J.; Nolin, K. A.; Gunterman, H. P.; Toste, F. D. *J. Am. Chem. Soc.* **2003**, *125*, 4056–4057.
179. Thiel, W. R. *Angew. Chem. Int. Ed.* **2003**, *42*, 5390–5392.
180. (a) Sousa, S. C. A.; Cabrita, I.; Fernandes, A. C. *Chem. Soc. Rev.* **2012**, *41*, 5641–5653. (b) Du, G.; Abu-Omar, M. M. *Curr. Org. Chem.* **2008**, *12*, 1185–1198.
181. For examples of molybdenum based catalysts, see: (a) Ziegler, J. E.; Du, G.; Fanwick, P. E.; Abu-Omar, M. M. *Inorg. Chem.* **2009**, *48*, 11290–11296. (b) Peterson, E.; Khalimon, A. Y.; Simionescu, R.; Kuzmina, L. G.; Howard, J. A. K.; Nikonov, G. I. *J. Am. Chem. Soc.* **2009**, *131*, 908–909. (c) Maddani, M. R.; Moorthy, S. K.; Prabhu, K. R. *Tetrahedron* **2010**, *66*, 329–333. (d) Fernandes, A. C.; Romao, C. C. *Tetrahedron Lett.* **2005**, *46*, 8881–8883. (e) Shirobokov, O. G.; Gorelsky, S. I.; Simionescu, R.; Kuzmina, L. G.; Nikonov, G. I. *Chem. Commun.* **2010**, *46*, 7831–7833. (f) Reis, P. M.; Romao, C. C.; Royo, B. *Dalton Trans.* **2006**, 1842–1846.
182. For examples of rhenium based catalysts, see: (a) Nolin, K. A.; Krumper, J. R.; Pluth, M. D.; Bergman, R. G.; Toste, F. D. *J. Am. Chem. Soc.* **2007**, *129*, 14684–14696. (b) Du, G.; Fanwick, P. E.; Abu-Omar, M. M. *J. Am. Chem. Soc.* **2007**, *129*, 5180–5187. (c) de Noronha, R. G.; Romao, C. C.; Fernandes, A. C. *J. Org. Chem.* **2009**, *74*, 6960–

-
6964. (d) Cabrita, I.; Fernandes, A. C. *Tetrahedron* **2011**, *67*, 8183-8186. (d) Nolin, K. A.; Ahn, R. W.; Kobayashi, Y.; Kennedy-Smith, J. J.; Toste, F. D. *Chem. Eur. J.* **2010**, *16*, 9555–9562. (e) Nolin, K. A.; Ahn, R. W.; Toste, F. D. *J. Am. Chem. Soc.* **2005**, *127*, 12462–12463.
183. (a) Abbina, S.; Bian, S.; Oian, C.; Du, G. *ACS Catal.* **2013**, *4*, 678-684. (b) Truong, T. V.; Kastl, E. A.; Du, G. *Tetrahedron Lett.* **2011**, *52*, 1670–1672.
184. (a) Cabrita, I.; Sousa, S. C. A.; Fernandes, A. C. *Tetrahedron Lett.* **2010**, *51*, 6132–6135. (b) Pehlivan, L.; Metay, E.; Laval, S.; Dayoub, W.; Delbrayelle, D.; Mignani, G.; Lemaire, M. *Eur. J. Org. Chem.* **2011**, *36*, 7400–7406.
185. (a) Berry, J. F.; *Comm. Inorg. Chem.* **2009**, *30*, 28-66. (b) Eikey, R. A.; Abu-Omar, M. M. *Coord. Chem. Rev.* **2003**, *243*, 83–124.
186. Yiu, S. M.; Lam, W. W. Y.; Ho, C. M.; Lau, T. C. *J. Am. Chem. Soc.* **2007**, *129*, 803–809.
187. For computational studies on the mechanisms, see: (a) Chung, L. W.; Lee, H. G.; Lin, Z.; Wu, Y. –D. *J. Org. Chem.* **2006**, *71*, 6000–6009. (b) Calhorda, M. J.; Costa, P. J. *Dalton Trans.* **2009**, 8155–8161. (c) Drees, M.; Strassner, T. *Inorg. Chem.* **2007**, *46*, 10850–10859. (d) Costa, P. J.; Romao, C. C.; Fernandes, A. C.; Royo, B.; Reis, P. M.; Calhorda, M. J. *Chem. Eur. J.* **2007**, *13*, 3934–3941. (e) Gu, P.; Wang, W.; Wang, Y.; Wei, H. *Organometallics* **2013**, *32*, 47–51.
188. (a) Shirobokov, O. G.; Kuzmina, L. G.; Nikonov, G. I. *J. Am. Chem. Soc.* **2011**, *133*, 6487–6489. (b) Khalimon, A. Y.; Ignatov, S. K.; Simionescu, R.; Kuzmina, L. G.; Howard, J. A.; Nikonov, G. I. *Inorg. Chem.* **2012**, *51*, 754–756. (c) Khalimon, A. Y.; Shirobokov, O. G.; Peterson, E.; Simionescu, R.; Kuzmina, L. G.; Howard, J. A.; Nikonov, G. I. *Inorg. Chem.* **2012**, *51*, 4300–4313.
189. Smeltz, J. L.; Boyle, P. D.; Ison, E. A. *Organometallics* **2012**, *31*, 5994–5997.
190. Yang, D.; Tanner, D. D. *J. Org. Chem.* **1986**, *51*, 2267–2270.
191. (a) Sun, J.; Lu, R. S.; Bau, R.; Yang, G. K. *Organometallics* **1994**, *13*, 1317–1325. (b) Schubert, U. *Adv. Organomet. Chem.* **1990**, *30*, 151–187.
192. S. M. Yiu, W. W. Y. Lam, C. M. Ho, T. C. Lau, *J. Am. Chem. Soc.* **2007**, *129*, 803–809.
193. Spielmann, J.; Harder, S. *Eur. J. Inorg. Chem.* **2008**, 1480–1486.
194. Dieskau, A. P.; Begouin, J.-M.; Plietker, B. *Eur. J. Org. Chem.* **2011**, (27), 5291–5296.
195. Fox, D. J.; Pedersen, D. S.; Warren, S. *Org. Biomol. Chem.* **2006**, *4*, 3102–3107.

196. Smeltz, J. L.; Boyle, P. D.; Ison, E. A. *Organometallics* **2012**, *31*, 5994–5997.

CHAPTER 6

VERSATILE MANGANESE CATALYSIS FOR THE SYNTHESIS OF POLYSILYLEETHERS FROM DIOLS AND DICARBONYLS WITH HYDROSILANES

6.1. Introduction

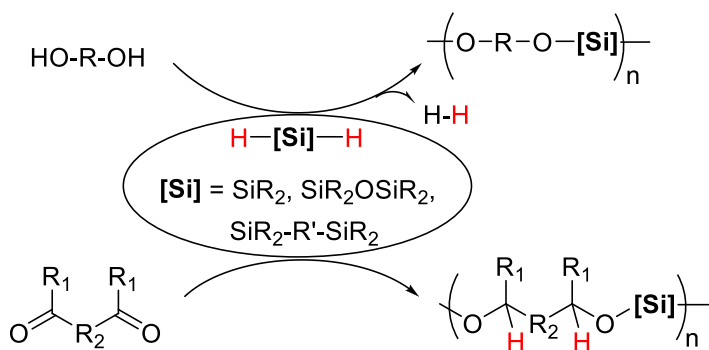
Polymers with silicon in the main chain have received much attention in organic and material chemistry due to their various industrial and academic applications.^{197,198} Polysilanes with Si-Si repeating units are promising in organic electronic devices because of their conductivity.¹⁹⁹ Poly(siloxane)s with Si-O-Si linkages and their copolymers are used extensively as elastomers, plastics and in other industrial applications because of their low-temperature flexibility and high temperature stability.^{200,201} Hydro-sensitive silicon polymers can be used in the medical applications such as controlled released of drugs.²⁰² Poly(siloxane)s can serve as the precursors to synthesize silicon oxy carbides (SiOC) via pyrolysis and direct photo-crosslinking methods.²⁰³ The Si-O-C ceramic has been applied in coatings and as electrode materials in lithium batteries.²⁰⁴ Recently there has been renewed interest in silicon-containing polymers, particularly poly(silylether)s with Si-O-C linkages, on account of their sustainability.²⁰⁵ Silicon and oxygen are practically inexhaustible due to their abundance and carbon can be more readily sourced from biomass. The Si-O-C linkages are hydrolytically degradable, different from the biodegradable ester linkages that typically requires enzymes for degradation. This makes the poly(silylether)-based materials attractive in short-term and/or single use

applications.²⁰⁶ Importantly, the degradation behavior, along with the thermomechanical properties, can be adjusted by changing substituent groups on silicon and/or carbon backbones of poly(silylether)s,²⁰⁷ and by copolymerization with other segments.²⁰⁸

Synthetically, poly(silylether)s have been prepared by various methods depending on the nature of the actual linkages. Similar to the synthesis of silylethers, reaction of dichlorosilanes with diols through polycondensation leads to formation of poly(silylether)s.²⁰⁹ Chlorosilanes can also react with bis(epoxide)s and bis(oxetane)s through additions catalyzed by quaternary onium salts to afford poly(silylether)s.^{210,211,212} However, use of chlorosilanes has limitations.²¹³ Chlorosilanes are moisture sensitive and usually produce hydrochloric acid and other unwanted byproducts in polymerization reactions that require additional methods for separation, which makes it an expensive process.²¹⁴ To overcome these problems, chlorosilanes have been replaced with diamino- and dialkoxysilanes as the coupling partners; in particular, diphenoxy- and dianilinosilanes have shown good activity towards the synthesis of high molecular weight polymers.²¹⁵ Still these methods may have limited substrate scope or require maintaining high-temperature conditions (200–300 °C) throughout the reaction.^{216,217}

Alternatively, hydrosilanes have been deemed an optimal replacement for chlorosilanes because of their stability to air and ease of handling. Reactions with diols through dehydrogenative coupling²¹⁸ and with dicarbonyls through hydrosilylation polymerization²¹⁹ afford a variety of poly(silylether)s (Scheme 12). More significantly, these methods are highly atom economical, producing H₂ as the sole byproduct or no byproduct. In general, these reactions are effected by catalysts derived from expensive transition metals, usually ruthenium, palladium, and rhodium.^{218,219,220} However, high cost,

low abundance of metals and high catalyst loading (up to 10 mol%) are the main drawbacks of these methods.²²¹ Other catalysts based on boranes²²² and alkali metals^{205a,223} are also known. Recently the catalytic systems derived from abundant metals such as iron have been reported.²²⁴



Scheme 12. Poly(silylether)s from hydrosilanes.

We have been interested in the high-valent transition metal complexes for their roles in catalytic reductions and silane activation.²²⁵ We found that an air-stable and easily prepared salen-manganese complex $[\text{MnN}(\text{salen}-3,5\text{-}^t\text{Bu}_2)]$ ²²⁶ (**1**) is an effective catalyst for hydrosilylation of carbonyl compounds and dehydrogenative coupling of hydroxyl compounds with hydrosilanes.²²⁷ Encouraged by these results, we sought to synthesize poly(silylether)s from a variety of diols and dicarbonyls under manganese catalysis. Furthermore, taking advantage of the dual activity of **1**, substrates with mixed functional groups have been used in the reaction with hydrosilanes to generate poly(silylether)s. No metal catalyst has been reported that could catalyze the synthesis of poly(silylether)s from all three types of substrates (diols, dicarbonyls and hydroxyl carbonyl) with hydrosilanes.

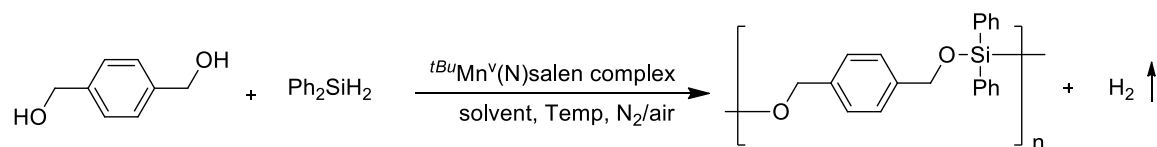
6.2. Results and discussion

6.2.1. Optimization reactions. Our initial experiments started with optimizing suitable reaction conditions for the polycondensation of diols and disilanes. 1,4-

Benzenedimethanol and diphenylsilane were chosen as the representative coupling partners in the presence of catalytic amounts of manganese complex **1** (1 mol%), and selected results are presented in Table 11. Based on the conditions in our previous work, reaction was first performed using acetonitrile as the solvent at reflux temperature (Table 11, entry **1**). As expected, the initial green color of the reaction mixture arising from **1** turned brown, indicating onset of the reaction. After 12 h, ¹H NMR spectroscopy showed greater than 95% conversion of diphenylsilane. Despite of the high conversion, however, the number average molecular weight (M_n) of the polymer was determined by GPC as 4000 g/mol (M_w/M_n 1.5). To improve M_n , several solvents were next screened. When acetonitrile was replaced by tetrahydrofuran (THF) (Table 11, entry **2**), low M_n (1850 g/mol) polymers were obtained with only 50 % conversion of diphenylsilane in 12 h. Use of 1,4-dioxane as solvent resulted in 95 % conversion and high molecular weight (M_n 7900 g/mol) (Table 11, entry **3**), suggesting that the coordination ability of cyclic ethers might not be the main culprit for the low conversion observed with THF. Reaction in refluxing toluene led to even higher M_n (9200 g/mol) within 12 h (Table 11, entry **4**). Given the above observations, it seemed that the reaction temperature played a key role in the polymerization reaction. Indeed, reaction performed at ambient temperature in toluene showed no reaction even after 48 h, and the green color remained the same during the period (Table 11, entry **5**). Finally, as air extrusion seemed to have little effect in our previous dehydrogenative coupling,²²⁷ a reaction was performed under air in refluxing toluene for convenience (Table 11, entry **6**). However, conversion of monomers remained only 58% even after extending the reaction time to 48 h, and M_n also dropped by half (4500 g/mol, 1.15 PDI). These results

suggested the importance of inert conditions for the generation of high molecular weight polymers.

Table 11. Dehydrogenative coupling of 1,4-benzenedimethanol with diphenylsilane.^a



Entry	Solvent ^b	Temp	Condition	t (h)	Conv. %	M_n (g/mol) ^c	M_w/M_n ^c
1	CD ₃ CN	reflux (81)	Under N ₂	12	> 95	4000	1.28
2	THF	reflux (66)	Under N ₂	12	50	1850	1.36
3 ^d	1,4-Dioxane	reflux (101)	Under N ₂	20	> 95	7900	1.57
4 ^e	Toluene	reflux (110)	Under N ₂	12	> 95	9200	1.66
5	Toluene	25 °C	Under N ₂	48	0	-	-
6	Toluene	reflux (110)	In air	48	58	4500	1.15

^aReaction conditions: substrate (0.8–0.9 mmol), silane – 1 equivalent and MnN catalyst – 1.0 mol%. ^b solvent used was 2.4–2.8 ml. ^cDetermined by GPC instrument. ^dYield – 75.9%. ^eYield – 75.6%.

The brown-colored reaction mixtures of two reactions (Table 11, entries 3 and 4) were later purified by precipitation with methanol from a CH₂Cl₂ solution of the reaction mixture. The resulting whitish-gray poly(silylether)s were obtained in 75% yields. In the ¹H NMR spectrum, disappearance of hydroxyl groups at 2.0 ppm and silane hydrogens at 4.84 ppm, and the shift of benzylic protons from 4.65 to 4.81 ppm suggested the formation of poly(silylether) of 1,4-benzenedimethanol and diphenylsilane (Figure 20). ¹³C NMR spectrum also supported the formation of poly(silylether), as only six peaks in aromatic region (129.71 to 139.47 ppm, four from silane two from substrate) and one peak at 64.98 ppm (benzylic carbon) were observed. In addition, the absence of both the hydroxyl (3500 cm⁻¹) and SiH groups (2133 cm⁻¹) in the FT-IR spectra further supported the NMR

assignments (Figure 21). The characteristic stretching frequency at $\sim 1040\text{ cm}^{-1}$ indicated the formation of Si–O–C connections.

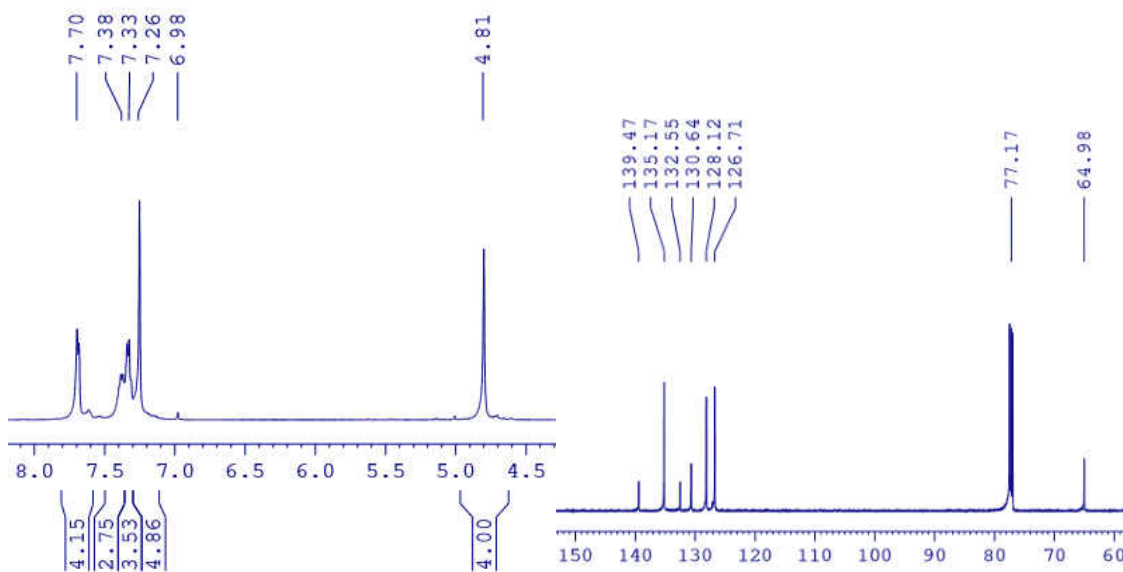


Figure 20. ^1H (left) and ^{13}C (right) NMR of the poly(silylether) from 1,4-benzenedimethanol and diphenylsilane.

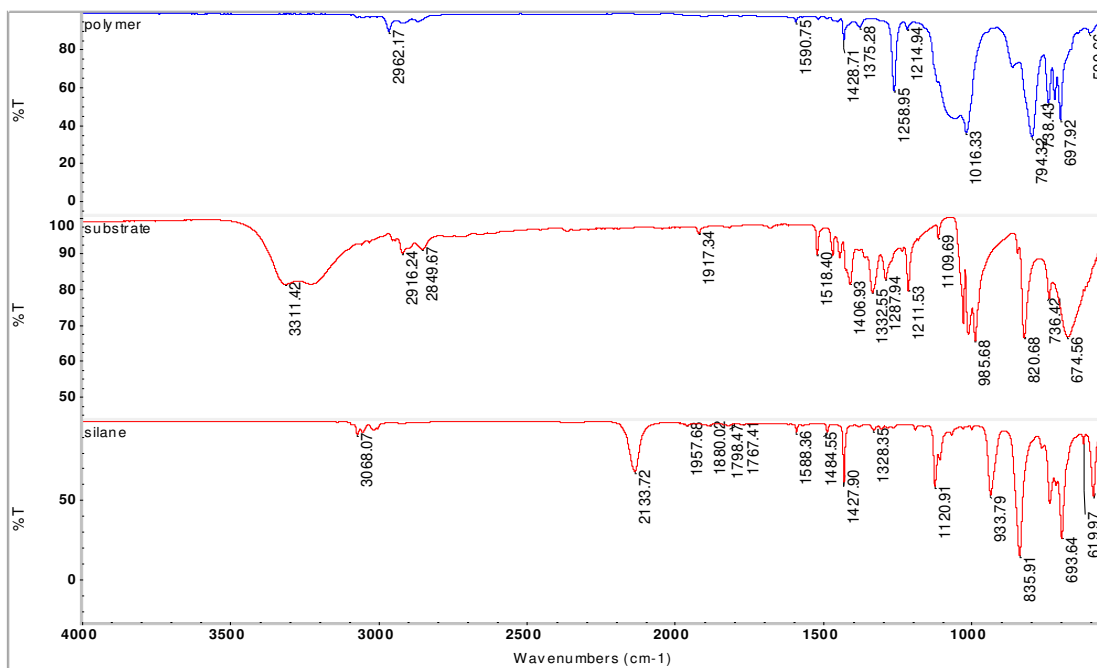


Figure 21. FT-IR spectra of 1,4-benzenedimethanol, diphenylsilane and their poly(silylether).

6.2.2. Step-growth polymerization. Before going to the various substrates, we performed a set of reactions in refluxing toluene under nitrogen between 1,4-benzenedimethanol and diphenylsilane to explore the correlation between conversion, time, and molecular weight of the polymer (Figure 22 and 23). During the reaction, samples were taken at each time interval and were subjected to analysis by NMR and GPC. Conversion of reactants was 19% in 1 h and reached around 50% in 4 h. However, at this point, the molecular weight of the polymer was only 1600 g/mol (M_w/M_n 1.33) indicating mostly oligomers were formed in the starting hours. At 8 h, the conversion increased slowly to 91% with M_n 4600 g/mol and at 22 h, the conversion was 96% with 13000 g/mol. The sharp increase in the molecular weight in the later stage of the reaction suggested that the oligomers formed in the initial reaction time were still active and were later incorporated to form long chain polymers. The behavior is typical of step-growth polymerization reactions.²²⁸ The non-linear growth of the dispersities also supported that these are step-growth type polymerization reactions.

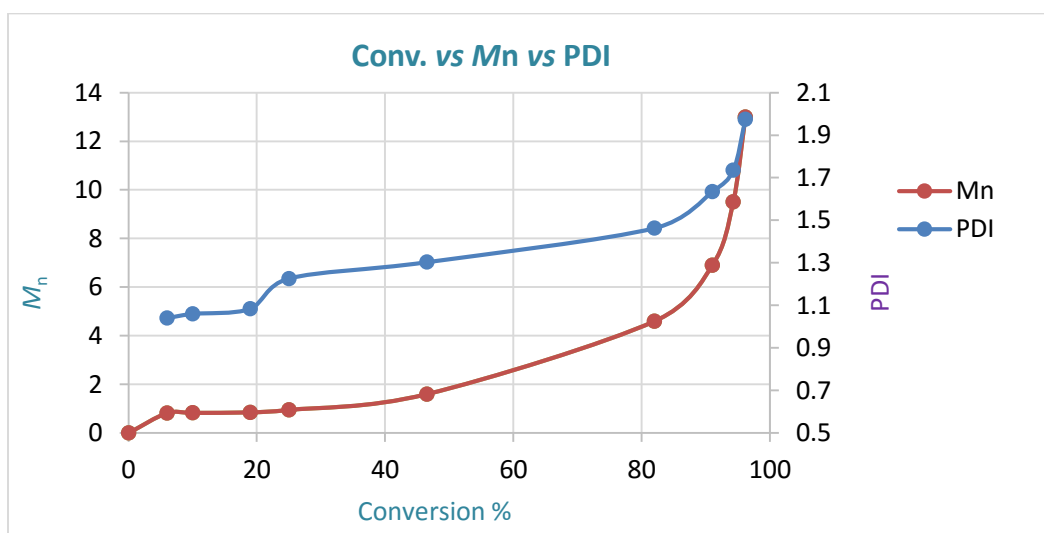


Figure 22. Conversion vs molecular weight of 1,4-benzenedimethanol and diphenylsilane poly(silylether)

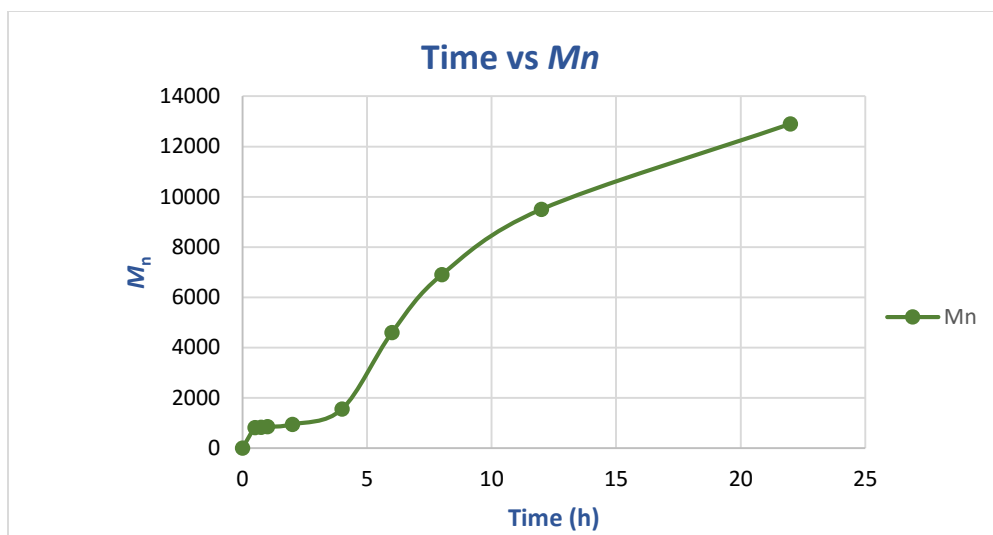
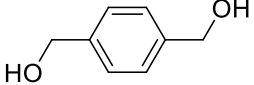
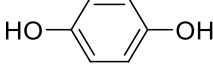
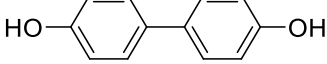
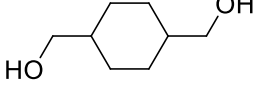
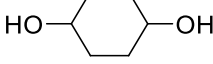
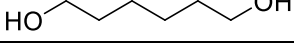


Figure 23. Time profile for 1,4-benzenedimethanol and diphenylsilane poly(silylether).

6.2.3. Substrate scope: Diols. To extend the substrate scope, we first chose a simple aryl diol 1,4-benzenediol (1,4-hydroquinone), because polymers with π -conjugated groups in the main or side chains have high interest for their prospective applications as electronic, photoic and ceramic materials (Table 12, entry **2**).²²⁹ Copolymerization reaction between 1,4-benzenediol and a disiloxane (1,3-bis(diethylamino)tetramethyldisiloxane) at melt conditions was reported in the literature, however the reported molecular weight of the polymer was low (M_n 3600 g/mol).^{209c} In our current dehydrogenative coupling process between, 4-benzenediol and diphenylsilane the silane conversion of more than 95 % was observed in 12h, and a white solid was obtained in 80% yield after purification. The disappearance of both hydroxyl and silicon hydrogen peaks in both ^1H NMR and FT-IR spectroscopies confirmed the formation of the expected poly(silylether). In the ^{29}Si NMR spectrum, a single peak at -37.42 ppm was observed. GPC analysis showed high molecular weight polymer with M_n 15000 g/mol (M_w/M_n 2.4). To expand on aryl diols, a dehydrogenative coupling reaction between a highly π -conjugated biphenyl-4,4'-diol (4,4'-bisphenol) and diphenylsilane was performed (entry **3**) under same conditions. The

conversion reached 95% in 15h and a whitish-gray polymer was obtained in 88% yield after purification. However, low molecular weight polymers ($M_n = 7200$ g/mol, PDI = 1.86) were obtained, which suggest that substrates with high π -conjugation are less active in this polymerization reaction.

Table 12. Dehydrogenative coupling of symmetrical diols with diphenylsilane.^a

Entry	Substrate	t (h)	M_n (g/mol) ^b	M_w/M_n ^b	Yield % ^c
1		12	9200	1.66	76
2		12	15000	2.38	80
3		15	7200	1.87	88
4		20	5100	1.41	62
5		20	3060	1.73	70
6		26	11400	2.00	84

^aReaction conditions: substrate (0.8–0.9 mmol), silane – 1 equivalent and MnN catalyst – 1.0 mol%. The reactions were carried out in refluxing toluene under N₂ and the conversions of silane were greater than 95%. ^b Determined by GPC instrument. ^c Based on the ¹H NMR and weight of the purified polymer.

Next, we carried out polycondensation reactions with aliphatic diols, namely 1,4-cyclohexanedimethanol and 1,4-cyclohexanediol (Table 12, entries **4** and **5**). These two substrates can be viewed as the aliphatic analogs of 1,4-benzenedimethanol and 1,4-benzenediol respectively. Reaction between the primary diol 1,4-cyclohexanedimethanol and diphenylsilane was monitored up to 24 h, by which time a silane conversion of 90% was achieved. Purification afforded the corresponding polysilylether with 64% isolated yield, and the observed M_n was 5700 g/mol, PDI = 1.4. Reaction with a bulkier secondary diol, 1,4-cyclohexanediol required longer reaction times, as only 80% conversion was

achieved after 48 h, although the isolated yield was 70%. Given the slow conversion, it was not surprising that the molecular weight of the resulting polymer was rather low, $M_n = 2700$ g/mol (PDI = 2.2). In agreement with the low molecular weight, a peak at 5.46 ppm was observed in the ^1H NMR spectrum, which could be attributed to the tertiary Si–H end groups in the polymer. Multiple peaks in ^{29}Si NMR also support the presence of Si–H units in the polymer structure. Our previous results showed that diphenylsilane could react with secondary alcohols but the second step was considerably slower than the first step.²²⁷ Similarly here the steric hindrance plays a vital role in these two polycondensation reactions as reflected in the extended reaction times and low molecular weights of the polymers.

Conversely, when 1,6-hexanediol was used as the substrate, a high molecular weight polymer ($M_n = 11400$ g/mol) was produced in high yields (Table 12, entry **6**). These results suggest that sterically less hindered monomers will react quickly to give the high molecular weight polymers. On the other hand, when another monomer 1,4-butanediol was used, cyclic silylether was obtained as the main product rather than poly(silylether)s.²²⁷ Obviously a rigid and/or long linker between the two hydroxyl groups of diols is conducive to the formation of poly(silylether)s.

6.2.4. Dicarboxyls. Considering our previous result that the manganese complex **1** is also an efficient catalyst for the hydrosilylation of organic carbonyls,²²⁵ we decided to apply the current system to dicarbonyl compounds for the synthesis of poly(silylether)s. In this study, benzene-1,4-dicarboxaldehyde (terephthalaldehyde) was chosen as the reaction partner with diphenylsilane, in part because the resulting polymer should be same as the polymer obtained from 1,4-benzenedimethanol (Table 12, entry **1** vs Table 13, entry **1**). Under

similar conditions, the consumption of terephthalaldehyde and the hydrosilylation of the carbonyl group were confirmed by the appearance of benzylic signals at 4.81 ppm in ^1H NMR and 65.0 ppm in ^{13}C NMR. The conversion of terephthalaldehyde reached 90% in 24 h, after which workup by precipitation gave 58% isolated yield. The FT-IR spectrum of the polymer showed the disappearance of C=O stretching frequency at 1663 cm^{-1} and of silane hydrogens at 2134 cm^{-1} and a single peak at -30.29 was observed in ^{29}Si NMR. These spectroscopic data are highly comparable with the data resulting from 1,4-benzenedimethanol. The main difference is that the molecular weight was low, $M_n = 2400$ g/mol with PDI = 1.86. The low molecular weight is believed to come from the less active nature of carbonyls in comparison to the hydroxyl groups. This difference in reactivity with hydrosilanes has been observed in other systems in the literature and is proposed to be a result of enhanced electrophilicity in hydroxyls. To further compare the activity of dicarbonyl monomers with diols, reactions were performed with 1,6-hexanedial and 1,4-cyclohexanedione, the analogous structures of 1,6-hexanediol and 1,4-cyclohexane diol respectively (Table 13, entries **2** and **3**). As expected, reaction with 1,6-hexanedial took 24 h to reach 90% conversion and the isolated yield was only 40%; it took even longer (48 h) for 1,4-cyclohexanedione to reach 90% conversion with a slightly higher isolated yield (49%). Both reactions resulted in low molecular weight polymers, $M_n = 1800$ and 2100 g/mol, respectively, consistent with the slow rate of reaction. The low yields in these reactions, despite of the >90% conversion, might be a result of the increased presence of short chain oligomers in these reactions that were lost during the precipitation process.

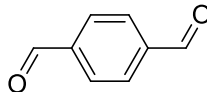
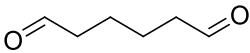
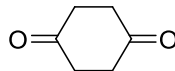
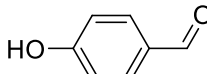
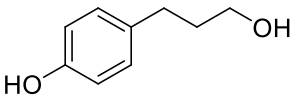
Entry	Substrate	t (h)	M_n (g/mol) ^b	M_w/M_n ^b	Yield % ^c
1		24	2400	1.88	58
2		24	1800	1.59	40
3		48	2100	1.73	49
4		18	3800	1.77	69
5		19	9000	1.59	80

Table 13. Poly(silylethers) of dicarbonyls, hydroxy carbonyls and unsymmetrical diols.^a

^aReaction conditions: substrate (0.8–0.9 mmol), silane – 1 equivalent and MnN catalyst – 1.0 mol%. ^bDetermined by GPC instrument. ^cBased on the ¹H NMR and weight of the purified polymer.

6.2.5. Substrates with mixed functional groups. So far, all the substrates used are structurally symmetrical with two identical functional groups. Encouraged by the results that polysilylethers can be prepared both diols and dicarbonyls using the same manganese catalyst, we sought to employ substrates with unsymmetrical, mixed functional groups to further extend the substrate scope. Thus, *p*-hydroxybenzaldehyde was first selected as a monomer to react with diphenylsilane (Table 13, entry **4**). Though the reaction time (18 h) required to reach 90% conversion of silane was less than the three reactions in entries 1–3, the isolated yield and the molecular weight ($M_n = 3800$ g/mol, PDI = 2.02) were greater than those reactions. Relatively speaking, these values fall right in between those obtained from 1,4-benzenediol and terephthalaldehyde, in line with the difference in their respective reactivities toward polymerization reactions under manganese catalysis. As *p*-hydroxybenzaldehyde has two different ends, it can form polymers with different

connectivities, which was supported by the presence of two peaks for the benzylic signals in both the ^1H NMR and ^{13}C NMR spectra. These observations were consistent with the ^{29}Si NMR spectrum, in which two peaks at -29.56 and -30.15 ppm was observed with the latter being the stronger peak. One would expect to see three distinct peaks corresponding to the three different silicon environments resulting from the head-to-head, head-to-tail, and tail-to-tail connections. One possibility is that two of them collapse to one signal, which seems to be not very likely. We suspect that due to the large difference in reactivity between aryl alcohols and aldehydes towards silane, the $-\text{OH}$ end reacted with silane mostly to generate a dialdehyde in the early stage of the reaction; later the dialdehyde reacted further with silane to produce the oligo- and polysilylether. By this way only two types of silicon environments were present in the polymer. The third type, if any, existed in very small amounts, was thus not observed by the ^{29}Si NMR. Also, supports this point but the huge difference in peak intensities may explains that one type of the connections is predominant than other.

To support the formation of polymers with different connectivities, we finally performed a reaction between another unsymmetrical monomer 3-(4-hydroxyphenyl)-1-propanol and diphenylsilane (Table 13, entry **5**). As this substrate has two hydroxyl groups at both ends, more than 95% conversion was achieved in 19h with 80% isolated yield. The molecular weight ($M_n = 9000$ g/mol) was high when compared with polymers from dicarbonyls and hydroxyl carbonyl. As expected, three distinct peaks appeared in the ^{29}Si NMR, in agreement with the formation of three different types of connectivities. The high yield and M_n constitute further evidence that hydroxyl compounds are much faster than carbonyls in the polymerization reactions.

6.3. Conclusions

In conclusion, a variety of poly(silylether)s were synthesized from diols, dicarbonyls and mixed functional group substrates with hydrosilanes using a salen manganese complex. Diol monomers were very active in polymerization process which produced the corresponding polymers in high yields and molecular weights than dicarbonyls. The unsymmetrical monomers were produced polymers with different connectivities contrast to the symmetrical monomers. We assume that a reduced manganese species might be the active catalyst in this polycondensation reactions, the supporting and mechanistic studies are underway.

6.4. Experimental section

General

All solvents and liquid substrates were degasified and dried over molecular sieves prior to use. Deuterated solvents were purchased from Cambridge Isotope Laboratory. All ^1H NMR and All ^{13}C NMR spectra were recorded on a Bruker AVANCE-500 NMR spectrometer and referenced to CDCl_3 . Gel permeation chromatography (GPC) analysis was performed on a Varian Prostar, using PLgel 5 μm Mixed-D column, a Prostar 355 RI detector, and THF as eluent at a flow rate of 1 mL/min (20 °C). Polystyrene standards were used for calibration.

General Procedure for the Dehydrogenative coupling of alcohols and silanes:

All the reactions were performed under inert conditions unless otherwise mentioned in the paper. A schlenk flask (50–100 mL) were used as the reaction flask and oil bath with digital

thermometer were used to set and read the temperature. The general procedure includes, loading the 1 mol% catalyst in a Schlenk flask, stoichiometric equivalents of substrate and diphenylsilane followed by the addition of 2.5 to 2.8 mL of solvent in a glove box. The resulting reaction mixture was taken out and refluxed under inert conditions on a Schlenk line. Later, the reaction mixture was heated at reflux temperature for a specific length of time.

Purification process

All the polymers were purified via precipitation method. As all the polymers were soluble in dichloromethane (DCM) and insoluble in methanol (MeOH), these two solvents were used in the precipitation process. Initially, the brown, viscous reaction mixture was turned as the homogenous mixture by the addition of as low as possible amount of DCM (1–2 mL). To the resulting homogenous reaction mixture, 8–10 mL MeOH was added until it is turned to a biphasic mixture. The top layer, which contains the unreacted materials was removed by pipette and the viscous bottom layer was washed 2–3 times with 6–8 mL of MeOH each time until it gave a white/light–yellow color viscous/solid polymer. Later, the resulting polymer was dried under hood and the corresponding yields were calculated by taking the weight of the polymer and characterized by ^1H NMR, ^{13}C NMR, IR spectroscopy and Gel permeation chromatography.

NMR characterization data

Table 12, entry 1: (1,4-benzenedimethanol polymer): Scale – catalyst-5.0 mg, substrate 0.89 mmol, polymer weight-214.0 mg, molecular weight of a repeating unit-318.0 g/mol, yield – 75.61%. ^1H NMR (500 MHz, CDCl_3 , 298K, δ): 4.81 (s, 4H, OCH_2), 7.26 (m, 4H, *p* & *o*, Ph), 7.33 (m, 4H, *m*, SiPh_2), 7.38 (m, 2H, *p*, SiPh_2), 7.70 (m, 4H, *o*, SiPh_2). ^{13}C {1H} NMR (500 MHz, CDCl_3 , 298K, δ): 64.98 (OCH_2). 126.71 (CH_2), 128.12 (*m*, SiPh_2), 130.64 (*p*, SiPh_2), 132.55 (*i*, SiPh_2), 135.17 (*o*, SiPh_2), 139.47 (*i*, Ph). ^{29}Si NMR: δ –30.41.

Table 12, entry 2: (1,4-benzenediol polymer): Scale – catalyst-5.0 mg, substrate-131.8 mg (0.89 mmol), polymer weight-207.0 mg, molecular weight of a repeating unit-292.42 g/mol, yield – 79.5%. ¹H NMR (500 MHz, CDCl₃, 298K, δ): 6.64 (m, 4H, Ph), 7.28 (m, 4H, *m*, SiPh₂), 7.36 (m, 2H, *p*, SiPh₂), 7.63 (m, 4H, *o*, SiPh₂). ¹³C {1H} NMR (500 MHz, CDCl₃, 298K, δ): 120.57 (*Ph*), 128.20 (*m*, SiPh₂), 131.04 (*p*, SiPh₂), 131.53 (*i*, SiPh₂), 135.29 (*o*, SiPh₂), 148.98 (*i*, Ph). ²⁹Si NMR: δ –35.22

Table 12, entry 3: (4,4'-dihydroxybisphenol polymer): Scale – catalyst-5.0 mg, substrate-0.89 mmol, polymer weight-299.0 mg molecular weight. of a repeating unit-368.0 g/mol, yield-91.2%. ¹H NMR (500 MHz, CDCl₃, 298K, δ): 6.64 (m, 4H, Ph), 7.28 (m, 4H, *m*, SiPh₂), 7.36 (m, 2H, *p*, SiPh₂), 7.63 (m, 4H, *o*, SiPh₂). ¹³C {1H} NMR (500 MHz, CDCl₃, 298K, δ): 120.57 (*Ph*), 128.20 (*m*, SiPh₂), 131.04 (*p*, SiPh₂), 131.53 (*i*, SiPh₂), 135.29 (*o*, SiPh₂), 148.98 (*i*, Ph). ²⁹Si NMR: δ -37.42. . *T*_g: 100.66 °C

Table 12, entry 4: (1,4-cyclohexanedimethanol polymer): Scale – catalyst-5.0 mg, substrate-0.89 mmol, polymer weight-214.0 mg, molecular weight of a repeating unit-324.5 g/mol, yield – 76.45%. ¹H NMR (500 MHz, CDCl₃, 298K, δ): 0.98 (m, 4H, CH₂), 1.54 (m, 2H, OCH), 1.86 (m, 4H, CH₂), 3.77 (m, 4H, OCH₂), 7.41 (m, 6H, *m* & *p*, SiPh₂), 7.66 (m, 4H, *o*, SiPh₂). ¹³C {1H} NMR (500 MHz, CDCl₃, 298K, δ): 29.28 (CH₂), 40.63 (CH₂), 68.72 (OCH), 127.96, (*m*, SiPh₂), 130.34 (*p*, SiPh₂), 133.54 (*i*, SiPh₂), 135.19(*o*, SiPh₂). ²⁹Si NMR: δ –29.90. *T*_g: 12.92 °C

Table 12, entry 5: (1,4-cyclohexanediol polymer): Scale – catalyst-5.0 mg, substrate-0.89 m. moles, polymer weight-184.8 mg, molecular weight of a repeating unit-298.0 mg, yield-70.0%. ¹H NMR (500 MHz, CDCl₃, 298K, δ): 1.41 (m, 4H, CH₂), 1.84 (m, 4H, CH₂), 3.91 (m, 2H, OCH), 5.46 (m, 1H, -SiH), 7.35 (m, 4H, *m*, SiPh₂), 7.39 (m, 2H, *p*, SiPh₂), 7.64 (m, 4H, *o*, SiPh₂). ¹³C {1H} NMR (500 MHz, CDCl₃, 298K, δ): 30.72 (CH₂), 32.35 (CH₂), 68.92, 70.16 (OCH), 127.76, 128.14 (*m*, SiPh₂), 130.12, 131.36 (*p*, SiPh₂), 134.31, 134.74 (*i*, SiPh₂), 135.11, 135.18 (*o*, SiPh₂). ²⁹Si NMR: δ –35.47, -35.61, -35.69. *T*_g: 55.9 °C

Table 12, entry 6: (1,6-hexanediol polymer): Scale – catalyst-5.0 mg, substrate-105.2 mg (0.89 mmol), polymer weight-222.5 mg, molecular weight. of a repeating unit-298.16 g/mol, yield – 84.0%. ¹H NMR (500 MHz, CDCl₃, 298K, δ): 1.32 (m, 4H, CH₂), 1.56 (m, 4H, CH₂CH₂), 3.74 (m, 4H, OCH₂), 7.33 (m, 4H, *m*, SiPh₂), 7.38 (m, 2H, *p*, SiPh₂), 7.63 (m, 4H, *o*, SiPh₂). ¹³C {1H} NMR (500 MHz, CDCl₃, 298K, δ): 25.74 (CH₂), 32.66 (CH₂CH₂), 63.31 (OCH₂), 127.99 (*m*, SiPh₂), 130.3 (*p*, SiPh₂), 133.4 (*i*, SiPh₂), 135.1 (*o*, SiPh₂). ²⁹Si NMR: δ –32.57

Table 13, entry 1: (1,4-dicarboxaldehyde (terephthalaldehyde) polymer): Scale – catalyst-5.0 mg, substrate-1 0.89 mmol, polymer weight-178.0 mg, molecular weight of a repeating unit-318.0 g/mol, yield-63.0%. ¹H NMR (500 MHz, CDCl₃, 298K, δ): 4.81 (m, 4H, OCH₂), 7.26 (m, 4H, *p* & *o*, Ph), 7.37 (m, 4H, *m*, SiPh₂), 7.71 (m, 6H, *p* & *o*, SiPh₂). ¹³C {1H} NMR (500 MHz, CDCl₃, 298K, δ): 65.0 (OCH₂). 126.73 (*p* & *o*, Ph), 128.17 (*m*,

SiPh₂), 130.65 (*p*, SiPh₂), 132.55 (*i*, SiPh₂), 135.17 (*o*, SiPh₂), 139.42 (*i*, Ph). ²⁹Si NMR: δ -30.29. *T*_g: 17.02 °C

Table 13, entry 2: (1,6-hexanedial polymer): Scale – catalyst-5.0 mg, substrate-123.0 mg (0.89 mmol), polymer weight-105.6 mg, molecular weight of a repeating unit-298.6.0 g/mol, yield – 40.0%. ¹H NMR (500 MHz, CDCl₃, 298K, δ): 1.26-1.62 (m, 8H, CH₂), 3.82 (m, 4H, OCH₂), 7.30-7.40 (m, 10H, SiPh₂). ¹³C {1H} NMR (500 MHz, CDCl₃, 298K, δ): 26.82 (CH₂), 33.21 (CH₂CH₂), 64.15 (OCH₂), 127.8 (*m*, SiPh₂), 131.1(*p*, SiPh₂), 133.8 (*i*, SiPh₂), 135.2 (*o*, SiPh₂).

Table 13, entry 3: (1,4-cyclohexanedione polymer): Scale – catalyst-5.0 mg, substrate-112.13 mg (0.89 mmol), polymer weight-130.1 mg, molecular weight of a repeating unit-298 g/mol, yield-49%. ¹H NMR (500 MHz, CDCl₃, 298K, δ): 1.38 (m, 4H, CH₂), 1.81 (m, 4H, CH₂), 3.87 (m, 2H, OCH), 7.27 (m, 6H, *m* & *p*, SiPh₂), 7.58 (m, 4H, *o*, SiPh₂). ¹³C {1H} NMR (500 MHz, CDCl₃, 298K, δ): 30.96, 32.02 (CH₂), 68.85, 70.09 (OCH), 127.77 (*m*, SiPh₂), 130.12 (*p*, SiPh₂), 134.14 (*i*, SiPh₂), 135.03 (*o*, SiPh₂). ²⁹Si NMR: δ -35.62, -35.70. *T*_g: 40.63 °C

Table 13, entry 4: (*p*-hydroxy benzaldehyde polymer): Scale – catalyst-5.0 mg, substrate-122.2 mg (0.89 m. moles), polymer weight-188.0 mg, molecular weight of a repeating unit-306.0 g/mol, yield-69.0%. ¹H NMR (500 MHz, CDCl₃, 298K, δ): 4.66, 4.81 (m, 2H, OCH₂), 6.88 (m, 2H, *ortho* to phenolic side Ph), 7.08 (m, 2H, *meta* to phenolic side Ph), 7.32 (m, 6H, *m* & *p*, SiPh₂), 7.68 (m, 2H, *o*, SiPh₂). ¹³C {1H} NMR (500 MHz, CDCl₃, 298K, δ): 64.78, 65.19 (OCH₂), 119.60, 119.71 (*Ph*), 128.21, 130.55, 130.79, 131.09, 132.09, 133.79, 134.55, 135.14 (*m*, *p*, *i* & *o*, SiPh₂), 153.50 (*i*, Ph). ²⁹Si NMR: δ -29.48, -30.35. *T*_g: 14.76 °C

Table 13, entry 5: 3-(4-hydroxyphenyl)-1- propanol polymer): Scale – catalyst-5.0 mg, substrate-152.19 mg (0.89 m. moles), polymer weight-238.0 mg, molecular weight of a repeating unit-335.0 g/mol, yield-80.0%. ¹H NMR (500 MHz, CDCl₃, 298K, δ): 1.73 (m, 2H, CH₂), 2.51 (m, 2H, CH₂Ph), 3.75 (m, 2H, OCH₂), 6.79 (m, 4H, *Ph*), 7.30 (m, 6H, *m* & *p*, SiPh₂), 7.65 (m, 2H, *o*, SiPh₂). ¹³C {1H} NMR (500 MHz, CDCl₃, 298K, δ): 31.32, 31.39 (CH₂), 34.13, 34.28 (CH₂Ph), 62.55, 63.02 (OCH₂), 119.52, 119.65 (*Ph*), 128.06, 128.15, 129.52, 130.45, 130.73, 131.74, 132.55, 133.23, 135.13 (*m*, *p*, *i* & *o*, SiPh₂), 152.20, 152.62 (*i*, Ph). ²⁹Si NMR: δ -37.81. *T*_g: 18.79 °C

6.5. References

197. (a) Anderson, M. T.; Sawyer, P. S.; Rieker, T. *Microporous Mesoporous Mater.* **1998**, *20*, 53–65. (b) Huesing, N.; Raab, C.; Torma, V.; Roig, A.; Peterlik, H. *Chem. Mater.* **2003**, *15*, 2690–2692. (c) Hsiuea, G., -H.; Weib, H., -F.; Shiaob, S., -J.; Kuoa, W., -J.; Sha, Y., -A. *Polymer Degradation and Stability.* **2001**, *73*, 309–318. (d) Dvornic, P. R.; Lenz, R. W. *Macromolecules* **1994**, *27*, 5833–5838. (e) Ohshita, J.; Watanabe, T.; Kanaya, D.; Ohsaki, H.; Ishikawa, M. *Organometallics* **1994**, *13*, 5002–5012.
198. Weber, W. P. “Silicone Reagents for Organic synthesis” Springer, Berlin, **1983**, 21–39.
199. Feigl, A.; Bockholt, A.; Weis, J.; Rieger, B. *Adv. Polym. Sci.* **2010**, *235*, 1–31.
200. (a) Mazurek, M. H. “Silicones”, Ed. Mingos, D. M. P.; Crabtree, R. H. in *Comprehensive Organometallic Chemistry III* **2007**, *3*, 651–697. (b) Meng, Y.; Wei, Z.; Lu, Y, L.; Zhang, L, Q. *eXPRESS Polymer Letters* **2012**, *6*, 882–894.
201. (a) Merker, R. L.; Scott, M. J. *J. Polym. Sci. Part A* **1964**, *2*, 15. (b) Merker, R. L.; Scott, M. J.; Haberland, G. G. *J. Polym. Sci., Part A* **1964**, *2*, 31. (c) Lauter, U.; Kantor, S. W.; Schmidt-Rohr, K.; MacKnight, W. J. *Macromolecules* **1999**, *32*, 3426–3431. (d) Dorset, D.; McCourt, M. P. *Polymer* **1997**, *38*, 1985. (e) Dunnavant, W. R.; Markle, R. A.; Sinclair, R. G.; Stickney, P. B.; Curry, J. E.; Byrd, J. D. *Macromolecules* **1968**, *1*, 244–249. (f) Liu, Y.; Imae, I.; Makishima, A.; Kawakami, Y. *Sci. Technol. Adv. Mater.* **2003**, *4*, 27–34.
202. Nagasaki, Y.; Matsukura, F.; Masao, K.; Aoki, H.; Tokuda, T. *Macromolecules* **1996**, *29*, 5859–5863.
203. (a) Martinez-Crespiera, S.; Ionescu, E.; Kleebe, H. Z.; Riedel, R. *J. Eur. Ceram. Soc.* **2011**, *31*, 913–919. (b) Harshe, R.; Balan, C.; Riedel, R. *J. Eur. Ceram. Soc.* **2004**, *24*, 3471–3482.
204. (a) Ji, F.; Li, Y. L.; Feng, J. M.; Su, D.; Wen, Y. Y.; Feng, Y.; Hou, F. *J. Mater. Chem.* **2009**, *19*, 9063–9067. (b) Liu, X.; Xie, K.; Wang, J.; Zheng, C. M.; Pan, Y. *J. Mater. Chem.* **2012**, *22*, 19621–19624. (c) Graczyk-Zajac, M.; Wimmer, M.; Neumann, C.; Riedel, R. *J. Solid State Electrochem.* **2015**, *19*, 2763–2769. (d) Lu, K.; Erb, D.; Liu, M. *J. Mater. Chem. C* **2016**, *4*, 1829–1837 (e) Colombo, P.; Mera, G.; Riedel, R.; Soraru, G. D. *J. Am. Ceram. Soc.* **2010**, *93*, 1805–1837. (f) Gregori, G.; Kleebe, H. J.; Blum, Y. D.; Babonneau, F. *Int. J. Mater. Res.* **2006**, *97*, 710–720.
205. (a) Cheng, C.; Watts, A.; Hillmyer, M. A.; Hartwig, J. F. *Angew. Chem. Int. Ed.* **2016**, *55*, 11872–11876. (b) Sahmetlioglu, E.; Nguyen, H. T. H.; Nsengiyumva, O.; Göktürk, E.; Miller, S. A. *ACS Macro Lett.* **2016**, *5*, 466–470.

-
206. Miller, S. A. *ACS Macro Lett.* **2013**, *2*, 550–554.
207. (a) Li, Y.; Kawakami, Y. *Macromolecules* **1999**, *32*, 8768–8773. (b) Mabry, M. J.; Runyon, M. K.; Weber, W. P. *Macromolecules* **2002**, *35*, 2207–2211. (c) Minegishi, S.; Ito, M.; Kameyama, A.; Nishikubo, T. *J. Polym. Sci.: Part A: Polym. Chem.* **2000**, *38*, 2254–2259.
208. Wang, M.; Zhang, Q.; Wooley, K. L. *Biomacromolecules* **2001**, *2*, 1206–1213.
209. (a) Drake, K.; Mukherjee, I.; Mirza, K.; Ji, H.-F.; Bradley, J.-C.; Wei, Y. *Macromolecules* **2013**, *46*, 4370–4377. (b) Yun, S. B.; Park, Y. T. *Bull. Korean Chem. Soc.* **2008**, *29*, 2373–2378. (c) Jung, I. K.; Park, Y. T. *Bull. Korean Chem. Soc.* **2011**, *32*, 1303–1309. (d) Jung, E. A.; Park, Y. T. *Bull. Korean Chem. Soc.* **2012**, *33*, 2031–2037. (e) Jung, E. A.; Park, Y. T. *Bull. Korean Chem. Soc.* **2013**, *34*, 1637–1642. (f) Liaw, D. J.; Liaw, B. Y. *J. Polym. Sci., Part A: Polym. Chem.* **1999**, *37*, 4591–4595. (g) Carraher, C. E., Jr.; Klimiuk, C. H. *J. Polym. Sci., Part A-1* **1970**, *8*, 973–978. (h) Issam, A. M.; Haris, M. *J. Inorg. Organomet. Polym.* **2009**, *19*, 454–458.
210. (a) Nishikubo, T.; Kameyama, A.; Hayashi, N. *Polym. J.* **1993**, *25*, 1003–1005. (b) Liaw, D.-J. *Polymer* **1997**, *38*, 5217–5219. (c) Nishikubo, T.; Kameyama, A.; Kimura, Y.; Fukuyo, K. *Macromolecules* **1995**, *28*, 4361–4365.
211. Nishikubo, T.; Kameyama, A.; Kimura, Y.; Nakamura, T. *Macromolecules*, **1996**, *29*, 5529–5534.
212. Minegishi, S.; Ito, M.; Kameyama, A.; Nishikubo, T. *Journal of Polymer Science: Part A: Polymer Chemistry.* **2000**, *38*, 2254–2259.
213. An introductory guide to the safe handling of chlorosilanes - www.dowcorning.com
214. Nye, S. A.; Swint, S. A. *J. Polym. Sci., Part A: Polym. Chem.* **1994**, *32*, 131–138.
215. (a) Curry, J. E.; Byrd, J. D. *Macromolecules* **1968**, *1*, 249. (b) Dunnavant, W. R.; Markle, R. A.; Stickney, P. B.; Curry, J. E.; Byrd, J. D. *J. Polym. Sci., Part A: Polym. Chem.* **1967**, *5*, 707.
216. (a) Padmanabon, M.; Kakimoto, M.; Imai, Y. *J. Polym. Sci., Part A: Polym. Chem.* **1989**, *28*, 2997. (b) Henglei, F. A.; Schmulder, P. *Makromol. Chem.* **1954**, *13*, 53. (c) Imai, Y. *J. Macromol. Sci., Chem. A.* **1991**, *28*, 1115.
217. (a) Curry, J. E.; Byrd, J. D. *Macromolecules* **1968**, *1*, 249. (b) Dunnavant, W. R.; Markle, R. A.; Stickney, P. B.; Curry, J. E.; Byrd, J. D. *J. Polym. Sci., Part A: Polym. Chem.* **1967**, *5*, 707.
218. (a) Li, Y.; Kawakami, Y. *Macromolecules* **1999**, *32*, 3540–3542. (b) Li, Y.; Kawakami, Y. *Macromolecules* **1999**, *32*, 8768–8773. (c) Li, Y.; Seino, M.; Kawakami, Y. *Macromolecules* **2000**, *33*, 5311–5314. (c) Li, Y.; Kawakami, Y. *Macromolecules* **1999**, *32*, 6871–6873.

-
219. (a) Paulasaari, J. K.; Weber, W. P. *Macromolecules*. **1998**, *31*, 7105–7107. (b) Mabry, J.M. Paulasaari, J. K.; Weber, W. P. *Polymer*. **2000**, *41*, 4423–4428. (c) Mabry, M. J.; Runyon, M. K.; Weber, W. P. *Macromolecules*, **2002**, *35*, 2207–2211. (d) Mabry, M. J.; Runyon, M. K.; Weber, W. P. *Macromolecules*, **2001**, *34*, 7264–7268.
220. (a) Lázaro, G.; Fernández-Alvarez, F. J.; Iglesias, M.; Horna, C.; Vispe, E.; Sancho, R.; Lahoz, F. J.; Iglesias, M.; Pérez-Torrente, J. J.; Oro, L. A. *Catal. Sci. Technol.* **2014**, *4*, 62–70. (b) Lázaro, G.; Iglesias, M.; Fernández-Alvarez, F. J.; Sanz Miguel, P. J.; Pérez-Torrente, J. J.; Oro, L. A. *ChemCatChem* **2013**, *5*, 1133–1141. (c) Purkayastha, A.; Baruah, J. B. *Appl. Organometal. Chem.* **2000**, *14*, 477–483.
221. Catalysis without Precious Metals, ed. Bullock, R. M. WileyVCH, Weinheim, Germany, 2010.
222. Cella, J.; Rubinsztajn, S. *Macromolecules* **2008**, *41*, 6965–6971.
223. Zhao, M.; Xie, W.; Cui, C. *Chem. Eur. J.* **2014**, *20*, 9259–9262.
224. (a) Lichtenberg, C.; Viciu, L.; Adelhardt, M.; Sutter, J.; Meyer, K.; de Bruin, D.; Grützmacher, H. *Angew. Chem. Int. Ed.* **2015**, *54*, 5766–5771. (b) Lichtenberg, C.; Adelhardt, M.; Wörle, M.; Büttner, T.; Meyer, K.; Grützmacher, H. *Organometallics* **2015**, *34*, 3079–3089.
225. (a) Abbina, S.; Bian, S.; Oian, C.; Du, G. *ACS Catal.* **2013**, *3*, 678–684; (b) Truong, T. V.; Kastl, E. A.; Du, G. *Tetrahedron Lett.* **2011**, *52*, 1670–1672. (c) Du, G.; Abu-Omar, M. M. *Cur. Org. Chem.* **2008**, *12*, 1185–1198. (d) Du, G.; Fanwick, P. E.; Abu-Omar, M. M. *J. Am. Chem. Soc.* **2007**, *129*, 5180–5187.
226. Yiu, S.-M.; Lam, W. W. Y.; Ho, C.-M.; Lau, T.-C. *J. Am. Chem. Soc.* **2007**, *129*, 803–809.
227. (a) Chidara, V. K.; Du, G. *Organometallics* **2013**, *32*, 5034–5037. (b) Vijjamarri, S.; Chidara, V. K.; Rousova, J.; Du, G. *Catal. Sci. Technol.* **2016**, *6*, 3886–3892.
228. Bryan, Z. J.; Hall, A. O.; Zhao, C. T.; Chen, J.; McNeil, A. C. *ACS Macro Lett.* **2016**, *5*, 69–72.
229. (a) Jenekhe, S. A. *Chem. Mater.* **2004**, *16*, 4381. (b) Brook, M. A. In *Silicon in Organic, Organometallic, and Polymer Chemistry*; John Wiley & Sons, Inc.: New York, **2000**. (c) Chen, J.; Cao, Y. *Macromol. Rapid Commun.* **2007**, *28*, 1714–1742.

CHAPTER 7

CATALYTIC EPOXIDATION OF BIOBASED ESTERS OF SUCROSE SOYATE

7.1. Introduction

Biobased materials derived from renewable sources have gained insight during the past few years because of their contribution towards sustainability. The most employed renewable resources are plant oils and carbohydrates. Vegetable oils constitute a valuable source of renewable feedstock due to their cost-effective, high abundance, environmental factors, and a variety of functional groups.^{230,231,232} On the other hand, carbohydrates are also the important class of renewable sources from plants, which can replace petroleum-derived products.

In the early 1960s, Walsh *et al.* reported sucrose esters of unsaturated fatty acids (SEFA), a hybrid of plant oil, triglycerides of fatty acids, and sucrose, a disaccharide.²³³ However, in the last decade, Proctor & Gamble (P&G) developed an improved synthesis of SEFA and commercialized under the brand name SEFOSE.²³⁴ Sucrose soyate (SS) is one example of SEFOSE, where, the sucrose moiety as a central core, and modified hydroxyl groups into esters with long chain fatty acids of soybean oil. The unsaturation in the fatty acid chains is used to introduce reactive functional groups that results in modified physical properties of the parent molecule.

Epoxidation of double bonds in SS generates more reactive, three-membered cyclic ethers also known as, oxiranes. They provide a convenient site for further transformations and represent a reactive intermediate for the synthesis of derivatives of SS that would be

difficult to obtain directly from the double bond.²³⁵ Epoxidized sucrose soyate (ESS) (Figure 24) is a promising candidate in the preparation of novel materials such as polyols, amino alcohols, alkoxy alcohols, hydroxyl esters, alkanol amines, epoxy resins and others.^{236,237,238,239} The thermosets and materials from ESS have shown a substantial increase in its hardness, storage modulus, and glass transition temperature compared to previous epoxidized vegetable oil-based resins.²⁴⁰

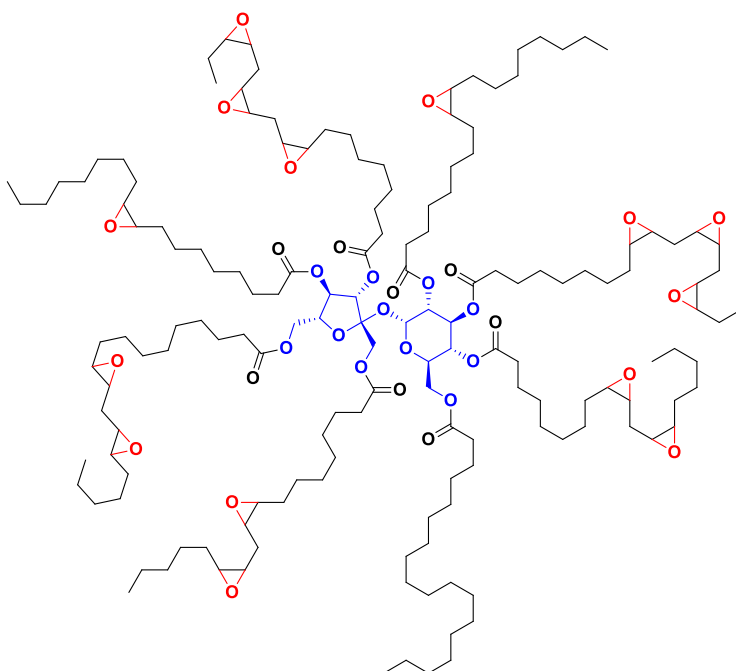


Figure 24. Completely epoxidized sucrose soyate (ESS). Blue color indicates sucrose moiety, black color indicates linoleic and linolenic acids as a constitute of soybean oil, and red color indicates the epoxide, formed from unsaturation in the parent sucrose soyate.

Even though, SS is derived from environment friendly substrates, sucrose and soybean oil, the ESS can be considered green only when non-toxic state-of-art procedures were used during its epoxidation. In general, epoxidation of olefins can be broadly classified into one of the following ways - (1) Acid resin or enzyme catalyzed epoxidation using percarboxylic acid synthesized either *in-situ* or preformed; (2) Metal complex catalyzed epoxidation using peroxides; (3) Metal supported activation of molecular

oxygen. Industrial epoxidation procedures use peroxy-carboxylic acid, generated *in-situ* from hydrogen peroxide and carboxylic acid, in presence of strong acid catalysts such as sulfuric acid and phosphoric acid. The acids unless neutralized prior to isolation of the product, favors ring-opening of epoxide in presence of water to form hydroxyl groups on SS fatty acid chains. These constitute major drawbacks for the isolation of clean products on a large scale industrial process. Therefore, clean, and selective epoxidation procedures with new efficient technologies following the principles of green chemistry are in demand.

In this perspective, permanganate, and chromate, which requires to be added in stoichiometric amounts and leaves toxic residues are neglected. For environmental and economic reasons, hydrogen peroxide and molecular oxygen are the greener choice of oxidants. However, H₂O₂ is easy to handle, produces only water as a byproduct and is relatively cheap, easy to store. The combination of green oxidant, H₂O₂ with non-toxic and inexpensive metal catalysts is undoubtedly an ideal system for epoxidation reactions.²⁴¹ Activation of molecular oxygen by a metal-catalyst is another area of interest, where a non-toxic, environment friendly oxygen can be used as an oxidant. The use of peracetic acid is also not ruled out in industries with combination of active metal catalysts.

In this paper, we evaluate different catalysts for the epoxidation of SS. Special attention is paid to environmentally friendly considerations whenever possible, for example, a solvent that can be derived from biomass, MeTHF, is particularly tested. Methyltrioxorhenium (MTO) (Chart 5, **a**) is one of the versatile catalyst used for epoxidation of olefins which are well described in review articles.²⁴² Previous reports with soybean oil as double bond substrates proved MTO to be effective CH₂Cl₂/H₂O₂ biphasic system. Complete conversion of double bonds with >90% selectivity towards epoxide

content was observed with H₂O₂ as oxidant and moderate results with peracetic acid (PAA).²⁴³ Addition of nitrogen base such as pyridine stabilizes the epoxide ring and existence of biphasic system lowers the interaction of epoxide to the aqueous phase and hence minimizes formation of ring-opened product. Hydrolysis of oxirane ring depends on various factors including rate of stirring, viscosity, pH, temperature.²⁴⁴ In spite of superior activity of MTO towards epoxidation, it cannot be recycled and reused.

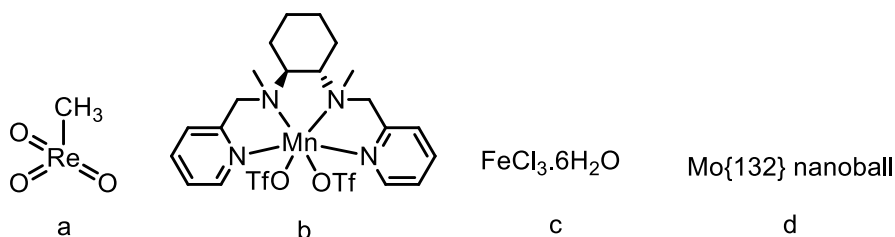


Chart 5. Various catalysts used in this study. 1. Methyltrioxorhenium(VII), 2. Mn^{II}(*R,R*-mcp)(CF₃SO₃)₂, 3. Iron(III)chloride hexahydrate, 4. {(NH₄)₄₂[Mo^V₇₂Mo^V₆₀O₃₇₂(CH₃COO)₃₀(H₂O)₇₂]}.
 1. CC(=O)O[Re](=O)=O
 2. C1=CC=C(C=C1)N2C(=C3C=CC=C3N2)C(=O)O
 3. [Fe](Cl)(Cl)Cl.O.O.O.O.O.O
 4. [Mo]

Salen-based catalysts, more importantly, Jacobsen-Katsuki catalysts are well developed for epoxidation of olefins ranging from simple to complex substrates.²⁴⁵ These groups reported manganese(III) salen complexes to be effective epoxidation catalyst for unfunctionalized olefins.²⁴⁶ Stack and co-workers reported a library of aminopyridine manganese complexes, of which Mn^{II}[(*R,R*)-mcp](OTf)₂ complex (Chart 5, **b**) is effective towards epoxidation of olefins with peracetic acid as an oxidant.²⁴⁷ Variants of these ligands was also recently used in the enantioselective epoxidation of alkenes with high conversions and excellent enantiomeric excess.²⁴⁸

Iron being biomimetic, high abundant, less toxic, environmentally benign, its complexes are studied as catalysts for certain reactions like hydrogenation and oxidation reactions.²⁴⁹ Numerous reports were observed for iron-porphyrin complexes for epoxidation, however, the synthesis of these ligands require tedious procedures that are

limited to industrial applications.²⁵⁰ Few iron containing non-porphyrin complexes have also reported for epoxidation of olefins.²⁵¹ In this context, iron salts like $\text{FeCl}_3 \cdot 6\text{H}_2\text{O}$ (Chart 5, **c**) is commercially available, less expensive metal source and it is used as epoxidation catalyst in combination with nitrogen based ligands. Hydrogen peroxide²⁵² and molecular oxygen²⁵³ are two popular oxidants used with iron containing complexes.

Activation of molecular oxygen by a metal-catalyst is another area of interest, where a non-toxic, environment friendly oxygen can be used as an oxidant. Hakimi and co-workers have reported the aerobic epoxidation of keplerate polyoxomolybdate complex (Chart 5, **d**) in water.²⁵⁴ Since the double bonds on the fatty acid chains of SS might have the same reactivity as the other substrates mentioned, this procedure was used in our process. In addition, the present protocol may be advantageous as MTO system, where the substrate exists as a suspension on water and catalyst is dissolved in aqueous phase.

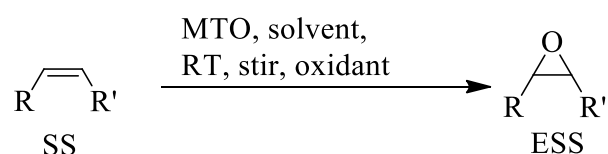
7.2. Results and discussion

7.2.1. Epoxidation of SS catalyzed by MTO

Initial optimization reactions were based on the choice of strength of the oxidant used to yield 100% ESS product. Complete conversion of SS can be achieved using both 10% and 30% H_2O_2 , however, the sensitivity of the epoxide ring towards acid in the reaction mixture lead to the formation of ring opened product was observed predominantly (Table 14, entries **1** and **2**). Usage of basic additives seems to avoid this problem to yield a clean product.²⁴⁴ When pyrazole and pyridine were used as additives, reaction proceeded clean and resulted in ESS with 100% epoxide content (Table 14, entries **3** and **4**). Conversion and amount of epoxide were calculated based on ^1H NMR. Having known the toxicity of DCM as a solvent, switching it with either ethyl acetate or 2-methyl THF (MeTHF) retained the initial

activity towards selectivity for formation of ESS (Table 14, entries **5** and **6**). The catalyst loading can be lowered to 0.5 mol% with the ability to form completely epoxide product but with comparatively longer reaction time (Table 14, entries **7**). In spite of the effective epoxidation reactions, this process has a downfall by lacking the reusability of the MTO. For this purpose, other metal complexes were also investigated to examine the activity of epoxidation as well as recyclability of the catalyst.

Table 14. Epoxidation of SS catalyzed by MTO.^a



entry	Oxidant ^b	MTO (mol%)	Additive ^c	Solvent	Time (h)	Conversion ^d (%)	Epoxide ^e (%)
1	10% H ₂ O ₂	1	-	DCM	24	100	10
2	30% H ₂ O ₂	1	-	DCM	14	100	11
3	30% H ₂ O ₂	1	pyrazole	DCM	4	100	100
4	30% H ₂ O ₂	1	pyridine	DCM	4	100	100
5	30% H ₂ O ₂	1	pyridine	EA	4	100	100
6	30% H ₂ O ₂	1	pyridine	MeTHF	2	100	100
7	30% H ₂ O ₂	0.5	pyridine	MeTHF	9	100	100

^aH₂O₂ was added drop wise over a period of 30 min and the reactions were performed at room temperature along with stirring. ^b1.2 eq oxidant was added for 1 eq double bond in SS. ^c5 mol% additive was used. ^dAmount of double bonds converted, calculated by ¹H NMR. ^eAmount of epoxide formed, calculated by ¹H NMR. If the value is <100%, the remaining amount indicates the percentage of ring opened product.

7.2.2. Epoxidation of SS catalyzed by Mn^{II}[(*R,R*)-mcp](OTf)₂ complex

Observed the activity of Mn^{II} complex (Chart 2, **b**) towards epoxidation of olefins, the same complex was used to catalyze the epoxidation of SS. Unlike commercially available MTO, **2b** is synthesized in three steps as per the literature protocols.²⁴⁷ Having used the successful reaction conditions reported for functionalized olefins, only 65%

conversion of double bonds in SS were observed in 5 h, 85% conversion in 36 h, and no further conversion was observed even at longer reaction times. However, this trial resulted only hydrolyzed product (Table 15, entry 1). Addition of **2b** in ethanol (EtOH) to a solution of SS in DCM, followed by the addition PAA resulted in 68% conversion and 16% epoxide content (Table 15, entry 2). It is clear from these runs that the epoxide ring is unstable in this environment and thus undergone hydrolysis, presumably with acid and water. Entry 2 was repeated with an extra addition of pyridine as a base with an idea if it can neutralize the acid and so as minimizes the hydrolyzed product. But, the actual result was still worse resulting in only 23% conversion for 48h with 11% epoxide content (Table 15, entry 3).

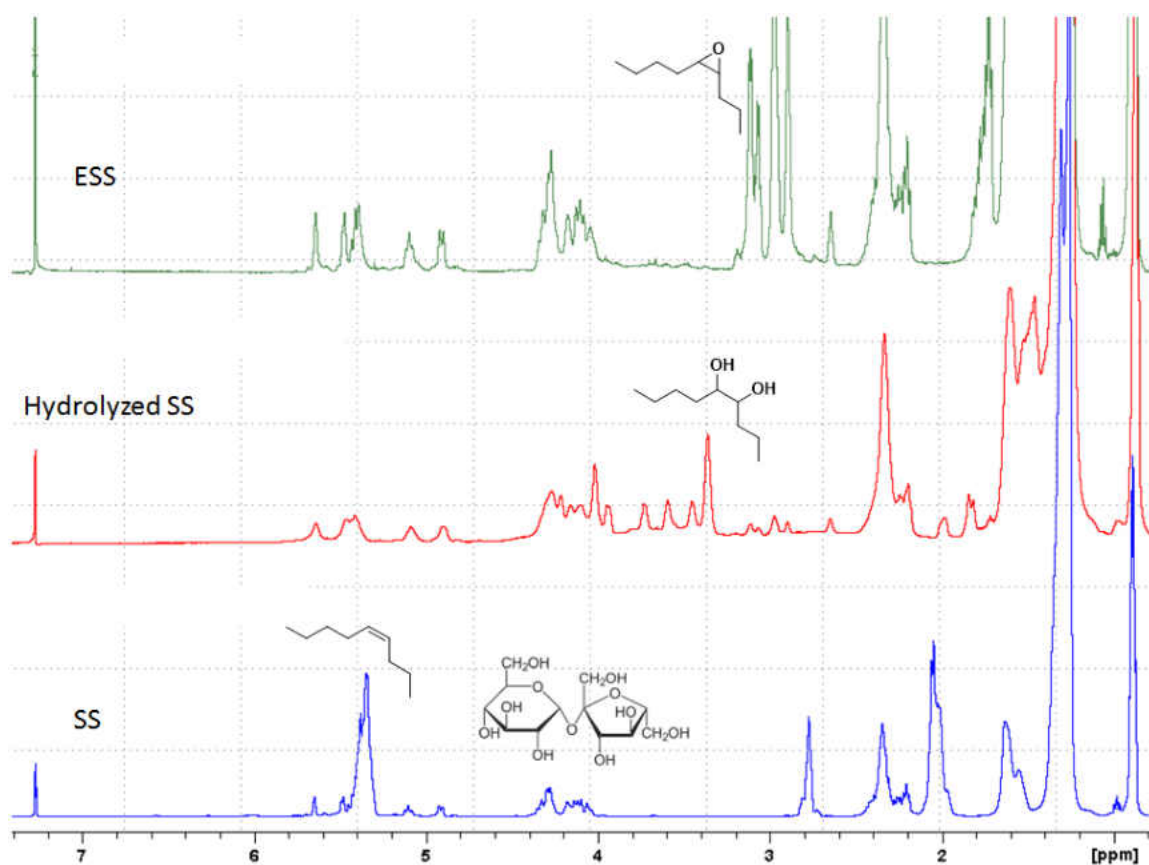
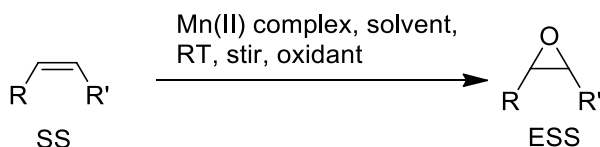


Figure 25. ¹H NMR spectrum of epoxidized sucrose soyate (top green), hydrolyzed sucrose soyate (middle red), sucrose soyate (bottom blue) in CDCl₃.

Observed the possible reaction dependence on the type of solvent used, PAA was added to a solution of SS in ethyl acetate (EA) and complete conversion of double bonds with no epoxide content at all (Table 15, entry 4). Lower conversion of 24% was observed the reaction mixture were dissolved in EA and EtOH (Table 15, entry 5) and no conversion was observed with acetonitrile (ACN) as solvent (Table 15, entry 6). Biomass derived solvent, 2-methyltetrahydrofuran (2-MeTHF) was also screened to make the reaction greener. However, only 51% conversion and 26% epoxide content were observed (Table 15, entry 7). And, using H₂O₂ instead of PAA doesn't improve the result (Table 15, entry 8). Overall, addition of 32% PAA to a solution of Mn^{II} and SS in 2-MeTHF worked well for this process.

Table 15. Epoxidation of SS catalyzed by Mn^{II}[(R,R)-mcp](OTf)₂ complex.^a



entry	Oxidant ^b	Mn ^{II} mol(%)	solvent	time (h)	Conversion ^c (%)	Epoxide ^d (%)
1	32% PAA	1	DCM	5	65	0
2	32% PAA	1	DCM/EtOH	3	68	16
3 ^e	32% PAA	1	DCM/EtOH	48	23	11
4	32% PAA	1	EA	2	100	0
5	32% PAA	1	EA/EtOH	70	24	5
6	32% PAA	1	ACN	36	0	0
7	32% PAA	1	2-MeTHF	24	51	26
8	30% H ₂ O ₂	1	DCM	48	0	0

^aOxidant was added drop wise over a period of 30 min and the reactions were performed at room temperature along with stirring. ^b1.2 eq oxidant was added with respect to 1 eq double bond in SS. ^cAmount of double bonds converted, calculated by ¹H NMR. ^dAmount of epoxide formed, calculated by ¹H NMR. If the value is <100%, the remaining amount indicates the percentage of ring opened product. ^e5 mol% pyridine was added as an additive.

7.2.3. Epoxidation of SS catalyzed by FeCl₃.6H₂O complex

Epoxidation of SS with commercially available, inexpensive, less toxic metal catalyst should be ideal for large scale production of ESS. A biomimetic iron system was reported with β -keto esters as sacrificial cosubstrate for the epoxidation of various olefins under open air without addition of any other oxidant.²⁵⁵ No conversion of double bonds to epoxide was observed when a mixture of 5 mol% FeCl₃.6H₂O (Chart 2, c), 1 eq. imidazole as an additive, 3 eq. ethyl-2-oxocyclopentane carboxylate (E₂OPC) were added to a solution of SS in ACN and the reaction mixture was stirred for 20 h at room temperature (Table 16, entry 1). Considering the disadvantage of using extra sacrificial substrate as well

Table 16. Epoxidation of SS catalyzed by FeCl₃.6H₂O^a

entry	oxidant ^b	mol (%)	additive	solvent	temp (°C)	time (h)	conversion ^c (%)	epoxide ^d (%)
1	O ₂	5	Imidazole, E ₂ OPC	ACN	RT	20	0	0
2	30% H ₂ O ₂	5	imidazole	EA	60	24	0	0
3	30% H ₂ O ₂	5	imidazole	EA/EtOH	60	31	39	0
4	30% H ₂ O ₂	5	imidazole	Acetone	60	24	52	0
5	30% H ₂ O ₂	5	1-Me imidazole	Acetone	60	10	92	0
6	30% H ₂ O ₂	5	1-Me imidazole	Acetone	RT	22	68	0

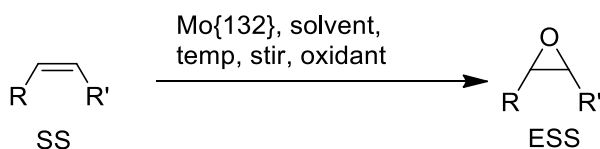
^aOxidant was added drop wise over a period of 30 min and the reactions were performed at room temperature along with stirring. ^b1.2 eq oxidant was added with respect to 1 eq double bond in SS. ^cAmount of double bonds converted, calculated by ¹H NMR. ^dAmount of epoxide formed, calculated by ¹H NMR. If the value is <100%, the remaining amount indicates the percentage of ring opened product.

as no reactivity was observed without oxidant, further screening was done using H₂O₂, which was proven to be efficient with this catalyst.²⁵⁶ The reaction did not yield ESS with 30% H₂O₂ and SS in EA even at longer reaction time (Table 16, entry **2**). On the contrary, the reaction can be activated with either EA/EtOH mixture or acetone as solvents. In both the cases, the basic additive (imidazole) was not capable to stabilize the three membered epoxide ring, hence no epoxide content was observed (Table 16, entries **3** and **4**). High conversions were observed with 1-methyl imidazole (1-Meimidazole) as an additive, but no epoxidized product was observed even at decreased temperature (Table 16, entries **5** and **6**).

7.2.4. Epoxidation of SS catalyzed by Mo{132} nanoball

Hakimi and co-workers have proved that the Mo{132} nanoball can catalyze the aerobic epoxidation of olefins under mild conditions. However, the same procedure did not work for the epoxidation of SS even at increased reaction time and higher catalyst loading (Table 17, entry **1**). The same catalyst was proven to catalyze the epoxidation using H₂O₂ as an oxidant,²⁵⁷ but SS remained unreactive with EtOH, DCM, or EA. (Table 17, entries **3–5**). Because of low solubility of Mo{132} in organic solvents, the runs without aqueous phase barely reacted with SS with no conversion. Solubility of both catalyst and SS might have played a key role in these reactions. 100% conversion was achieved when two different choice of solvents were used to dissolve Mo{132} and SS in each phase. When aqueous solution Mo{132} was added to SS in EA followed by a slow addition of 30% H₂O₂ resulted in complete conversion of double bonds to hydrolyzed product (Table 17, entry-**6**). The same result was observed with EA/EtOH solvent mixture in 10h (Table 17, entry-**7**).

Table 17. Epoxidation of SS catalyzed by Mo{132} nanoball.^a



entry	oxidant ^b	Mo{132} (mol%)	solvent	temp (°C)	time (h)	conversion ^c (%)	epoxide ^d (%)
1	O ₂	0.5	H ₂ O	RT	36	0	0
2	30% H ₂ O ₂	0.5	EtOH	RT	56	0	0
3	30% H ₂ O ₂	1	EtOH	60	46	0	0
4	30% H ₂ O ₂	1	DCM	RT	36	0	0
5	30% H ₂ O ₂	0.2	EA	RT	56	0	0
6	30% H ₂ O ₂	0.2	EA/H ₂ O	60	8	100	0
7	30% H ₂ O ₂	0.2	EA/EtOH	60	10	100	0

^aOxidant was added drop wise over a period of 30 min and the reactions were performed at room temperature along with stirring. ^b1.2 eq oxidant was added with respect to 1 eq double bond in SS. ^cAmount of double bonds converted, calculated by ¹H NMR. ^dAmount of epoxide formed, calculated by ¹H NMR. If the value is <100%, the remaining amount indicates the percentage of ring opened product.

7.3. Conclusions

We have examined four different types of metal catalysts to demonstrate efficient epoxidation methodology using environmentally benign oxidants. MTO in combination with pyridine or pyrazole was proven to be a successful epoxidation catalyst for SS with 100% double bond conversion and 100% epoxide content. Only 26% epoxide content can be achieved manganese catalyst and FeCl₃.6H₂O can catalyze the reaction to 90% conversion, however, this system failed to stabilize the formed epoxide and hence resulted in the 100% hydrolysis product. Being a heterogeneous catalyst, Mo{132} can be advantageous over the others because of its reusability and easy isolation procedures. Even though, complete conversion of SS was observed with EA/H₂O and EA/EtOH solvent mixtures, no selectivity was observed towards formation of epoxide.

7.4. Experimental section

General

Materials used in the present work are mentioned in the alphabetical order - (1s,2s)-(+)-1,2-diaminocyclohexane, ammonium heptamolybdate tetrahydrate, ethyl-2-oxocyclopentane carboxylate, 37% formaldehyde solution, glacial acetic acid, hydrazine sulfate, 30% aq. hydrogen peroxide, imidazole, Iron(III) chloride hexahydrate, manganese bis(trifluoromethanesulfonate), Methyltrioxorhenium, 2-methyltetrahydrofuran, 32% peracetic acid in acetic acid, Bis[3,5-bis(trifluoro-methyl)diphenyl]diselenide, 2-pyridine caroxaldehyde, sodium borohydride were purchased from Sigma-Aldrich chemicals. 1-methyl imidazole, pyridine, pyrazole were purchased from Acros chemicals. Anhydrous acetonitrile, ammonium acetate and 2-methyl THF were purchased from Fisher Scientific. Deuterated solvents like CDCl_3 and C_6D_6 were purchased from Cambridge isotope laboratories. Prepurified nitrogen and oxygen gas were purchased from Air gas. Epoxidation catalysts namely, $\text{Mn}^{\text{II}}(\text{R,R-mcp})(\text{CF}_3\text{SO}_3)_2$ (Chart 5, **b**) and $\text{MO}\{132\}$ (Chart 5, **d**) nanoball were prepared according to reported literature procedures. Sucrose soyate was obtained from Dr. Webster's group at NDSU, who in turn obtained the samples from Procter & Gamble Chemicals (Cincinnati, OH). ^1H NMR and ^{13}C NMR analyses were performed on a Bruker AVANCE-500 NMR spectrometer using Topspin 1.3 software, and signals were referenced to residual peaks of CDCl_3 .

General procedure for epoxidation of SS: The SS used in this study have a value an average degree of substitution of 7.7 with iodine value, $\text{IV} = 117$, and viscosity as 425 mPa.s. Double bond content in SS is estimated based on the relative integration of double bond protons in ^1H NMR and based on iodine value. Under normal benchtop conditions, pre-weighed SS was dissolved in respective solvent using a 25 mL round bottom flask,

followed by the addition 0.1–1 mol% catalyst (relative to double bonds), 1.2 eq. oxidant over a period of 15–20 min and stirred at constant speed. Reaction mixture was heated in an oil bath, equipped with thermocouple, whenever required. Reaction progress was monitored by collecting a small amount of sample and analyzing with ^1H NMR spectroscopy. Reaction was continued until 100% conversion of SS was observed. In case of reactions with MTO, 20% NaHSO_3 was added to the stirring reaction mixture and continued until 1 h. Then the organic layer containing ESS and by products, if present, were isolated from aqueous layer and dried over saturated NaCl . The purified and dried sample was analyzed for further characterizations based of ^1H NMR, ^{13}C NMR, IR spectroscopies.

Characterization:

^1H NMR. ^1H NMR spectra corresponding to SS, ESS, and hydrolyzed SS were shown in Figure 3. The spectrum of SS shows double bond protons ($-\text{CH}=\text{CH}-$) at 4.92–5.65 ppm, the protons of ($-\text{CH}=\text{CH}-\text{CH}_2-\text{CH}=\text{CH}-$) appears at 2.77 ppm, and the protons of ($-\text{CH}_2-\text{CH}=\text{CH}-$) at 2.04–2.35 ppm. The spectrum of ESS shows the disappearance of double bond protons ($-\text{CH}=\text{CH}-$) at 4.92–5.65 ppm and appearance of new peaks for ($-\text{CH}-\text{CHO}-$) protons at 2.89–3.12 ppm.

^{13}C NMR. ^{13}C NMR spectra corresponding to SS, ESS were shown in Figure 4. The spectrum of SS shows ester carbons ($\text{C}=\text{O}$) at 172–173 ppm, double bond carbons ($-\text{CH}=\text{CH}-$) at 128 ppm and 131 ppm. The spectrum of ESS shows the disappearance of double bond carbons ($-\text{CH}=\text{CH}-$) at 128 ppm and 131 ppm and appearance of new peaks for ($-\text{CH}-\text{CHO}-$) protons at 54 ppm and 56 ppm.

FT-IR. IR spectrum of SS shows an adsorption from sp^2 C-H stretch (-CH=CH-) at 3010 cm^{-1} , and ester carbonyl band at 1747 cm^{-1} . In the spectrum of ESS, the band corresponding to sp^2 C-H stretch (-CH=CH-) at 3010 cm^{-1} is disappeared and a new adsorption band due to epoxide C-O stretch was observed at 821 cm^{-1} .

7.5. References

230. Schwab, A. W.; Bagby, M. O.; Freeman, B. *Fuel* **1987**, *66*, 1372–1378.
231. Khot, S. N.; Lascala, J. J.; Can, E.; Morye, S. S.; Williams, G. I.; Palmese, G. R.; Kusefoglu, S. H.; Wool, R. P. *J. Appl. Polym. Sci.* **2001**, *82*, 703–723.
232. Raqueza, J.-M.; Deléglisea, M.; Lacrampea, M.-F.; Krawczaka, P. *Prog. Polym. Sci.* **2010**, *35*, 487–509.
233. Walsh, T.; Bobalek, E.; Hall, D. *Div. Org. Coatings Plastic Chem.* **1961**, *21*, 125–148.
234. Kenneally, C. J.; Busch, G. A.; Corrigan, P. J.; Granberg, E. P.; Howie, J. K.; Schafermeyer, R. G.; Trout, J. E., US Patent 6121440A 2000.
235. Dahlke, B.; Hellbardt, S.; Paetow, M.; Zech, W. H. *J. Am. Oil Chem. Soc.* **1995**, *72*, 349–353.
236. Nelson, T. J.; Galhenage, T. P.; Webster, D. C. *J. Coat. Technol. Res.* **2013**, *10*, 589–600.
237. Pan, X.; Webster, D. C. *Macromol. Rapid Commun.* **2011**, *32*, 1324–1330.
238. Pan, X.; Sengupta, P.; Webster, D. C. *Biomacromolecules* **2011**, *12*, 2416–2428.
239. Pan, X.; Webster, D.C. *ChemSusChem.* **2012**, *5*, 419–429.
240. Yan, J.; Webster, D. *Green Mater.* **2014**, *2*, 132–143.
241. (a) Colladon, M.; Scarso, A.; Sgarbossa, P.; Michelin, R. A.; Strukul, G. *J. Am. Chem. Soc.* **2006**, *128*, 14006–14007. (b) Sawada, Y.; Matsumoto, K.; Kondo, S.; Watanabe, H.; Ozawa, T.; Suzuki, K.; Saito, B.; Katsuki, T. *Angew. Chem. Int. Ed.* **2006**, *45*, 3478–3480.
242. (a) Kuhn, F. E.; Scherbaum, A.; Herrmann, W. A. *J. Organomet. Chem.* **2004**, *689*, 4149–4164. (b) Amato, M. E.; Ballistreri, F. P.; Pappalardo, A.; Tomaselli, G. A.; Toscano, R. M.; Sfrassetto, G. T. *molecules* **2013**, *18*, 13754–13768.
243. (a) Gerbase, A. E.; Gregorio, J. R.; Martinelli, M.; Brasil, M. C.; Mendes, A. N. F. *J. Am. Oil Chem. Soc.* **2002**, *79*, 179–181. (b) Santacesaria, E.; Renken, A.; Russo, V.; Turco, R.; Tesser, R.; Di Serio, M. *Ind. Eng. Chem. Res.* **2012**, *51*, 8760–8767. (c) Refvik, M. D.; Larock, R. C. *J. Am. Oil Chem. Soc.* **1999**, *76*, 99–102. (d) Refvik, M. D.; Larock, R. C. *J. Am. Oil Chem. Soc.* **1999**, *76*, 99–102. (e) Sales, H.; Cesquini, R.; Sato, S.; Mandelli, D.; Schuchardt, U. *Stud. Surf. Sci. Catal.* **2000**, *130*, 1661–1666.
244. (a) Campanella, A.; Baltanas, M. A. *Lat. Am. Appl. Res.* **2005**, *35*, 205–210. (b) Campanella, A.; Baltanas, M. A. *Lat. Am. Appl. Res.* **2005**, *35*, 211–216.

-
245. (a) Jacobsen, E. N. Transition Metal-catalyzed Oxidations: Asymmetric Epoxidation. In *Comprehensive Organometallic Chemistry II*, 1st ed.; Abel, E. W.; Stone, F. G. A.; Wilkinson, G. Eds.; Pergamon Press: New York, 1995; Vol. 12, 1097–1135. (b) Katsuki, T. Asymmetric Epoxidation of Unfunctionalized Olefins and Related Reactions. In *Catalytic Asymmetric Synthesis*, 2nd ed.; Ojima, I. Ed. Wiley-CVH: New York, 2000; 287–325.
246. (a) Zhang, W.; Loebach, J. L.; Wilson, S. R.; Jacobsen, E. N. *J. Am. Chem. Soc.* **1990**, *112*, 2801–2803. (b) Jacobsen, E. N.; Zhang, W.; Loebach, J. L.; Muci, A. R.; Ecker, J. R.; Deng, L. *J. Am. Chem. Soc.* **1991**, *113*, 7063–7064. (c) Irie, R.; Noda, K.; Ito, Y.; Matsumoto, N.; Katsuki, T. *Tetrahedron Lett.* **1990**, *31*, 7345–7348.
247. (a) Murphy, A.; Dubois, G.; Stack, T. D. P. *J. Am. Chem. Soc.* **2003**, *125*, 5250–5251. (b) Murphy, A.; Pace, A.; Stack, T. D. P. *Org. Lett.* **2004**, *6*, 3119–3122.
248. Maity, N. Ch.; Bera, P. K.; Ghosh, D.; Abdi, S. H. R.; Kureshy, R. I.; Khan, N. H.; Bajaj, H. C.; Suresh, H. *Catal. Sci. Technol.* **2014**, *4*, 208–217.
249. (a) Casey, C. P.; Guan, H. -r. *J. Am. Chem. Soc.* **2007**, *129*, 5816–5817. (b) S. C. Bart, E. Lobkovsky, P. J. Chirik, *J. Am. Chem. Soc.* **2004**, *126*, 13794–13807. (c) Shulpin, G. B.; Golfeto, C. C.; Suss-Fink, G.; Shulpina, L. S.; Mandelli, D. *Tetrahedron Lett.* **2005**, *46*, 4563–4567.
250. Meunier, B. *Chem. Rev.* **1992**, *92*, 1411–1456.
251. (a) Chen, K.; Costas, M.; Kim, J.; Tipton, A. K.; Que, L. *J. Am. Chem. Soc.* **2002**, *124*, 3026–3035. (b) White, M. C.; Doyle, A. G.; Jacobsen, E. N. *J. Am. Chem. Soc.* **2001**, *123*, 7194–7195.
252. Anilkumar, G.; Bitterlich, B.; Gelalcha, F. G.; Tse, M. K.; Beller, M. *Chem. Commun.* **2007**, 289–291.
253. (a) Dobler, C.; Mehlretter, G.M.; Sundermeier, U Beller, M. *J. Am. Chem. Soc.* **2000**, *122*, 10289–10297. (b) Dobler, C.; Mehlretter, G. M.; Beller, M. *Angew. Chem. Int. Ed.* **1999**, *38*, 3026–3028.
254. Rezaeifard, A.; Haddad, R.; Jafarpour, M.; Hakimi, M. *J. Am. Chem. Soc.* **2013**, *135*, 10036–10039.
255. Schroder, K.; Join, B.; Amali, A. J.; Junge, K.; Ribas, X.; Costas, M.; Beller, M. *Angew. Chem. Int. Ed.* **2011**, *50*, 1425–1429.
256. (a) Jiao, M.; Matsunaga, H.; Ishizuka, T. *Chem. Pharm. Bull.* **2011**, *59*, 799–801. (b) Hasan, K.; Brown, N.; Kozak, C. M. *Green Chem.* **2011**, *13*, 1230–1237.
257. Rezaeifard, A.; Haddad, R.; Jafarpour, M.; Hakimi, M. *ACS Sustainable Chem. Eng.* **2014**, *2*, 942–950.

APPENDICES

APPENDIX-A

X-RAY DATA TABLES OF COMPLEX 1d (Chapter 2)Table 18. Crystal data, data collection, structure solution and structure refinement for **1d**

formula	C ₃₈ H ₃₈ N ₄ O ₂
formula weight	582.72
crystal system	triclinic
space group	$\bar{P}1$
<i>a</i> , Å	9.3756 (14)
<i>b</i> , Å	9.05053(14)
<i>c</i> , Å	10.2668(15)
α , deg	97.973(2)
β , deg	111.748(2)
γ , deg	109.046(2)
<i>V</i> , Å ³	767.39
<i>Z</i>	1
<i>d</i> _{calc} , g cm ⁻³	1.261
temperature/K	180
μ , mm ⁻¹	0.079
Radiation	Mo 0.71073
2 θ range, deg	2.236-27.545
data collected	17787
<i>R</i> _{int}	0.0451
data in refinement	7059
data with <i>I</i> > 2.0 σ (<i>I</i>)	5521
number of variables	432
<i>R</i> (<i>F</i> _o) ^a	0.0419
<i>R</i> _w (<i>F</i> _o ²) ^b	0.0611
GOF	1.018
Flack	-0.2(5)

^a $R = \sum ||F_o| - |F_c|| / \sum |F_o|$ for $F_o^2 > 2\sigma(F_o^2)$; ^b $R_w = [\sum w (|F_o^2| - |F_c^2|)^2 / \sum w |F_o^2|]^1/2$

Table 19. Selected bond lengths for **1b** (Chapter 2).

Atoms 1,2	d 1,2 [Å]	Atoms 1,2	d 1,2 [Å]
N1—C4AA	1.485(3)	C20—H20	0.9500
N1—C4	1.281(3)	C20—C21	1.383(4)
C2AA—H2AA	0.9500	C21—H21	0.9500
C2AA—C9	1.400(3)	C22—H22	0.9500
C2AA—C10	1.397(4)	C22—C23	1.410(4)
O3—C15	1.369(3)	C23—H23	0.9500
O3—C16	1.446(5)	C23—C24	1.348(4)
O4—C4	1.362(3)	C24—H24	0.9500
O4—C30	1.450(3)	C24—C25	1.437(4)
C1AA—H1AA	0.9800	C25—C36	1.390(4)
C1AA—H1AB	0.9800	C26—H26	0.9500
C1AA—H1AC	0.9800	C26—C27	1.384(4)
C1AA—C0AA	1.528(4)	C27—H27	0.9500
C0AA—H0AA	1.0000	C27—C28	1.389(4)
C0AA—C4AA	1.531(4)	C28—H28	0.9500
C0AA—C31	1.523(4)	C28—C29	1.380(4)
C4AA—H4AA	1.0000	C29—H29	0.9500
C4AA—C30	1.539(4)	C30—H30A	0.9900
C4—C3AA	1.469(3)	C30—H30B	0.9900
C3AA—C6	1.423(3)	C31—H31A	0.9800
C3AA—C26	1.397(4)	C31—H31B	0.9800
C6—N7	1.379(3)	C31—H31C	0.9800
C6—C29	1.406(3)	C32—H32	0.9500
N7—H7	0.8800	C32—C33	1.411(4)
N7—C8	1.409(3)	C33—H33	0.9500
C8—C9	1.440(4)	C33—C34	1.353(4)
C8—C32	1.371(4)	C34—H34	0.9500
C9—C35	1.437(3)	C34—C35	1.431(4)
C10—C11	1.443(4)	C35—C36	1.396(4)
C10—C25	1.437(4)	C36—H36	0.9500
C11—N12	1.408(3)	C1A—H1AD	0.9800
C11—C22	1.371(4)	C1A—H1AE	0.9800

N12—H12	0.8800	C1A—H1AF	0.9800
N12—C13	1.384(3)	C1A—C2A	1.532(11)
C13—C14	1.412(4)	C2A—H2A	1.0000
C13—C21	1.407(4)	C2A—C5A	1.533(10)
C14—C15	1.461(4)	C5A—H5AA	0.9800
C14—C18	1.405(4)	C5A—H5AB	0.9800
C15—N37	1.274(4)	C5A—H5AC	0.9800
C16—H16A	0.9900	C1B—H1BA	0.9800
C16—H16B	0.9900	C1B—H1BB	0.9800
C16—C17	1.532(5)	C1B—H1BC	0.9800
C17—H17	1.0000	C1B—C2B	1.516(10)
C17—H17A	1.0000	C2B—H2B	1.0000
C17—N37	1.486(4)	C2B—C5B	1.501(13)
C17—C2A	1.505(7)	C5B—H5BA	0.9800
C17—C2B	1.654(9)	C5B—H5BB	0.9800
C18—H18	0.9500	C5B—H5BC	0.9800
C18—C19	1.366(5)	N1—H7	2.0232(30)
C19—H19	0.9500	H12—N37	2.0707(26)
C19—C20	1.381(5)		

Table 20. Selected bond angles for **1b** (Chapter 2).

Atoms 1,2,3	Angle 1,2,3 [°]	Atoms 1,2,3	Angle 1,2,3 [°]
C4—N1—C4AA	107.3(2)	C11—C22—H22	119.500
C9—C2AA—H2AA	118.900	C11—C22—C23	121.1(3)
C10—C2AA—H2AA	118.900	C23—C22—H22	119.500
C10—C2AA—C9	122.2(2)	C22—C23—H23	119.200
C15—O3—C16	105.8(2)	C24—C23—C22	121.6(3)
C4—O4—C30	105.7(2)	C24—C23—H23	119.200
H1AA—C1AA—H1AB	109.500	C23—C24—H24	120.100
H1AA—C1AA—H1AC	109.500	C23—C24—C25	119.9(3)
H1AB—C1AA—H1AC	109.500	C25—C24—H24	120.100
C0AA—C1AA—H1AA	109.500	C24—C25—C10	119.4(2)
C0AA—C1AA—H1AB	109.500	C36—C25—C10	119.1(2)
C0AA—C1AA—H1AC	109.500	C36—C25—C24	121.4(3)

C1AA—C0AA—H0AA	107.500	C3AA—C26—H26	119.300
C1AA—C0AA—C4AA	111.2(2)	C27—C26—C3AA	121.5(3)
C4AA—C0AA—H0AA	107.500	C27—C26—H26	119.300
C31—C0AA—C1AA	110.6(2)	C26—C27—H27	120.600
C31—C0AA—H0AA	107.500	C26—C27—C28	118.7(3)
C31—C0AA—C4AA	112.4(2)	C28—C27—H27	120.600
N1—C4AA—C0AA	111.0(2)	C27—C28—H28	119.200
N1—C4AA—H4AA	109.200	C29—C28—C27	121.6(3)
N1—C4AA—C30	103.1(2)	C29—C28—H28	119.200
C0AA—C4AA—H4AA	109.200	C6—C29—H29	119.800
C0AA—C4AA—C30	115.0(2)	C28—C29—C6	120.5(3)
C30—C4AA—H4AA	109.200	C28—C29—H29	119.800
N1—C4—O4	117.6(2)	O4—C30—C4AA	104.5(2)
N1—C4—C3AA	126.7(2)	O4—C30—H30A	110.900
O4—C4—C3AA	115.7(2)	O4—C30—H30B	110.900
C6—C3AA—C4	121.2(2)	C4AA—C30—H30A	110.900
C26—C3AA—C4	119.3(2)	C4AA—C30—H30B	110.900
C26—C3AA—C6	119.5(2)	H30A—C30—H30B	108.900
N7—C6—C3AA	119.4(2)	C0AA—C31—H31A	109.500
N7—C6—C29	122.2(2)	C0AA—C31—H31B	109.500
C29—C6—C3AA	118.2(2)	C0AA—C31—H31C	109.500
C6—N7—H7	115.700	H31A—C31—H31B	109.500
C6—N7—C8	128.7(2)	H31A—C31—H31C	109.500
C8—N7—H7	115.700	H31B—C31—H31C	109.500
N7—C8—C9	116.8(2)	C8—C32—H32	119.500
C32—C8—N7	123.3(2)	C8—C32—C33	121.1(3)
C32—C8—C9	119.9(2)	C33—C32—H32	119.500
C2AA—C9—C8	123.0(2)	C32—C33—H33	119.400
C2AA—C9—C35	118.8(2)	C34—C33—C32	121.1(3)
C35—C9—C8	118.2(2)	C34—C33—H33	119.400
C2AA—C10—C11	123.1(2)	C33—C34—H34	119.900
C2AA—C10—C25	118.7(2)	C33—C34—C35	120.3(3)
C25—C10—C11	118.2(2)	C35—C34—H34	119.900
N12—C11—C10	117.8(2)	C34—C35—C9	119.3(2)

C22—C11—C10	119.8(2)	C36—C35—C9	118.8(2)
C22—C11—N12	122.4(2)	C36—C35—C34	121.9(2)
C11—N12—H12	116.900	C25—C36—C35	122.3(2)
C13—N12—C11	126.2(2)	C25—C36—H36	118.800
C13—N12—H12	116.900	C35—C36—H36	118.800
N12—C13—C14	120.0(2)	C15—N37—C17	107.8(3)
N12—C13—C21	121.4(3)	H1AD—C1A—H1AE	109.500
C21—C13—C14	118.5(2)	H1AD—C1A—H1AF	109.500
C13—C14—C15	121.4(2)	H1AE—C1A—H1AF	109.500
C18—C14—C13	119.2(3)	C2A—C1A—H1AD	109.500
C18—C14—C15	119.4(3)	C2A—C1A—H1AE	109.500
O3—C15—C14	115.7(2)	C2A—C1A—H1AF	109.500
N37—C15—O3	117.2(3)	C17—C2A—C1A	113.7(6)
N37—C15—C14	127.1(3)	C17—C2A—H2A	108.700
O3—C16—H16A	110.700	C17—C2A—C5A	106.0(5)
O3—C16—H16B	110.700	C1A—C2A—H2A	108.700
O3—C16—C17	105.0(3)	C1A—C2A—C5A	110.9(6)
H16A—C16—H16B	108.800	C5A—C2A—H2A	108.700
C17—C16—H16A	110.700	C2A—C5A—H5AA	109.500
C17—C16—H16B	110.700	C2A—C5A—H5AB	109.500
C16—C17—H17	104.000	C2A—C5A—H5AC	109.500
C16—C17—H17A	114.400	H5AA—C5A—H5AB	109.500
C16—C17—C2B	108.2(4)	H5AA—C5A—H5AC	109.500
N37—C17—C16	103.0(3)	H5AB—C5A—H5AC	109.500
N37—C17—H17	104.000	H1BA—C1B—H1BB	109.500
N37—C17—H17A	114.400	H1BA—C1B—H1BC	109.500
N37—C17—C2A	117.8(3)	H1BB—C1B—H1BC	109.500
N37—C17—C2B	100.9(3)	C2B—C1B—H1BA	109.500
C2A—C17—C16	121.9(4)	C2B—C1B—H1BB	109.500
C2A—C17—H17	104.000	C2B—C1B—H1BC	109.500
C2B—C17—H17A	114.400	C17—C2B—H2B	111.000
C14—C18—H18	119.300	C1B—C2B—C17	109.8(6)
C19—C18—C14	121.3(3)	C1B—C2B—H2B	111.000
C19—C18—H18	119.300	C5B—C2B—C17	103.6(7)

C18—C19—H19	120.200	C5B—C2B—C1B	110.4(7)
C18—C19—C20	119.6(3)	C5B—C2B—H2B	111.000
C20—C19—H19	120.200	C2B—C5B—H5BA	109.500
C19—C20—H20	119.500	C2B—C5B—H5BB	109.500
C19—C20—C21	121.0(3)	C2B—C5B—H5BC	109.500
C21—C20—H20	119.500	H5BA—C5B—H5BB	109.500
C13—C21—H21	119.800	H5BA—C5B—H5BC	109.500
C20—C21—C13	120.3(3)	H5BB—C5B—H5BC	109.500
C20—C21—H21	119.800		

Table 21. Selected torsional angles for **1b** (Chapter 2).

Atoms 1,2,3,4	Tors. an. 1,2,3,4 [°]	Atoms 1,2,3,4	Tors. an. 1,2,3,4 [°]
N1—C4AA—C30—O4	-12.9(3)	N12—C13—C14—C18	175.3(3)
N1—C4—C3AA—C6	-0.8(4)	N12—C13—C21—C20	-175.9(3)
N1—C4—C3AA—C26	179.5(3)	C13—C14—C15—O3	-173.9(2)
C2AA—C9—C35—C34	-176.7(2)	C13—C14—C15—N37	6.4(4)
C2AA—C9—C35—C36	3.1(3)	C13—C14—C18—C19	0.1(4)
C2AA—C10—C11—N12	-4.3(3)	C14—C13—C21—C20	-0.1(4)
C2AA—C10—C11—C22	178.2(2)	C14—C15—N37—C17	177.4(3)
C2AA—C10—C25—C24	-177.6(2)	C14—C18—C19—C20	1.0(5)
C2AA—C10—C25—C36	2.7(3)	C15—O3—C16—C17	9.6(4)
O3—C15—N37—C17	-2.2(4)	C15—C14—C18—C19	180.0(3)
O3—C16—C17—N37	-10.6(4)	C16—O3—C15—C14	175.3(3)
O3—C16—C17—C2A	124.4(5)	C16—O3—C15—N37	-5.1(4)
O3—C16—C17—C2B	95.7(4)	C16—C17—N37—C15	8.0(4)
O4—C4—C3AA—C6	178.8(2)	C16—C17—C2A—C1A	178.8(5)
O4—C4—C3AA—C26	-0.9(3)	C16—C17—C2A—C5A	-59.1(6)
C1AA—C0AA—C4AA—N1	-66.7(3)	C16—C17—C2B—C1B	58.6(7)
C1AA—C0AA—C4AA—C30	176.8(2)	C16—C17—C2B—C5B	176.5(6)
C0AA—C4AA—C30—O4	108.1(2)	C18—C14—C15—O3	6.3(4)
C4AA—N1—C4—O4	-1.3(3)	C18—C14—C15—N37	-173.4(3)
C4AA—N1—C4—C3AA	178.4(2)	C18—C19—C20—C21	-1.8(5)
C4—N1—C4AA—C0AA	-114.7(2)	C19—C20—C21—C13	1.3(5)

C4—N1—C4AA—C30	8.9(3)	C21—C13—C14—C15	179.6(3)
C4—O4—C30—C4AA	12.4(3)	C21—C13—C14—C18	-0.6(4)
C4—C3AA—C6—N7	-5.7(3)	C22—C11—N12—C13	-35.1(4)
C4—C3AA—C6—C29	178.3(2)	C22—C23—C24—C25	-1.7(4)
C4—C3AA—C26—C27	-178.8(2)	C23—C24—C25—C10	-0.8(4)
C3AA—C6—N7—C8	164.8(2)	C23—C24—C25—C36	178.9(2)
C3AA—C6—C29—C28	1.2(4)	C24—C25—C36—C35	179.5(2)
C3AA—C26—C27—C28	0.0(4)	C25—C10—C11—N12	175.4(2)
C6—C3AA—C26—C27	1.5(4)	C25—C10—C11—C22	-2.0(3)
C6—N7—C8—C9	146.2(2)	C26—C3AA—C6—N7	174.0(2)
C6—N7—C8—C32	-36.6(4)	C26—C3AA—C6—C29	-2.0(3)
N7—C6—C29—C28	-174.7(2)	C26—C27—C28—C29	-1.0(4)
N7—C8—C9—C2AA	-7.9(3)	C27—C28—C29—C6	0.3(4)
N7—C8—C9—C35	173.0(2)	C29—C6—N7—C8	-19.3(4)
N7—C8—C32—C33	-174.2(2)	C30—O4—C4—N1	-7.6(3)
C8—C9—C35—C34	2.4(3)	C30—O4—C4—C3AA	172.8(2)
C8—C9—C35—C36	-177.7(2)	C31—C0AA—C4AA— N1	57.9(3)
C8—C32—C33—C34	0.5(4)	C31—C0AA—C4AA— C30	-58.6(3)
C9—C2AA—C10—C11	178.1(2)	C32—C8—C9—C2AA	174.8(2)
C9—C2AA—C10—C25	-1.6(3)	C32—C8—C9—C35	-4.3(3)
C9—C8—C32—C33	2.9(4)	C32—C33—C34—C35	-2.4(4)
C9—C35—C36—C25	-2.1(4)	C33—C34—C35—C9	0.9(4)
C10—C2AA—C9—C8	179.6(2)	C33—C34—C35—C36	-178.9(3)
C10—C2AA—C9—C35	-1.2(3)	C34—C35—C36—C25	177.7(3)
C10—C11—N12—C13	147.5(2)	N37—C17—C2A—C1A	-52.4(7)
C10—C11—C22—C23	-0.4(4)	N37—C17—C2A—C5A	69.7(6)
C10—C25—C36—C35	-0.8(4)	N37—C17—C2B—C1B	166.4(5)
C11—C10—C25—C24	2.6(3)	N37—C17—C2B—C5B	-75.7(6)
C11—C10—C25—C36	-177.1(2)	C2A—C17—N37—C15	-129.3(4)
C11—N12—C13—C14	158.8(2)	C2A—C17—C2B—C1B	-64.8(8)
C11—N12—C13—C21	-25.5(4)	C2A—C17—C2B—C5B	53.1(8)
C11—C22—C23—C24	2.3(4)	C2B—C17—N37—C15	-103.8(4)

N12—C11—C22—C23	-177.7(2)	C2B—C17—C2A—C1A	-112.2(9)
N12—C13—C14—C15	-4.5(4)	C2B—C17—C2A—C5A	9.9(7)

APPENDIX B
X-RAY DATA TABLES OF COMPLEX 3b (Chapter 2)

Table 22. Crystal data, data collection, structure solution and structure refinement for **3b**

formula	C ₆₄ H ₇₂ N ₈ O ₄ Zn ₂ · 4(C ₇ H ₈)
formula weight	1516.57
crystal system	triclinic
space group	P $\bar{1}$
<i>a</i> , Å	10.8657 (5)
<i>b</i> , Å	12.4925 (6)
<i>c</i> , Å	15.6029 (8)
α , deg	106.928 (3)
β , deg	97.805 (3)
γ , deg	91.204 (3)
<i>V</i> , Å ³	2003.29
<i>Z</i>	1
<i>d</i> _{calc} , g cm ⁻³	1.257
temperature/K	100
μ , mm ⁻¹	1.174
Radiation	Cu K α 1.54178
2 θ range, deg	2.994-67.187
data collected	21073
R _{int}	0.0622
data in refinement	8347
data with <i>I</i> > 2.0 σ (<i>I</i>)	7451
number of variables	878
R(<i>F</i> _o) ^a	0.0593
R _w (<i>F</i> _o ²) ^b	0.0667
GOF	1.081
Flack	0.02(4)

^a $R = \sum ||F_o| - |F_c|| / \sum |F_o|$ for $F_o^2 > 2\sigma(F_o^2)$; ^b $R_w = [\sum w (|F_o^2| - |F_c^2|)^2 / \sum w |F_o^2|]^1/2$

Table 23. Selected bond lengths for **3b** (Chapter 2).

Atoms 1,2	d 1,2 [Å]	Atoms 1,2	d 1,2 [Å]
Zn1—N1	1.957(7)	C35—C36	1.490(11)
Zn1—N2	2.018(7)	C36—C37	1.518(11)
Zn1—N3	1.998(7)	C37—C38	1.511(14)
Zn1—N4	1.953(7)	C37—C39	1.540(12)
Zn2—N5	2.001(7)	C40—C41	1.441(11)
Zn2—N6	1.954(7)	C40—C45	1.429(11)
Zn2—N7	1.951(7)	C41—C42	1.365(12)
Zn2—N8	1.995(7)	C42—C43	1.405(13)
O1—C1BA	1.358(11)	C43—C44	1.391(13)
O1—C0CA	1.433(11)	C44—C45	1.415(12)
O2—C20	1.367(9)	C45—C46	1.441(13)
O2—C21	1.471(10)	C47—C48	1.536(12)
O3—C46	1.347(10)	C48—C49	1.523(11)
O3—C47	1.459(11)	C49—C50	1.522(12)
O4—C33	1.373(10)	C50—C51	1.563(17)
O4—C34	1.443(10)	C50—C52	1.490(12)
N1—C0AA	1.379(11)	C53—C54	1.391(11)
N1—C53	1.421(11)	C53—C58	1.397(11)
N2—C1BA	1.299(11)	C54—C55	1.397(13)
N2—C9	1.476(10)	C55—C56	1.396(12)
N3—C20	1.268(11)	C56—C57	1.419(10)
N3—C22	1.492(9)	C57—C58	1.386(12)
N4—C2AA	1.364(11)	C59—C60	1.410(12)
N4—C59	1.439(10)	C59—C64	1.377(11)
N5—C46	1.318(12)	C60—C61	1.388(12)
N5—C48	1.477(10)	C61—C62	1.406(11)
N6—C40	1.359(11)	C62—C63	1.384(13)
N6—C57	1.419(10)	C63—C64	1.381(12)
N7—C27	1.355(11)	C75—C74	1.366(15)
N7—C61	1.422(11)	C75—C76	1.415(15)
N8—C33	1.314(11)	C90—C89	1.381(17)

N8—C35	1.509(10)	C90—C91A	1.60(3)
C0AA—C6AA	1.414(12)	C90—C91B	1.25(2)
C0AA—C0BA	1.430(12)	C89—C88A	1.32(2)
C6AA—C7AA	1.374(11)	C89—C88B	1.37(3)
C7AA—C8AA	1.407(12)	C73—C74	1.374(15)
C8AA—C9AA	1.362(13)	C73—C72	1.380(14)
C9AA—C0BA	1.414(11)	C76—C77	1.325(17)
C0BA—C1BA	1.444(13)	C85A—C91A	1.45(3)
C0CA—C9	1.517(11)	C72—C77	1.394(15)
C9—C1AA	1.520(11)	C72—C71	1.489(14)
C1AA—C2BA	1.520(12)	C88A—C87A	1.36(3)
C2BA—C3BA	1.518(13)	C86A—C87A	1.37(3)
C2BA—C13	1.513(13)	C86A—C91A	1.41(4)
C2AA—C3AA	1.416(12)	C79—C84	1.432(15)
C2AA—C19	1.430(11)	C79—C80	1.366(16)
C3AA—C4AA	1.360(13)	C79—C78	1.33(3)
C4AA—C5AA	1.412(13)	C82—C83	1.372(14)
C5AA—C18	1.352(12)	C82—C81	1.378(17)
C18—C19	1.417(12)	C84—C83	1.412(14)
C19—C20	1.444(12)	C80—C81	1.269(18)
C21—C22	1.522(11)	C96—C95	1.3900
C22—C23	1.509(11)	C96—C97	1.3900
C23—C24	1.552(11)	C95—C93	1.3900
C24—C25	1.498(14)	C93—C94	1.3900
C24—C26	1.540(15)	C94—C98	1.3900
C27—C28	1.413(12)	C94—C92A	1.38(3)
C27—C32	1.462(12)	C98—C97	1.3900
C28—C29	1.339(11)	C98—C92B	1.33(3)
C29—C30	1.417(12)	C85B—C86B	1.54(3)
C30—C31	1.350(12)	C86B—C87B	1.36(3)
C31—C32	1.430(12)	C86B—C91B	1.38(3)
C32—C33	1.422(13)	C87B—C88B	1.45(4)
C34—C35	1.501(10)		

Table 24. Selected bond angles for **3b** (Chapter 2).

Atoms 1,2,3	Angle 1,2,3 [°]	Atoms 1,2,3	Angle 1,2,3 [°]
N1—Zn1—N2	94.7(3)	N8—C33—O4	114.4(8)
N1—Zn1—N3	128.3(3)	N8—C33—C32	129.4(8)
N3—Zn1—N2	101.4(3)	O4—C34—C35	105.4(6)
N4—Zn1—N1	113.1(3)	C34—C35—N8	101.2(6)
N4—Zn1—N2	129.7(3)	C36—C35—N8	115.6(6)
N4—Zn1—N3	93.1(3)	C36—C35—C34	115.1(6)
N6—Zn2—N5	94.5(3)	C35—C36—C37	116.1(7)
N6—Zn2—N8	125.7(3)	C36—C37—C39	112.3(7)
N7—Zn2—N5	117.8(3)	C38—C37—C36	114.3(8)
N7—Zn2—N6	113.6(3)	C38—C37—C39	108.6(8)
N7—Zn2—N8	94.6(3)	N6—C40—C41	120.9(7)
N8—Zn2—N5	112.5(3)	N6—C40—C45	122.6(7)
C1BA—O1—C0CA	106.7(7)	C45—C40—C41	116.4(7)
C20—O2—C21	105.3(6)	C42—C41—C40	121.4(8)
C46—O3—C47	107.2(6)	C41—C42—C43	121.9(8)
C33—O4—C34	105.7(6)	C44—C43—C42	118.4(8)
C0AA—N1—Zn1	126.7(6)	C43—C44—C45	121.3(8)
C0AA—N1—C53	121.2(7)	C40—C45—C46	124.0(8)
C53—N1—Zn1	111.9(5)	C44—C45—C40	120.3(8)
C1BA—N2—Zn1	121.4(6)	C44—C45—C46	115.7(7)

C1BA—N2—C9	109.4(7)	O3—C46—C45	116.6(8)
C9—N2—Zn1	128.6(5)	N5—C46—O3	114.9(7)
C20—N3—Zn1	123.4(5)	N5—C46—C45	128.5(7)
C20—N3—C22	108.6(7)	O3—C47—C48	105.4(6)
C22—N3—Zn1	127.7(5)	N5—C48—C47	102.2(6)
C2AA—N4—Zn1	127.1(6)	N5—C48—C49	110.7(6)
C2AA—N4—C59	118.4(7)	C49—C48—C47	114.5(7)
C59—N4—Zn1	114.4(5)	C50—C49—C48	115.7(8)
C46—N5—Zn2	121.4(5)	C49—C50—C51	109.7(8)
C46—N5—C48	109.4(6)	C52—C50—C49	115.1(8)
C48—N5—Zn2	128.8(5)	C52—C50—C51	109.4(10)
C40—N6—Zn2	125.8(5)	C54—C53—N1	118.2(7)
C40—N6—C57	119.2(7)	C54—C53—C58	119.1(7)
C57—N6—Zn2	114.9(5)	C58—C53—N1	122.3(7)
C27—N7—Zn2	127.1(6)	C53—C54—C55	120.7(8)
C27—N7—C61	117.9(7)	C56—C55—C54	120.0(8)
C61—N7—Zn2	114.8(5)	C55—C56—C57	119.7(8)
C33—N8—Zn2	119.7(6)	C56—C57—N6	117.7(7)
C33—N8—C35	107.3(6)	C58—C57—N6	122.9(7)
C35—N8—Zn2	132.8(5)	C58—C57—C56	119.0(7)
N1—C0AA—C6AA	121.2(7)	C57—C58—C53	121.5(7)
N1—C0AA—C0BA	122.7(8)	C60—C59—N4	119.3(7)

C6AA—C0AA—C0BA	116.1(7)	C64—C59—N4	121.1(7)
C7AA—C6AA—C0AA	123.5(8)	C64—C59—C60	119.2(8)
C6AA—C7AA—C8AA	120.2(8)	C61—C60—C59	121.3(7)
C9AA—C8AA—C7AA	117.7(7)	C60—C61—N7	122.6(7)
C8AA—C9AA—C0BA	123.9(8)	C60—C61—C62	118.4(8)
C0AA—C0BA—C1BA	124.1(7)	C62—C61—N7	118.6(7)
C9AA—C0BA—C0AA	118.7(8)	C63—C62—C61	119.7(8)
C9AA—C0BA—C1BA	117.2(8)	C64—C63—C62	121.5(8)
O1—C1BA—C0BA	116.1(8)	C59—C64—C63	119.8(8)
N2—C1BA—O1	114.1(8)	C74—C75—C76	118.(1)
N2—C1BA—C0BA	129.8(8)	C89—C90—C91A	112.7(15)
O1—C0CA—C9	105.6(7)	C91B—C90—C89	130.6(15)
N2—C9—C0CA	101.3(6)	C88A—C89—C90	126.8(14)
N2—C9—C1AA	111.2(6)	C88B—C89—C90	111.4(17)
C0CA—C9—C1AA	114.0(7)	C74—C73—C72	122.9(10)
C9—C1AA—C2BA	115.0(6)	C75—C74—C73	119.8(10)
C3BA—C2BA—C1AA	109.6(8)	C77—C76—C75	120.7(10)
C13—C2BA—C1AA	113.3(8)	C73—C72—C77	115.7(10)
C13—C2BA—C3BA	109.6(8)	C73—C72—C71	122.1(10)
N4—C2AA—C3AA	122.1(7)	C77—C72—C71	122.1(9)
N4—C2AA—C19	121.6(8)	C89—C88A—C87A	120.2(19)
C3AA—C2AA—C19	116.3(8)	C87A—C86A—C91A	123.(2)

C4AA—C3AA—C2AA	123.2(8)	C76—C77—C72	122.8(10)
C3AA—C4AA—C5AA	120.5(8)	C88A—C87A—C86A	121.(2)
C18—C5AA—C4AA	117.7(8)	C80—C79—C84	119.1(11)
C5AA—C18—C19	123.8(8)	C78—C79—C84	124.6(16)
C2AA—C19—C20	123.6(8)	C78—C79—C80	116.3(16)
C18—C19—C2AA	118.5(7)	C83—C82—C81	115.2(11)
C18—C19—C20	117.9(7)	C83—C84—C79	119.6(10)
O2—C20—C19	115.0(7)	C81—C80—C79	116.9(13)
N3—C20—O2	115.9(7)	C82—C83—C84	118.8(10)
N3—C20—C19	129.0(7)	C80—C81—C82	130.2(14)
O2—C21—C22	103.5(6)	C85A—C91A—C90	119.(2)
N3—C22—C21	101.4(6)	C86A—C91A—C90	115.(2)
N3—C22—C23	113.5(6)	C86A—C91A—C85A	126.(3)
C23—C22—C21	115.0(7)	C95—C96—C97	120.000
C22—C23—C24	112.8(7)	C96—C95—C93	120.000
C25—C24—C23	110.4(8)	C95—C93—C94	120.000
C25—C24—C26	110.5(8)	C98—C94—C93	120.000
C26—C24—C23	111.1(7)	C92A—C94—C93	130.8(13)
N7—C27—C28	123.3(8)	C92A—C94—C98	109.2(13)
N7—C27—C32	120.2(8)	C94—C98—C97	120.000
C28—C27—C32	116.4(8)	C92B—C98—C94	135.5(17)
C29—C28—C27	123.0(8)	C92B—C98—C97	104.4(17)

C28—C29—C30	121.0(8)	C98—C97—C96	120.000
C31—C30—C29	119.4(8)	C87B—C86B—C85B	120.(2)
C30—C31—C32	121.8(8)	C87B—C86B—C91B	120.4(19)
C31—C32—C27	118.3(8)	C91B—C86B—C85B	119.8(18)
C33—C32—C27	124.7(8)	C86B—C87B—C88B	117.(2)
C33—C32—C31	116.7(8)	C90—C91B—C86B	117.4(19)
O4—C33—C32	116.1(7)	C89—C88B—C87B	122.(2)
